Adipocyte-specific inhibition of *Mir221/222* ameliorates diet-induced obesity through targeting *Ddit4*

Satoshi Yamaguchi, Dongxiao Zhang, Akihiro Katayama, Naoko Kurooka, Ryosuke Sugawara, Haya Hamed Hassan Albuayjan, Atsuko Nakatsuka, Jun Eguchi, and Jun Wada

Department of Nephrology, Rheumatology, Endocrinology and Metabolism, Okayama University Graduate School of Medicine, Dentistry and Pharmaceutical Sciences, Okayama, Japan

Correspondence:
Jun Wada, M.D., Ph.D.
Department of Nephrology, Rheumatology, Endocrinology and Metabolism
Okayama University
2-5-1 Shikata-cho, Kita-ku, Okayama 700-8558, Japan
Tel: +81-86-235-7232
FAX: +81-86-222-5214
E-mail: junwada@okayama-u.ac.jp

Keywords: Non-coding RNAs, microRNA, Adipose Tissues, Adipogenesis, mTORC1

ABSTRACT

MicroRNAs expressed in adipocytes are involved in transcriptional regulation of target mRNAs in obesity, but miRNAs critically involved in this process is not well characterized. Here, we identified upregulation of miR-221-3p and miR-222-3p in the white adipose tissues in C57BL/6 mice fed with high fat-high sucrose (HFHS) chow by RNA sequencing. *Mir221* and *Mir222* are paralogous genes and share the common seed sequence and *Mir221/222AdipoKO* mice fed with HFHS chow demonstrated resistance to the development of obesity compared with *Mir221/222*$^{flox/y}$. *Ddit4* is a direct target of *Mir221* and *Mir222*, and the upregulation of *Ddit4* in *Mir221/222AdipoKO* was associated with the suppression of TSC2 (tuberous sclerosis complex 2)/mammalian target of rapamycin complex 1 (mTORC1)/S6K (ribosomal protein S6 kinase) pathway. The inhibition of miR-221-3p and miR-222-3p linked to reduced adipogenesis, and it may be a potential candidate for miRNA-based therapy.

INTRODUCTION

In obesity, the excess and ectopic accumulation of adipose tissue leads to the clusters of metabolic disorders such as low-grade inflammation, type 2 diabetes (T2D), dyslipidemia, hypertension, nonalcoholic fatty liver disorder (NAFLD), cardiovascular diseases (CVDs), chronic kidney disease (CKD) and cancer. As an endocrine organ, the adipose tissue communicates with other tissues by secreting peptide hormones, inflammatory cytokines, signaling lipids and miRNAs packed in exosomes (1). The alteration of expression profile of miRNA both in cytoplasm and extracellular vesicles leads to changes in the transcriptional and translational activities of the genes, which control inflammation, whole body insulin sensitivity, lipid metabolism, adipogenesis of white, beige, and brown adipose tissues(2). For instance, miR-34a secreted by mature adipocytes in exosomes were transported into macrophages, suppresses M2 polarization, and stimulates inflammatory responses by repressing Krüppel-like factor 4(3). Lentivirus-mediated suppression of miR-34a increased

the beige and brown fat formation in diet-induced obese mice by increasing fibroblast growth factor 21 and sirtuin 1(4). The genetic ablation of miR-128-1 in mouse metabolic disease models resulted in increased energy expenditure, amelioration of diet-induced obesity and enhanced insulin sensitivity(5). In lipid metabolism, miR-425 overexpression in mice resulted in the promotion of diet-induced obesity and overexpression of miR-425 in 3T3-L1 cells accelerated adipogenesis and lipogenesis, while knock down of miR-425 remarkably enhanced lipolysis and lipid oxidation(6).

We also attempted to identify specific miRNAs critically involved in the process of obesity, we surveyed expression profile of miRNAs in liver, muscle, white adipose tissues (WATs), and sera of C57BL/6JJcl mice fed with standard (STD) and high fat-high sucrose (HFHS) chow by RNA sequencing (GSE61959)(7). miR-221-3p and miR-222-3p are highly up-regulated in epididymal adipose tissues in mice fed with high fat high sucrose (HFHS). miR-221 and miR-222 both locate in the close proximity on the X chromosome and share the identical seed sequence(8). In meta-analysis, circulating miR-221-3p was reduced in T2D, while miR-222-3p was elevated in obesity and T2D (9). Although miR-221-3p and miR-222-3p are differentially expressed in sera and adipose tissues, the functional *in vivo* experiments to elucidate the roles of *Mir221* and *Mir222* in obesity has not been reported. Here, we investigated the adipocyte specific *Mir221* and *Mir222* knockout (*Mir221/222AdipoKO*) mice fed with HFHS chow, and they were protected from the development of obesity by targeting DDIT4 (DNA damage inducible transcript 4)/TSC2 (tuberous sclerosis complex 2)/S6K (ribosomal protein S6 kinase) pathway.

MATERIALS AND METHODS

Animal Models

We obtained Mir 221 KO cond (*Mir221*^{tm2}; EMMA ID, EM:05507) from EMMA (the European Mouse Mutant Archive) and Helmholz Zentrum München (Neuherberg, Germany). The targeting vector cassette composed of *Neo* flanked by FRT and distal loxP

sites was inserted outside the genomic region encoding *Mir221* and *Mir222* precursors. *Neo* was removed by Flp in the conditional KO allele of Mir 221 KO cond. The conditional KO allele was confirmed by primer pair; 1544_29 (5'- GCT CTG TTT TCC TAA GTG ATG G-3') and 1544_30 (5'-CTG ACA GGA AGT AAA TCA TCT TAG C-3'). The expected fragments were 265 bp in wild and 384 bp in conditional KO allele. We also used B6.FVB-Tg (Adipoq-cre)1Evdr/J to produce *Mir221/222AdipoKO* mice by crossing to Mir 221 KO cond. Adipoq-cre transgene was screened by primers, 15381 (5'-ACG GAC AGA AGC ATT TTC CA-3') and 18564 (5'-GGA TGT GCC ATG TGA GTC TG-3'). The primers, oIMR7338 (5'-CTA GGC CAC AGA ATT GAA AGA TCT-3') and oIMR7339 (5'-GTA GGT GGA AAT TCT AGC ATC ATC C-3'), were used for internal positive control. The expected sizes for transgene and internal positive control were 200 bp and 324 bp, respectively. By crossing male Tg (Adipoq-cre) and female *Mir221*^{tm2}*/y* C57BL/6JJcl mice, we generated male *Mir221/222*$^{flox/y}$ and male *Mir221/222AdipoKO* littermates.

Five-week-old mice were randomly assigned to standard diet (STD) group (MF, Oriental Yeast, Japan) or high fat high sucrose diet (HFHS) group (D12331, Research Diets, New Brunswick, NJ). The detailed formulation of STD(10) (https://www.oyc.co.jp/bio/LAD-equipment/LAD/ingredient.html and https://www.oyc.co.jp/bio/LAD-equipment/LAD/rodents.html) and HFHS (https://www.eptrading.co.jp/service/researchdiets/pdf/D12328-D12331.pdf) diets are shown in **Supplementary Table 1**. At 22 weeks of age, we obtained various organs and they were subjected to following experiments.

3T3-L1 Cell Cultures

3T3-L1 pre-adipocytes were cultured in Dulbecco's modified eagle's medium (DMEM, 2124951, Gibco). On day 0, the cells were treated with the differentiation media; DMEM supplemented with 10% FBS, 10 μg/ml insulin (I1882, Sigma), 1 μM DEX (D2915, Sigma) and 0.5 mM IBMX (I5879, Sigma). Then, the media were changed to DMEM supplemented

with 10 μg/ml insulin and 10% FBS on day 2 and cultured for 10 or 20 days. Undifferentiated 3T3-L1 cells were subjected to Lentiviral miRNA expression, Lentiviral miRNA inhibition studies, and luciferase reporter assays.

Human Serum Samples

Human serum samples were collected from 69 patients with type 2 diabetes in Okayama University Hospital and 45 subjects with normal fasting glucose (NGT).

Insulin Tolerance Test and Glucose Tolerance Test (ITT and GTT)

The 13-week-old mice (n=4 in each experimental group) were fasted for 16 hours in GTT and for 3 hours in ITT. They were then intraperitoneally injected with glucose solution (1 mg/g body weight) and human insulin (1 unit/kg in HFHS groups and 0.75 unit/kg in STD groups) for GTT and ITT, respectively.

Basal Metabolic Rate, Locomotor Activity, and Food Intake

At 18 weeks of age, O_2/CO_2 metabolism measuring system (MK-5000, Muromachi Kikai, Tokyo, Japan) were used to quantify oxygen consumption rate and carbon dioxide production for the estimation of V̇O2 and respiratory quotient (RQ). The locomotor activity was recorded for 24 hours by the frequency of interrupting an infrared sensor (ACTIMO-100, Shinfactory, Fukuoka, Japan). Daily food intake was measured and calculated; daily food intake [g/day/body weight (BW)] = [initial food weight (g) – leftover food weight (g)]/measurement period (days)/BW (g). The 6-10 mice in each experimental group were examined.

Reverse Transcription-Quantitative Polymerase Chain Reaction (RT-qPCR)

RNAs were extracted from frozen tissues and cultured 3T3-L1 cells with RNeasy Mini kit (74106, Qiagen). The QIAamp Circulating Nucleic Acid Kit (Qiagen) were used for the

isolation of total RNAs from serum. For gene expression analyses, cDNAs were prepared with High-Capacity RNA-to-cDNA Kit (Thermo Fisher Scientific). TaqMan gene expression primers, *Ddit4* (Mm00512504_g1), *Rplp0* (Mm00725448_s1), *Rn18s* (Mm03928990_g1), *Adipoq* (Mm00456425_m1), *Lep* (Mm00434759_m1), *Lpl* (Mm01345523_m1), *Srebf1* (Mm00550338_m1), *Cebpa* (Mm00514283_s1), *Fabp4* (Mm00445878_m1), *Pparg* (Mm01184322_m1), *Lipe* (Mm00495359_m1), *Pnpla2* (Mm00503040_m1), *Ucp1* (Mm01244861_m1), *Cox8b* (Mm00432648_m1), *Prdm16* (Mm00712556_m1), *Cidea* (Mm00432554_m1), *Ppargc1a* (Mm01208835_m1), *G6pc* (Mm00839363_m1), *Gck* (Mm00439129_m1), *Fasn* (Mm00662319_m1), *Ppara* (Mm00440939_m1), *Il6* (Mm00446190_m1), *Ifng* (Mm01168134_m1), *Tnf* (Mm00443258_m1), *Il1b* (Mm01336189_m1) were used (Thermo Fisher Scientific). For miRNA expression studies, cDNAs were prepared from total RNAs by TaqMan MicroRNA Reverse Transcription Kit (Life Technologies). MicroRNA primers, *mmu-miR-222-3p* (CTAAJ3), *hsa-miR-221-3p* (000524), *hsa-miR-222-3p* (002276), snoRNA202 (001232), snoRNA234 (001234), and cel-miR-39 (000200) were used (Thermo Fisher Scientific). Rplp0, Rn18s, snoRNA202, snoRNA234, and cel-miR-39 were served as the invariant controls. The RT-qPCR was performed using TaqMan Universal PCR Master mix II (no UNG) at a StepOne Plus Real-Time PCR system. The quantification was performed by the $2^{-\Delta\Delta CT}$ analysis method.

Cloning of Mir221 Host Gene (*Mir221hg*)

Long non-coding RNA, *Mir221hg*, was cloned using SMARTer RACE 5'/3' Kit (634858, Clontech). 5'- and 3'-RACE-Ready cDNAs from epididymal adipose tissues poly A^+ RNA were prepared by SMARTScribe Reverse Transcriptase. 5'- and 3'-RACE-Ready cDNAs were amplified by PCR using 5' GSP (5'-GAT TAC GCC AAG CTT CCA GCA GAC AAT GTA GC TGT TGC-3') and 3' GSP (5'-GAT TAC GCC AAG CTT TCC AGG TCT GGG GCA TGA ACC TG-3'), respectively. Furthermore, nested PCR was performed using 5' NGSP (5'-GAT TAC GCC AAG CTT GTA TGC CAG GTT CAT GCC CCA GAC-3') and 3' NGSP

(5’-GAT TAC GCC AAG CTT GCA ACA GCT ACA TTG TCT GCT GG-3’). PCR products were analyzed by agarose/EtBr gel and purified by NucleoSpin Gel and PCR Clean-Up Kit. The purified RACE products were subcloned into pRACE vector by In-Fusion Cloning (Clontech). Independent 4 clones of both 5’- and 3’-RACE were sequenced.

Western Blot Analysis

The epididymal fat tissues from 22-week-old mice and cultured 3T3-L1 cells were homogenized in RIPA lysis buffer (radioimmunoprecipitation buffer) plus protease inhibitors. The samples were boiled in SDS-PAGE loading buffer, separated on 12% Mini-PROTEAN TGX Precast Protein Gels (Bio-Rad), and transferred to a PVDF Blotting Membrane (cytiva). After blocking with 5% nonfat milk for 1 hour at room temperature (RT), the blots were incubated with REDD-1/DDIT4 Antibody, rabbit polyclonal (ab106356, RRID: AB_10864294), C/EBPα Antibody, rabbit polyclonal (2295, RRID: AB_10692506), PPARγ (D69) Antibody, rabbit polyclonal (2430, RRID: AB_823599), mTOR (7C10) Rabbit mAb (2983, RRID: AB_2105622), Phospho-mTOR (Ser2448) (D9C2) XP Rabbit mAb (5536, RRID: AB_10691552), Akt Antibody, rabbit polyclonal (9272, RRID: AB_329827), Phospho-Akt (Thr308) Antibody, rabbit polyclonal (9275, RRID: AB_329828), p70 S6 Kinase (49D7) Rabbit mAb (2708, RRID: AB_390722), Phospho-p70 S6 Kinase (Thr389) Antibody, rabbit polyclonal (9205, RRID: AB_330944), Tuberin/TSC2 Antibody, rabbit polyclonal (3612, RRID: AB_2207804), Phospho-Tuberin/TSC2 (Thr1462) Antibody, rabbit polyclonal (3611, RRID: AB_329855, Cell Signaling Technology) overnight at 4°C. GAPDH (D16H11) XP Rabbit mAb (HRP Conjugate) (8884, RRID: AB_11129865) was used as a loading control (Cell Signaling Technology). After washing three times with Tris-buffered saline (TBS), the blots were incubated with ECL Donkey Anti-Rabbit IgG, HRP-Conjugated Antibodies (NA934V, GE healthcare Life science, 1:10000) at RT for 1 hour. The blots were developed with Pierce ECL Western Blotting Substrate (TE261327, Thermo Fisher Scientific). The chemiluminescence was analyzed using ImageQuant LAS-4000 mini (FUJIFILM).

Morphometric Analysis for Adipocyte Size

Epidydimal adipose tissues were fixed by 10% formalin, embedded with paraffin. The 5-μm paraffin sections were prepared and stained with PAS. The images were captured using an Olympus BX51 microscope. The size of the adipocytes was analyzed by Keyence Hybrid cell count software. Epidydimal adipose tissues were taken from 3-5 individual animals from each experimental group.

Isolation of Stromal Vascular Fraction (SVF) from White Adipose Tissues

SVF was isolated from epididymal adipose tissue of 24-week-old mice. Briefly, fresh mouse epididymal fat pads were minced and digested with collagenase type 1 (CLSS1, Worthington) in HBSS containing 10% FBS for 45 minutes at 37°C. The mixture was filtered through a nylon mesh (100 μm), then centrifuged at 400 *g* for 1 minute. The adipocyte fraction was obtained from the supernatant, they were again centrifuged at 800 *g* for 10 minutes, and the SVF was obtained from the pellet.

Identification of *Mir221/222* Target mRNAs

The mRNA microarray was performed by GeneChip Mouse Gene 2.0 array using total RNA of epidydimal fat obtained from 16-week-old mice (1 animal from each group) and analyzed by Filgen (Nagoya, Japan). The raw data are available in Gene Expression Omnibus (GEO; https://www.ncbi.nlm.nih.gov/geo/) (GSE163921). TargetScan (http://www.targetscan.org/vert_72/), miRDB (http://www.mirdb.org/), Pictar (https://pictar.mdc-berlin.de/) and DIANA-microT v5.0 (https://bio.tools/DIANA-microT) and were used to identify potential target genes for *Mir221/222*.

Lentiviral miRNA Expression and Lentiviral miRNA Inhibitor

Lentiviral transduction using pLV-miRNA and pLV-miR-Locker system to 3T3-L1 cells were performed according to the manufacturer's manual (Biosettia). After transformation to *E. coli* JM109 cells, pLV-[mmu-mir-221] plasmid (mir-p177m, Biosettia), pLV-[mmu-mir-222] plasmid (mir-p178m, Biosettia), pLV-[mmu-mir-221-3p] locker plasmid (mir-mp0337, Biosettia), pLV-[mmu-mir-222-3p] locker plasmid (mir-mp0339, Biosettia), pLV-[mir-control] plasmid (mir-p000, Biosettia), pLV-miR-locker control plasmid (mir-locker-ctrl, Biosettia), pMDLg/pRRE (12251, Addgene), pRSV/Rev (12253, Addgene), and pMD2.G (12259, Addgene) were isolated with EndoFree Plasmid Maxi Kit (12362, Qiagen). 293T cells (10×10^7/5 mL) were transfected with each pLV plasmid, pMDLg/pRRE, pRSV/Rev, pMD2.G, Lipofectamine LTX, and 1.5 mL Opti-MEM. The supernatants were collected after 48 hours after transfection. 3T3-L1 cells were transduced with lentivirus stock in complete media containing 10 μg/mL polybrene for 12 hours, replaced with fresh complete medium

Luciferase Reporter Assay

To quantitatively evaluate miRNA activity on cloned miRNA target sequence from 3'-untranslated region (3'-UTR) of *Ddit4*, pmirGLO dual luciferase miRNA Target expression vector (E1330, Promega) was used. Firstly, the pmirGLO plasmid was linearized by double digestion with *Xho*I and *Sal*I. The cDNA of *Ddit4* wild type (WT) 3′-UTR was amplified by PCR and ligated with CIP treated pmirGLO Vector. The primers are Forward-*Xho*I-3'UTR-*Ddit4*: 5'-GGG GGG CTC GAG CAG CTG CTC ATT GAA GAG TG-3′, and Reverse-*Sal*I-3'UTR-*Ddit4*: 5'-GGG GGG GTCGAC CAA ACC AAC AGA GGA GAC AG-3′. pmirGLO-*Ddit4* MT 3'-UTR was prepared by site directed mutagenesis by PCR using primers; Forward-MT-Seed-*Ddit4*: 5'-CTG GAT GTG TAT CTG CAT GTA C-3' and Reverse-MT-Seed-*Ddit4*: 5'-GTA CAT GCA GAT ACA CAT CCA G-3'. The seed sequence "CGATGTA" was mutated to "CGTCTA". After transformation to *E. coli* JM109 cells, pmirGLO-*Ddit4* WT 3'-UTR, pmirGLO-*Ddit4* MT 3'-UTR, and pmirGLO no-insert control plasmids were isolated with EndoFree Plasmid Maxi Kit (12362, Qiagen). 3T3-L1 cells were seeded at a density of

120,000 cells/mL, then co-transfected with Syn-mmu-miR-221-3p (MIMAT0000669, Qiagen), Syn-mmu-miR-222-3p (MIMAT0000670, Qiagen), negative control siRNA (1027280, Qiagen), inhibitor negative control (1027271, Qiagen), pmirGLO-*Ddit4* WT 3'-UTR, pmirGLO-*Ddit4* MT 3'-UTR, and pmirGLO no-insert control plasmids. Twenty-four hours after transfection, the cells were analyzed to measure luciferase activities using the Dual-Glo Luciferase Assay System and a GloMax 20/20 luminometer (Promega).

Statistical Analysis

All values were represented as the mean ± standard deviation (SD). Statistical analyses were conducted using IBM SPSS Statistics 23 and GraphPad Prism (version 8.0). Independent *t*-test, Mann-Whitney's U test, and one-way ANOVA with Tukey test was used to determine the differences. For correlation, non-parametric Spearman r coefficient was used. $p<0.05$ was considered statistically significant.

RESULTS

Mir221/222AdipoKO mice are resistant to diet-induced obesity

To identify miRNAs critically involved in the disease process of obesity and type 2 diabetes (T2D), we performed miRNA profiling of serum, liver and epididymal fat tissues in C57BL/6JJcl mice fed with standard (STD) and high fat-high sucrose (HFHS) chow. The Illumina RNA sequencing data (Gene Expression Omnibus number GSE61959) demonstrated that the read numbers of *Mir221* and *Mir222* were 5.7 and 8.2-fold up-regulated in epididymal adipose tissues in HFHS group compared with STD group (**Supplementary Table 2**). *Mir221* and *Mir222* are paralog genes located in proximity on X chromosome and they share identical seed sequence. To further investigate the role of *Mir221/222* in obesity and diabetes, we crossed male Tg (Adipoq-cre) mice and female *Mir221*$^{tm2/y}$ C57BL/6JJcl mice and generated male *Mir221/222*$^{flox/y}$ and male *Mir221/222AdipoKO* littermates.

Body weight of *Mir221/222AdipoKO* mice fed with HFHS chow was significantly reduced compared with *Mir221/222*$^{flox/y}$ mice (**Figure 1A**). The weight of epididymal, mesenteric, subdermal, and brown fat was also reduced in *Mir221/222AdipoKO* mice (**Figure 1B**). The *Mir221/222*$^{flox/y}$ and *Mir221/222AdipoKO* mice fed with STD chow demonstrated no significant differences in their body and tissue weight (**Figure 1A and 1B**). The average size of adipocytes in epididymal adipose tissues derived from *Mir221/222AdipoKO* mice fed with HFHS chow was smaller compared with *Mir221/222*$^{flox/y}$ mice (**Figure 1C**). To investigate glucose homeostasis, we performed insulin tolerance test (ITT) and glucose tolerance test (GTT). The blood glucose levels of *Mir221/222AdipoKO* mice fed with HFHS chow were reduced in GTT and ITT compared with *Mir221/222*$^{flox/y}$, but they did not reach significant differences (**Figure 1D**). The serum insulin concentrations of *Mir221/222AdipoKO* mice were significantly lower than *Mir221/222*$^{flox/y}$, suggesting the improvement of insulin sensitivity in *Mir221/222AdipoKO* mice (**Figure 1D**). To investigate whether reduced adiposity in *Mir221/222AdipoKO* mice was due to changes in energy expenditure or energy intake, we measured basal metabolic rates, locomotor activity and food intake. Basal metabolic rate such as respiratory quotient and oxygen consumption were not altered between *Mir221/222*$^{flox/y}$ and *Mir221/222AdipoKO* mice fed with HFHS chow (**Supplementary Figure 1A and 1B**). The locomotor activity was recorded for 24 hours, most of the activities were observed during the dark phase. Increased activity was observed in *Mir221/222AdipoKO* mice under HFHS chow compared with *Mir221/222*$^{flox/y}$ during light (0.944 ± 0.309 vs 1.60 ± 0.764 counts/min, p=0.036) and dark (6.67 ± 4.38 *vs* 7.94 ± 4.38 counts/min, p=0.497) periods (**Supplementary Figure 1C**). Food consumption were not altered in *Mir221/222AdipoKO* and *Mir221/222*$^{flox/y}$ fed with HFHS (**Supplementary Figure 1D**). Under HFHS chow, serum leptin concentrations were significantly reduced in *Mir221/222AdipoKO* compared with *Mir221/222*$^{flox/y}$ (24.5 ± 2.35 *vs* 21.5 ± 1.85 ng/ml, p=0.043), while serum adiponectin concentrations were not altered (**Supplementary Figure 1E and 1F**). In quantitative RT-PCR in epididymal adipose

tissues, mRNA expression of *Lep* was significantly reduced in *Mir221/222AdipoKO*. The genes related to adipogenesis, such as *Pparg*, *Cebpa*, *Ppargc1* and *Prdm16*, were not altered in *Mir221/222AdipoKO* (**Supplementary Figure 2**).

Expression *Mir221* and *Mir222* are highly induced by HFHS chow feeding in mature adipocytes from epididymal adipose tissue

We investigated the expression of *Mir221* and *Mir222* in various organs. Both miR-221-3p and miR-222-3p were abundantly expressed in brain, kidney, and lung in *Mir221/222*$^{flox/y}$ and they were down-regulated or not altered by the HFHS feeding compared with STD chow. In contrast, both miR-221-3p and miR-222-3p were significantly upregulated in the epididymal fat tissues, and such upregulation was canceled in the epididymal fat tissues of *Mir221/222AdipoKO* fed with HFHS chow (**Figure 2A and 2B**). Next, we investigated the localization of *Mir221* and *Mir222* in the cell fractions of epididymal adipose tissues. Both miR-221-3p and miR-222-3p were significantly induced by HFHS chow in mature adipocytes of *Mir221/222*$^{flox/y}$, while the upregulation was significantly reversed in the mature adipocyte of *Mir221/222AdipoKO* fed with HFHS chow. In contrast, miR-221-3p and miR-222-3p were not significantly upregulated in the stromal vascular fraction (SVF) from *Mir221/222*$^{flox/y}$ fed with HFHS chow (**Figure 2C**). We also assessed the expression of miR-221-3p and miR-222-3p during 3T3-L1 adipocyte differentiation. Both miR-221-3p and miR-222-3p continuously down-regulated after the induction of adipocyte differentiation (**Supplementary Figure 3A**). Finally, we assessed the serum concentrations of mmu-miR-221-3p and mmu-miR-222-3p by quantitative PCR and they were not altered in *Mir221/222*$^{flox/y}$ and *Mir221/222AdipoKO* fed with STD and HFHS chow, suggesting serum mature forms of *Mir221* and *Mir222* were derived from various organs but not exclusively from adipose tissues (**Supplementary Figure 4A**). In human samples from the subjects with normal glucose tolerance (NGT, n=45) and impaired glucose tolerance (IGT, n=69), hsa-miR-221-3p and hsa-miR-222-3p demonstrated negative (R^2=0.1311, p<0.0001) and

positive correlations (R2=0.03841, p=0.0441) with HbA1c levels, respectively (**Supplementary Figure 4B and 4C**).

Identification of *Mir221hg* and its expression

The miRNA genes are classified as intergenic and intragenic miRNAs, and the intragenic miRNAs and related host genes share the common transcriptional regulation. The long non-coding RNA (lncRNA), namely mir-221 host gene (MIR221HG), has been reported in bovine, which inhibits the adipocyte differentiation in cultured cells(11). Thus, we performed 5' and 3' rapid amplification of cDNA ends (5'/3'RACE) using poly A^+ RNA purified from epididymal fat tissues of C57BL/6JJcl mice and cloned 1537 bp single exon lncRNA (*Mir221hg*, MW581002) which overlap *Mir221* (**Supplementary Figure 5A**). Next, we designed primers for quantitative PCR of *Mir221hg* and evaluated gene expression in various tissue. *Mir221hg* was abundantly expressed in brain in *Mir221/222*$^{flox/y}$ and they were upregulated in brain, heart, liver, intestine, spleen by the HFHS feeding compared with STD chow. The expression of *Mir221hg* was rather low in various adipose tissues and its lncRNA expression was not changed in *Mir221/222AdipoKO* fed with STD and HFHS chow (**Supplementary Figure 5B and 5C**). Although *Mir221hg* lncRNA may be functional as a reservoir for miR-221-3p, the role of *Mir221hg* lncRNA in adipose tissues was limited in our experiments.

miR-221-3p and miR-222-3p target *Ddit4*

To investigate the mechanism for the resistance to diet-induced obesity in *Mir221/222AdipoKO*, we attempted to identify the potential target genes for miR-221-3p and miR-222-3p. We performed mRNA profiling by GeneChip Mouse Gene 2.0 array using total RNA purified from epididymal fat tissues of *Mir221/222*$^{flox/y}$ fed with STD or HFHS, *Mir221/222AdipoKO* fed with STD or HFHS chow (**Supplementary Table 3, 4 and 5**). Then, we made the list of 355 target genes commonly predicted by TargetScan, miRDB,

and DIANA-microT, and their seed sequences were conserved in both human and mouse genome (**Supplementary Table 6**). By searching upregulated genes in *Mir221/222AdipoKO* compared with *Mir221/222*$^{flox/y}$ in both STD and HFHS fed groups, we identified that DNA-damage-inducible transcript 4 (*Ddit4*) demonstrated 1.9-fold and 2.58-fold upregulation in *Mir221/222AdipoKO* fed with HFHS and STD chow, respectively (**Supplementary Table 7**). To evaluate miRNA activity of miR-221-3p and miR-222-3p by the binding to 3'-untranslated region (3'-UTR) of *Ddit4*, we performed luciferase reporter assay in 3T3-L1 cells. We cloned 3'-UTR regions of *Ddit4* gene and prepared the wild-type reporter vector, pmirGLO-*Ddit4* WT 3'-UTR, and the mutant vector, pmirGLO-*Ddit4* MT 3'-UTR, in which mutagenesis was induced on the seed sequence binding site (**Figure 3A**). The luciferase reporter vectors were co-transfected with Syn-mmu-miR-221-3p or Syn-mmu-miR-222-3p or negative control siRNA in 3T3-L1 cells. As a result, reporter activity of pmirGLO-*Ddit4* WT 3'-UTR were significantly inhibited in the presence of both Syn-mmu-miR-221-3p and Syn-mmu-miR-222-3p. In contrast, Syn-mmu-miR-221-3p or Syn-mmu-miR-222-3p had almost no effect on the reporter activity of pmirGLO-*Ddit4* MT 3'-UTR (**Figure 3A**). Next, we checked the expression of *Ddit4* in the epididymal adipose tissues of *Mir221/222*$^{flox/y}$ and *Mir221/222AdipoKO* fed with HFHS by quantitative PCR and Western blot. Although the mRNA expression of *Ddit4* was increased in *Mir221/222AdipoKO* without statistical significance, DDIT4 protein expression was significantly upregulated in the *Mir221/222AdipoKO* compared with *Mir221/222*$^{flox/y}$ (**Figure 3B**), suggesting the possible involvement of translational repression by miR-221-3p and miR-222-3p.

miR-221/222 promotes adipogenesis by *DDIT4*-mediated inhibition of mTORC1

DDIT4 is known to activate tuberous sclerosis complex 1 (TSC1)/TSC2 complex by the inhibition of AKT (protein kinase B) and the release of 14-3-3 from TSC2(12). It further negatively regulates mammalian target of rapamycin complex 1 (mTORC1) (13). Increased activity of the mTORC1 signaling has been associated with obesity(14), and the knockout

mice for the mTORC1 downstream ribosomal protein S6 kinase (S6K) are protected against diet-induced-obesity(15). Thus, we further checked the inactivated form of p-TSC2 (Thr-1462) and activated form of p-S6K(16) in the epididymal adipose tissues of *Mir221/222*$^{flox/y}$ and *Mir221/222AdipoKO*. After overnight fasting, the mice were injected intraperitoneally with insulin and the epididymal fat tissues were harvested at 7 min after insulin injection. In *Mir221/222AdipoKO* mice, both p-AKT and p-TSC2 (Thr-1462) were significantly reduced, and accordingly p-S6K was also significantly reduced (**Figure 4A and 4B**). p-mTOR was reduced in *Mir221/222AdipoKO* mice, however, it did not reach the statistically significant differences (**Figure 4A and 4B**).

Since mTOR has been shown to positively regulate adipogenesis and lipogenesis while inhibiting lipolysis, fatty acid oxidation and ketogenesis(17), we performed adipogenesis and glycerol assays in 3T3-L1 adipocytes. We constructed lentiviral vector expressing miRNA inhibitors (pLV-locker 221, pLV-locker 222, pLV-locker control) and miRNA mimics (pLV 221, pLV 222, pLV control). The efficiency for inhibitors and mimics was confirmed in 3T3-L1 cells at 3-7 days after the transduction (**Supplementary Figure 3B and 3C**). Lentiviral vectors were transduced to 3T3-L1 cells at 2 days before the induction of differentiation and cultured for 7 days. The pLV-locker 221, pLV-locker 222, and pLV-locker 221/222 did not alter the accumulation of lipid droplets demonstrated by oil red O staining measured by absorbance at 490 nm (**Figure 5A**). Similarly, pLV 221, pLV 222, and pLV221/222 only show slight increase in the accumulation of lipid droplets in 3T3-L1 cells without statistical significance (**Figure 5B**). Western blot analysis demonstrated that the expression of C/EBPα and PPARγ were not changed by pLV-locker 221 and pLV-locker 222 (**Figure 5C**), while they were significantly up-regulated by treatment with pLV 221 and pLV 222 (**Figure 5D**). To investigate lipolysis, lentiviral vectors were transduced to the fully differentiated 3T3-L1 adipocyte and we performed glycerol assay 7 days after lentiviral transduction. pLV-locker 221/222 and pLV 221/222 did not alter the glycerol release (**Figure 5E**).

DISCUSSION

The adipocyte-specific inhibition of *Mir221/Mir222* expression protected the mice fed with HFHS chow from the obesity. We demonstrated that the direct target of miR-221-3p and miR-222-3p was *Ddit4* and the inhibition of *Mir221/Mir222* expression resulted in upregulation of DDIT4, inactivation of AKT, activation of TSC2 and subsequent inactivation of S6K, the latter is a major target of mTORC1. The lentivirus-mediated transfer of *Mir222* gene promoted the adipogenesis demonstrated by up-regulation of C/EBPα and PPARγ in differentiated 3T3-L1 cells. We concluded that the inhibition of miR-221-3p and miR-222-3p and DDIT4-mediated inhibition of mTORC1 signaling is one of the major mechanisms for the protection from diet-induced obesity. The role of *Mir221* in adipogenesis has been focused by series of investigation and Ahonen et al. reported miR-221-3p overexpression in Simpson-Golabi-Behmel syndrome (SGBS) preadipocytes inhibited *de novo* lipogenesis and adipogenesis(18). In our investigation, overexpression by pLV 221 did not alter the lipogenesis and adipogenesis in 3T3-L1 cells; however, pLV 222 enhanced the adipogenesis. In bovine adipocyte differentiation, long non-coding RNA (lncRNA), *MIR221HG*, significantly increased adipocyte differentiation associated with dramatic increment of PPARγ(11). We also cloned mouse *Mir221hg* with 1,537 bp and identified that 1,054 bp of 5'-flanking region was deleted in *Mir221/222AdipoKO* mice. The expression of *Mir221hg* is barely detected in brown and WATs in wild type mice and we speculated that the influence of deletion of *Mir221hg* is minimal in *Mir221/222AdipoKO* mice. Although the functional studies to elucidate the role of *Mir222* in adipogenesis and lipogenesis were not reported in cultured adipocytes in previously published studies, we demonstrated that *Mir222* expression was upregulated in WATs and serum in both obese patients. The importance of *Mir222* in the pathogenesis of obesity is supported by the analysis of adipose tissue-specific Dicer knockout mice, in which gonadal adipose tissue was the main source of serum exosomal miR-222(19). The exosome-packed *Mir222* influenced remote organs,

and overexpression of *Mir222* inhibits the expression of IRS-1 by directly binding to untranslated regions in the muscle(20) and liver(21). In current investigation, we firstly demonstrated that overexpression of *Mir222* enhanced mTORC1 pathway and promoted the adipogenesis in 3T3-L1 cells.

Under the presence of amino acids, mTORC1 is activated by GTP-bound Rheb. In the upstream of the Rheb, AKT inhibits TSC2 and TBC1D7 (TBC1 Domain Family Member 7) complex, which further inhibits the activation of mTORC1 by acting as a GTPase-activating protein. mTORC1 promotes the lipid synthesis and storage and adipogenesis, while it inhibits the lipolysis, β-oxidation and ketogenesis. SREBP (sterol regulatory element-binding protein) processing and activation is promoted by mTORC1 by the activation of S6K and lipin 1 leading to transcriptional activation of SREPB1, SREBP2, and many other lipogenic genes. mTORC1 also committed mesenchymal stem cells to adipocyte lineage by the activation of S6K, promotes the initial step of adipocyte differentiation by inhibiting 4E-BP1/2 (eIF4E-binding protein 1/2), and completes the final differentiation by the activation of PPARγ(22). Many researchers screened the agents or intrinsic factors to inhibit mTORC1 signaling and lipogenesis for the treatment of obesity. Lee et al. reported that ezetimibe reduced lipid accumulation by inhibiting mTORC1 signaling, leading to the downregulation of lipogenesis-related genes(23). Shi et al. reported that the inhibition of miR-196b-5p blocked adipogenesis and lipogenesis by directly targeting TSC1 and TGFBR1 (transforming growth factor-β receptor 1)(24). We demonstrated that the inhibition of miR-221-3p and miR-222-3p and subsequent DDIT4-mediated inhibition of mTORC1 signaling is a therapeutic target for the treatment of obesity.

The activation of mTORC1 links to various pathological processes in adipose tissues such as inflammation, beige adipogenesis and angiogenesis. mTORC1 loss and gain of function studies in macrophages resulted in amelioration and exacerbation of inflammatory response, as well as macrophage polarization to both M1 and M2 profiles(25). miR-221 mediates M1 macrophage polarization(26, 27), while suppression of miR-222 alleviate the

462 inflammatory response(28, 29). However, we did not observe the apparent changes in
463 gene expression of cytokines such as *Il1b*, *Il6*, *Ifng*, and *Tnf* in adipose tissues in
464 *Mir221/222AdipoKO* mice (**Supplementary Figure 2**). The phenotyping of T cells and
465 macrophages in WATs should be performed in the future investigation. In beige
466 adipogenesis, the adipose-specific deletion of Raptor, a key component of mTORC1,
467 promoted beige adipogenesis by inhibiting prostaglandins (PGs) synthesized by
468 cyclooxygenase-2 (COX-2)(30). Supporting this notion, ketoprofen alleviated diet-induced
469 obesity and promotes the fat browning by the COX-2 and mTORC1-p38 signaling
470 pathway(31). In our investigation, the genes related to beige adipogenesis such as *Ppargc1*
471 and *Prdm16* tended to be upregulated in WATs without statistical differences. However, in
472 WATs in *Mir221/222AdipoKO* mice, apparent beige adipogenesis was not observed by
473 histological examinations. In tumor microenvironment and angiogenesis, mTORC1 under a
474 hypoxic condition promotes the translation of hypoxia-inducible factor (HIF) 1-2, which lead
475 to the expression of angiogenic growth factors such as vascular endothelial growth factor
476 (VEGF), TGF-α, and platelet-derived growth factor β (PDGF-β)(32). *Mir221* and *Mir222*
477 demonstrated the angiogenic activities in vascular cells(33) and cancers(34), however, we
478 did not observe the angiogenesis activities in WATs in *Mir221/222AdipoKO* mice.
479
480 **Limitation of Study**
481 We hypothesized that circulating miR-221-3p and miR-222-3p play important roles in both
482 mouse obese models and the patients with obesity and T2D. However, the circulating
483 levels of miR-221-3p and miR-222-3p were not altered in *Mir221/222*$^{flox/y}$ and
484 *Mir221/222AdipoKO* mice fed with STD and HFHS. In addition, the human serum levels of
485 miR-221-3p and miR-222-3p showed correlations with HbA1c, however, they did not show
486 significant correlations with body weight and BMI. Although we show the roles of miR-221-
487 3p and miR-222-3p in the adipocytes, we did not clearly demonstrate the role of circulating
488 miR-221-3p and miR-222-3p in the pathogenesis of obesity. Another limitation is that it is

still unknown why *Mir221/222AdipoKO* mice did not show significant improvement of insulin sensitivity although the body weight was significantly reduced compared with *Mir221/222*$^{flox/y}$ fed with HFHS. Finally, the micronutrient composition is not matched between the STD and HFHS diets and it may possibly impact the observed outcomes. Ideally, a matched diet should be used for mineral and vitamin mix.

DATA AVAILABILITY

RNA sequencing and mRNA microarray data generated in this study is available at GEO: GSE61959 and GSE163921.

ETHICS STATEMENT

All animal experiments were approved by the Animal Care and Use Committee of the Department of Animal Resources, Advanced Science Research Center, Okayama University (OKU-2015547, 2016201, 2016202, 2018479, 2018480, and 2018481). The observational clinical study was approved by Okayama University Graduate School of Medicine, Dentistry and Pharmaceutical Sciences and Okayama University Hospital, Ethics Committee (#1708-045).

CONFLICT OF INTEREST

Jun Wada receives speaker honoraria from Astra Zeneca, Daiichi Sankyo, Novartis, Novo Nordisk Pharma, Tanabe Mitsubishi and receives grant support from Astellas, Baxter, Bayer, Chugai, Dainippon Sumitomo, Kyowa Kirin, Novo Nordisk Pharma, Ono, Otsuka, Tanabe Mitsubishi, and Teijin.

Author contributions

SY, DZ, AK, and JW designed the project and experiments and wrote the manuscript. SY, DZ, AK, NK, RS, and HHHA performed animal experiments and analyzed and interpreted

data. AN and JE performed culture and molecular biology experiments. SY, AK, NK, RS, AN, JE, and JW designed and performed clinical study.

FUNDING

This work was supported by Grant-in-Aid for Young Scientists (19K17984), Grant-in-Aid for Scientific Research (B) (19H03675), Japan Agency for Medical Research and development (AMED, grant no: 17ek0210095h0001, 20ek0109445h0001).

ACKNOWLEDGEMENTS

We acknowledge support from Central Research Laboratory, Okayama University Medical School; usage of BECKMAN COULTER XL 80, ABI PRISM3130, and producing paraffin blocks and sections.

SUPPLEMENTARY MATERIAL

The supplementary Material for this article can be found online.

References

1. Kahn CR, Wang G, Lee KY. Altered adipose tissue and adipocyte function in the pathogenesis of metabolic syndrome. *J Clin Invest.* (2019) 129:3990-4000. doi: 10.1172/JCI129187
2. Huang Z, Xu A. Adipose Extracellular Vesicles in Intercellular and Inter-Organ Crosstalk in Metabolic Health and Diseases. *Front Immunol.* (2021) 12:608680. doi: 10.3389/fimmu.2021.608680
3. Pan Y, Hui X, Hoo RLC, Ye D, Chan CYC, Feng T, et al. Adipocyte-secreted exosomal microRNA-34a inhibits M2 macrophage polarization to promote obesity-induced adipose inflammation. *J Clin Invest.* (2019) 129:834-49. doi: 10.1172/JCI123069
4. Fu T, Seok S, Choi S, Huang Z, Suino-Powell K, Xu HE, et al. MicroRNA 34a inhibits beige and brown fat formation in obesity in part by suppressing adipocyte fibroblast growth factor 21 signaling and SIRT1 function. *Mol Cell Biol.* (2014) 34:4130-42. doi: 10.1128/MCB.00596-14

5. Wang L, Sinnott-Armstrong N, Wagschal A, Wark AR, Camporez JP, Perry RJ, et al. A MicroRNA Linking Human Positive Selection and Metabolic Disorders. *Cell.* (2020) 183:684-701 e14. doi: 10.1016/j.cell.2020.09.017
6. Qi R, Wang J, Wang Q, Qiu X, Yang F, Liu Z, et al. MicroRNA-425 controls lipogenesis and lipolysis in adipocytes. *Biochim Biophys Acta Mol Cell Biol Lipids.* (2019) 1864:744-55. doi: 10.1016/j.bbalip.2019.02.007
7. Higuchi C, Nakatsuka A, Eguchi J, Teshigawara S, Kanzaki M, Katayama A, et al. Identification of circulating miR-101, miR-375 and miR-802 as biomarkers for type 2 diabetes. *Metabolism.* (2015) 64:489-97. doi: 10.1016/j.metabol.2014.12.003
8. Deiuliis JA. MicroRNAs as regulators of metabolic disease: pathophysiologic significance and emerging role as biomarkers and therapeutics. *Int J Obes (Lond).* (2016) 40:88-101. doi: 10.1038/ijo.2015.170
9. Villard A, Marchand L, Thivolet C, Rome S. Diagnostic Value of Cell-free Circulating MicroRNAs for Obesity and Type 2 Diabetes: A Meta-analysis. *J Mol Biomark Diagn.* (2015) 6. doi: 10.4172/2155-9929.1000251
10. Nakagawa Y, Ishimura K, Oya S, Kamino M, Fujii Y, Nanba F, et al. Comparison of the sympathetic stimulatory abilities of B-type procyanidins based on induction of uncoupling protein-1 in brown adipose tissue (BAT) and increased plasma catecholamine (CA) in mice. *PLoS One.* (2018) 13:e0201203. doi: 10.1371/journal.pone.0201203
11. Li M, Gao Q, Tian Z, Lu X, Sun Y, Chen Z, et al. MIR221HG Is a Novel Long Noncoding RNA that Inhibits Bovine Adipocyte Differentiation. *Genes (Basel).* (2019) 11. doi: 10.3390/genes11010029
12. Britto FA, Dumas K, Giorgetti-Peraldi S, Ollendorff V, Favier FB. Is REDD1 a metabolic double agent? Lessons from physiology and pathology. *Am J Physiol Cell Physiol.* (2020) 319:C807-C24. doi: 10.1152/ajpcell.00340.2020
13. Tirado-Hurtado I, Fajardo W, Pinto JA. DNA Damage Inducible Transcript 4 Gene: The Switch of the Metabolism as Potential Target in Cancer. *Front Oncol.* (2018) 8:106. doi: 10.3389/fonc.2018.00106
14. Khamzina L, Veilleux A, Bergeron S, Marette A. Increased activation of the mammalian target of rapamycin pathway in liver and skeletal muscle of obese rats: possible involvement in obesity-linked insulin resistance. *Endocrinology.* (2005) 146:1473-81. doi: 10.1210/en.2004-0921
15. Yu R, Li Z, Liu S, Huwatibieke B, Li Y, Yin Y, et al. Activation of mTORC1 signaling in gastric X/A-like cells induces spontaneous pancreatic fibrosis and derangement of glucose metabolism by reducing ghrelin production. *EBioMedicine.* (2018) 36:304-15. doi: 10.1016/j.ebiom.2018.09.027

16. Manning BD, Tee AR, Logsdon MN, Blenis J, Cantley LC. Identification of the tuberous sclerosis complex-2 tumor suppressor gene product tuberin as a target of the phosphoinositide 3-kinase/akt pathway. *Mol Cell.* (2002) 10:151-62. doi: 10.1016/s1097-2765(02)00568-3
17. Pena-Leon V, Perez-Lois R, Seoane LM. mTOR Pathway is Involved in Energy Homeostasis Regulation as a Part of the Gut-Brain Axis. *Int J Mol Sci.* (2020) 21. doi: 10.3390/ijms21165715
18. Ahonen MA, Asghar MY, Parviainen SJ, Liebisch G, Horing M, Leidenius M, et al. Human adipocyte differentiation and composition of disease-relevant lipids are regulated by miR-221-3p. *Biochim Biophys Acta Mol Cell Biol Lipids.* (2021) 1866:158841. doi: 10.1016/j.bbalip.2020.158841
19. Li D, Song H, Shuo L, Wang L, Xie P, Li W, et al. Gonadal white adipose tissue-derived exosomal MiR-222 promotes obesity-associated insulin resistance. *Aging (Albany NY).* (2020) 12:22719-43. doi: 10.18632/aging.103891
20. de Mendonca M, de Sousa E, da Paixao AO, Araujo Dos Santos B, Roveratti Spagnol A, Murata GM, et al. MicroRNA miR-222 mediates pioglitazone beneficial effects on skeletal muscle of diet-induced obese mice. *Mol Cell Endocrinol.* (2020) 501:110661. doi: 10.1016/j.mce.2019.110661
21. Ono K, Igata M, Kondo T, Kitano S, Takaki Y, Hanatani S, et al. Identification of microRNA that represses IRS-1 expression in liver. *PLoS One.* (2018) 13:e0191553. doi: 10.1371/journal.pone.0191553
22. Epstein Y, Seidman DS, Moran D, Arnon R, Arad M, Varssano D. Heat-exercise performance of pyridostigmine-treated subjects wearing chemical protective clothing. *Aviat Space Environ Med.* (1990) 61:310-3. doi:
23. Lee YS, Park JS, Lee DH, Han J, Bae SH. Ezetimibe ameliorates lipid accumulation during adipogenesis by regulating the AMPK-mTORC1 pathway. *FASEB J.* (2020) 34:898-911. doi: 10.1096/fj.201901569R
24. Shi Y, Li F, Wang S, Wang C, Xie Y, Zhou J, et al. miR-196b-5p controls adipocyte differentiation and lipogenesis through regulating mTORC1 and TGF-beta signaling. *FASEB J.* (2020) 34:9207-22. doi: 10.1096/fj.201901562RR
25. Festuccia WT. Regulation of Adipocyte and Macrophage Functions by mTORC1 and 2 in Metabolic Diseases. *Mol Nutr Food Res.* (2021) 65:e1900768. doi: 10.1002/mnfr.201900768
26. Cai M, Shi Y, Zheng T, Hu S, Du K, Ren A, et al. Mammary epithelial cell derived exosomal MiR-221 mediates M1 macrophage polarization via SOCS1/STATs to promote inflammatory response. *Int Immunopharmacol.* (2020) 83:106493. doi: 10.1016/j.intimp.2020.106493

27. Quero L, Tiaden AN, Hanser E, Roux J, Laski A, Hall J, et al. miR-221-3p Drives the Shift of M2-Macrophages to a Pro-Inflammatory Function by Suppressing JAK3/STAT3 Activation. *Front Immunol.* (2019) 10:3087. doi: 10.3389/fimmu.2019.03087
28. Zhang H, Luan S, Xiao X, Lin L, Zhao X, Liu X. Silenced microRNA-222 suppresses inflammatory response in gestational diabetes mellitus mice by promoting CXCR4. *Life Sci.* (2021) 266:118850. doi: 10.1016/j.lfs.2020.118850
29. Zhang Y, Yang J, Zhou X, Wang N, Li Z, Zhou Y, et al. Knockdown of miR-222 inhibits inflammation and the apoptosis of LPS-stimulated human intervertebral disc nucleus pulposus cells. *Int J Mol Med.* (2019) 44:1357-65. doi: 10.3892/ijmm.2019.4314
30. Zhang X, Luo Y, Wang C, Ding X, Yang X, Wu D, et al. Adipose mTORC1 Suppresses Prostaglandin Signaling and Beige Adipogenesis via the CRTC2-COX-2 Pathway. *Cell Rep.* (2018) 24:3180-93. doi: 10.1016/j.celrep.2018.08.055
31. Kang NH, Mukherjee S, Jang MH, Pham HG, Choi M, Yun JW. Ketoprofen alleviates diet-induced obesity and promotes white fat browning in mice via the activation of COX-2 through mTORC1-p38 signaling pathway. *Pflugers Arch.* (2020) 472:583-96. doi: 10.1007/s00424-020-02380-7
32. Conciatori F, Bazzichetto C, Falcone I, Pilotto S, Bria E, Cognetti F, et al. Role of mTOR Signaling in Tumor Microenvironment: An Overview. *Int J Mol Sci.* (2018) 19. doi: 10.3390/ijms19082453
33. Poliseno L, Tuccoli A, Mariani L, Evangelista M, Citti L, Woods K, et al. MicroRNAs modulate the angiogenic properties of HUVECs. *Blood.* (2006) 108:3068-71. doi: 10.1182/blood-2006-01-012369
34. Xu CH, Liu Y, Xiao LM, Chen LK, Zheng SY, Zeng EM, et al. Silencing microRNA-221/222 cluster suppresses glioblastoma angiogenesis by suppressor of cytokine signaling-3-dependent JAK/STAT pathway. *J Cell Physiol.* (2019) 234:22272-84. doi: 10.1002/jcp.28794

FIGURE LEGENDS

Figure 1. The metabolic phenotypes of *Mir221/222*$^{flox/y}$ and *Mir221/222AdipoKO* male mice fed with high fat high sucrose (HFHS) or standard (STD) chow. (**A**) Body weight of *Mir221/222*$^{flox/y}$ and *Mir221/222AdipoKO* mice fed with HFHS (n=7) or STD chow (n=6), respectively. (**B**) Tissue weight of *Mir221/222*$^{flox/y}$ and *Mir221/222AdipoKO* mice fed with HFHS or STD chow at 24 weeks of age. (Epi, epididymal; Mes, mesenteric; Sub, inguinal; Brown, Brown adipose tissues) (**C**) Adipocyte area in epididymal adipose tissues of *Mir221/222*$^{flox/y}$ (n=3) and *Mir221/222AdipoKO* (n=5) mice fed with HFHS or STD.

Quantitative analyses were carried out on PAS-stained paraffin sections. (**D**) Insulin tolerance test (ITT) and glucose tolerance test (GTT) in mice fed with HFHS (n=7) or STD chow (n=6). Data shown as mean ± SD and analyzed by one-way ANOVA with Tukey test in **A** and **B**, and Mann-Whitney's U test in **C** and **D** (*p<0.05; **p<0.01; ***p<0.001; ****p<0.0001).

Figure 2. Expression of Mir221 and Mir222 in *Mir221/222*$^{flox/y}$ and *Mir221/222AdipoKO* male mice fed with high fat high sucrose (HFHS) or standard (STD) chow. (**A and B**) In various tissues, the expression of miR-221-3p and miR-222-3p is normalized by snoRNA202 and snoRNA234. The HFHS-induced up-regulation of miR-221-3p and miR-222-3p in epididymal adipose tissues was reversed in *Mir221/222AdipoKO* (red asterisks). (Epi, epididymal; Mes, mesenteric; Sub, inguinal; Brown, Brown adipose tissues) (**C**) Serum concentration of miR-221-3p and miR-222-3p. HFHS *Mir221/222*$^{flox/y}$ (n=3), HFHS *Mir221/222AdipoKO* (n=5), STD *Mir221/222*$^{flox/y}$ (n=5) and STD *Mir221/222AdipoKO* mice (n=6). Data shown as mean ± SD and analyzed by one-way ANOVA with Tukey test (*p<0.05; **p<0.01; ***p<0.001; ****p<0.0001).

Figure 3. Dual-luciferase reporter assay for *Ddit4* 3'UTR and expression of *Ddit4* in mice. (**A**) Dual-luciferase reporter assay using pmirGLO-*Ddit4* WT 3'-UTR, pmirGLO-*Ddit4* MT 3'-UTR, and pmirGLO no-insert control plasmids. 3T3-L1 cells were co-transfected with Syn-mmu-miR-221-3p (n=4), Syn-mmu-miR-222-3p (n=4), negative control siRNA (n=8). (**B**) Quantitative RT-PCR for *Ddit4* in epididymal adipose tissues of *Mir221/222*$^{flox/y}$ (n=4) and *Mir221/222AdipoKO* (n=8) mice fed with high fat high sucrose (HFHS). Western blot analyses for DDIT4 and GAPDH (glyceraldehyde-3-phosphate dehydrogenase) in epididymal adipose tissues of *Mir221/222*$^{flox/y}$ (n=3) and *Mir221/222AdipoKO* (n=7) mice fed with high fat high sucrose (HFHS). Data shown as mean ± SD and analyzed by Mann-Whitney's U test (*p<0.05; **p<0.01).

Figure 4. Western blot analyses. (**A**) Western blot analyses for AKT (protein kinase B), TSC2 (tuberous sclerosis complex 2), mTOR (mammalian target of rapamycin) and S6K (ribosomal protein S6 kinase) in *Mir221/222*$^{flox/y}$ (n=3) and in epididymal adipose tissues of *Mir221/222AdipoKO* (n=5) male mice fed with high fat high sucrose (HFHS). Activated form of p-AKT and Inactivated form of p-TSC2 (Thr-1462) and activated form of p-S6K are shown. (**B**) Densitometric analyses of Western blots. Data shown as mean ± SD and analyzed by Mann-Whitney's U test (*p<0.05).

Figure 5. Adipogenesis, lipogenesis and lipolysis in 3T3-L1 cells. Lentiviral vectors were transduced to 3T3-L1 cells at 2 days before the induction of differentiation and cultured for 7 days. (**A**) Oil-red O staining of differentiated 3T3-L1 cells treated with pLV-locker control, pLV-locker 221, pLV-locker 222, and pLV-locker 221/222. (**B**) Oil-red O staining of differentiated 3T3-L1 cells treated with pVL control, pLV 221, pLV 222, and pLV221/222. (**C**) Western blot analysis of PPARγ in differentiated 3T3-L1 cells treated with pLV-locker control, pLV-locker 221, pLV-locker 222, and pLV-locker 221/222. (**D**) Western blot analysis of PPARγ in differentiated 3T3-L1 cells treated with pVL control, pLV 221, pLV 222, and pLV221/222. (**E**) Lipolysis assay in 3T3-L1 cells stimulated with isoproterenol. Differentiated 3T3-L1 cells were treated with pLV-locker 221/222 and pLV 221/222. Data shown as mean ± SD and analyzed by one-way ANOVA with Tukey test (*p<0.05; **p<0.01).

Figure 1

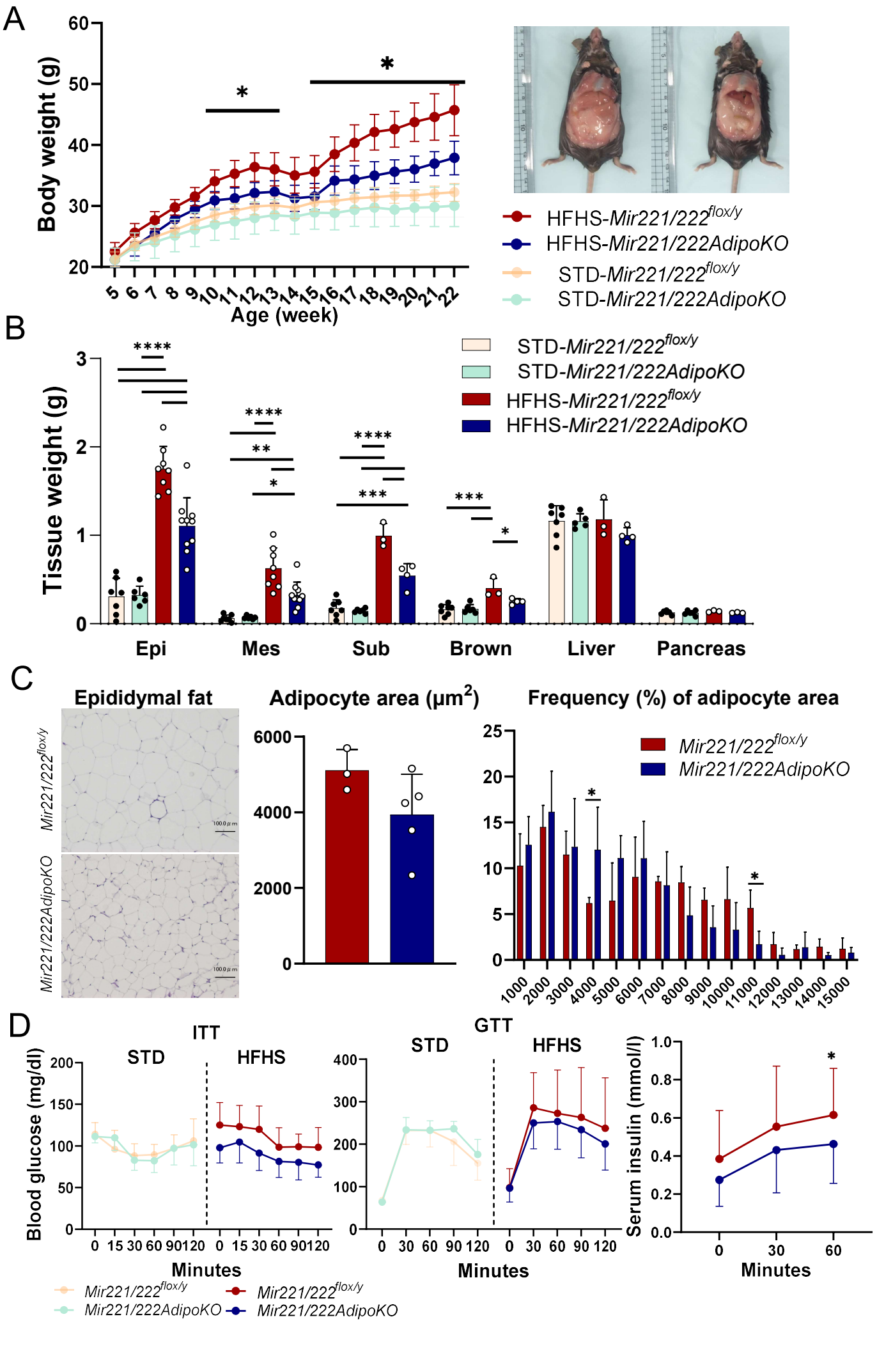
A
Body weight (g)
Age (week)
HFHS-Mir221/222flox/y
HFHS-Mir221/222AdipoKO
STD-Mir221/222flox/y
STD-Mir221/222AdipoKO
B
Tissue weight (g)
Epi
Mes
Sub
Brown
Liver
Pancreas
C
Epididymal fat
Adipocyte area (μm2)
Frequency (%) of adipocyte area
Mir221/222flox/y
Mir221/222AdipoKO
D
ITT
GTT
STD
HFHS
Blood glucose (mg/dl)
Minutes
Serum insulin (mmol/l)

Figure 2

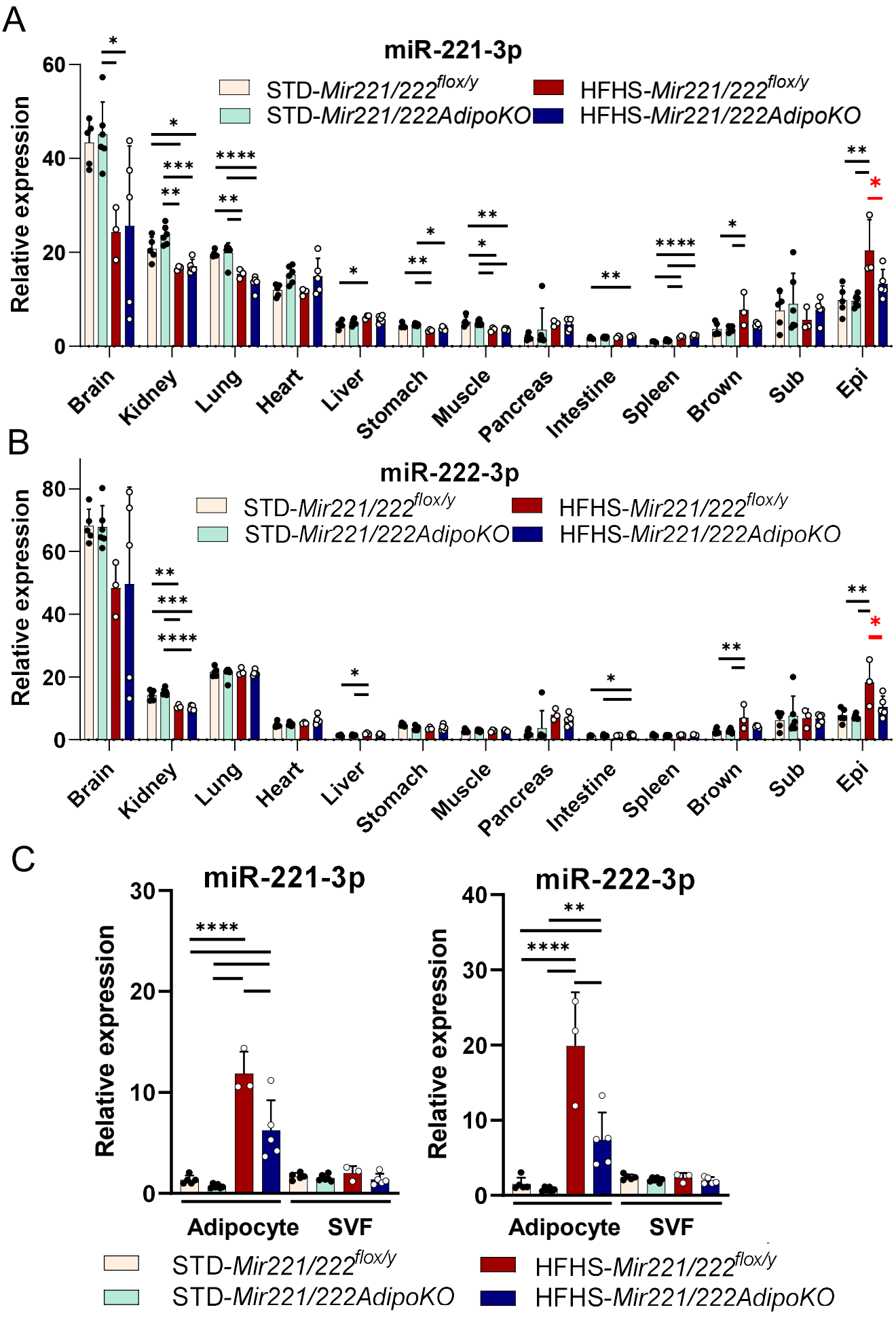
A
miR-221-3p
Relative expression
STD-Mir221/222flox/y
STD-Mir221/222AdipoKO
HFHS-Mir221/222flox/y
HFHS-Mir221/222AdipoKO
Brain
Kidney
Lung
Heart
Liver
Stomach
Muscle
Pancreas
Intestine
Spleen
Brown
Sub
Epi
B
miR-222-3p
C
miR-221-3p
miR-222-3p
Adipocyte
SVF

Figure 3

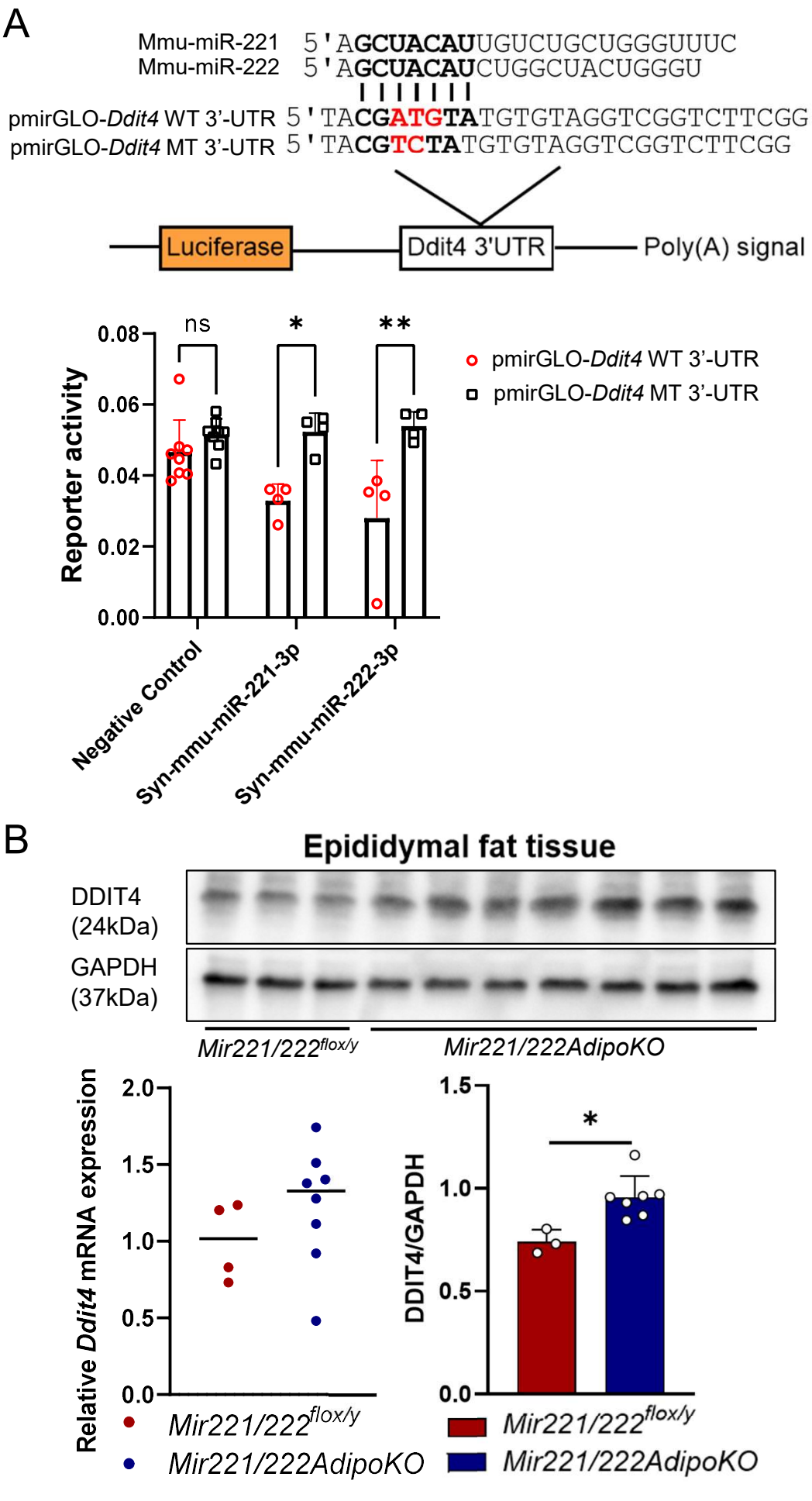
A
Mmu-miR-221 5'AGCUACAUUGUCUGCUGGGUUUC
Mmu-miR-222 5'AGCUACAUCUGGCUACUGGGU
pmirGLO-Ddit4 WT 3'-UTR 5'TACGATGTATGTGTAGGTCGGTCTTCGG
pmirGLO-Ddit4 MT 3'-UTR 5'TACGTCTATGTGTAGGTCGGTCTTCGG
Luciferase
Ddit4 3'UTR
Poly(A) signal
Reporter activity
0.08
0.06
0.04
0.02
0.00
ns
*
**
pmirGLO-Ddit4 WT 3'-UTR
pmirGLO-Ddit4 MT 3'-UTR
Negative Control
Syn-mmu-miR-221-3p
Syn-mmu-miR-222-3p
B
Epididymal fat tissue
DDIT4
(24kDa)
GAPDH
(37kDa)
Mir221/222flox/y
Mir221/222AdipoKO
Relative Ddit4 mRNA expression
2.0
1.5
1.0
0.5
0.0
Mir221/222flox/y
Mir221/222AdipoKO
DDIT4/GAPDH
1.5
1.0
0.5
0.0
*
Mir221/222flox/y
Mir221/222AdipoKO

Figure 4

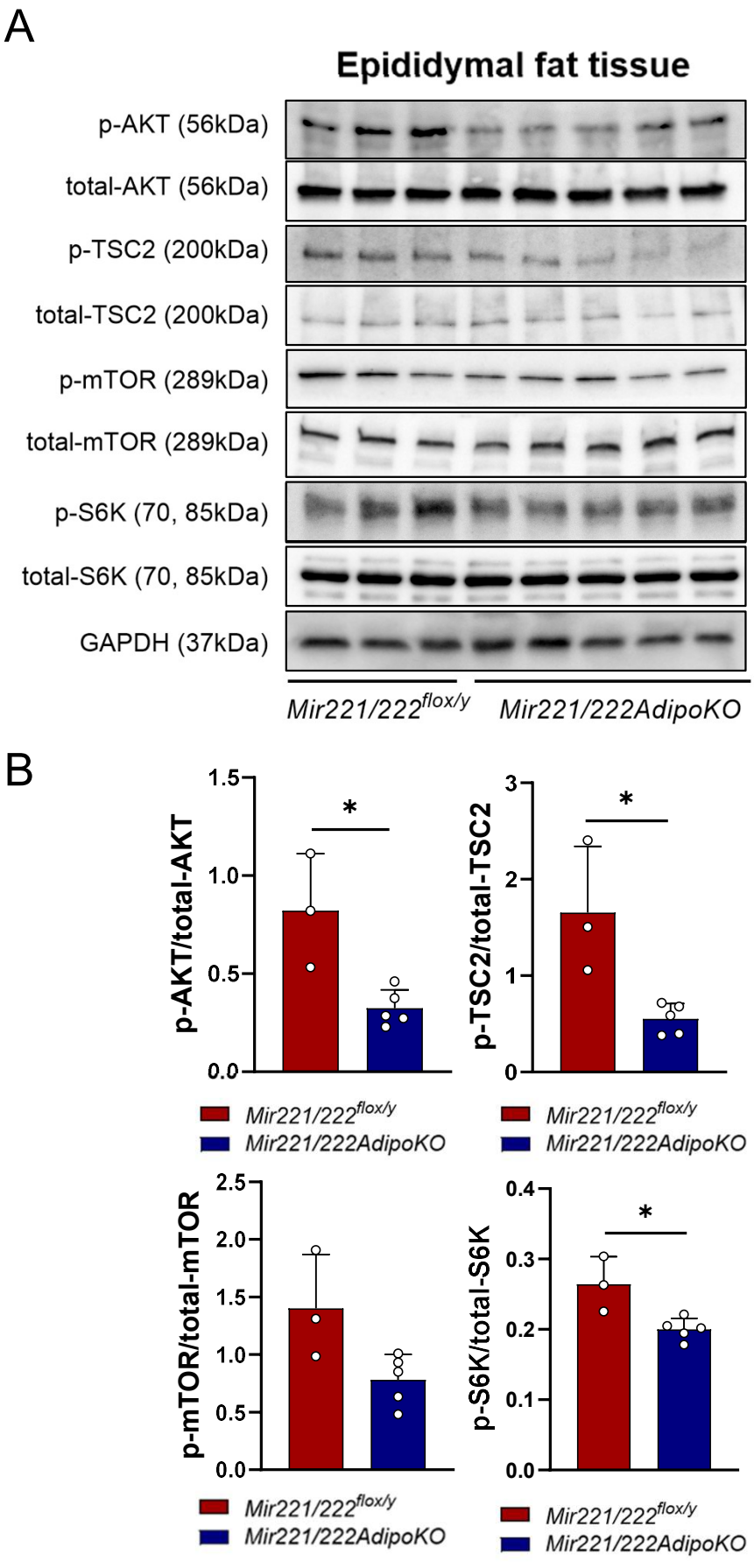
A
Epididymal fat tissue
p-AKT (56kDa)
total-AKT (56kDa)
p-TSC2 (200kDa)
total-TSC2 (200kDa)
p-mTOR (289kDa)
total-mTOR (289kDa)
p-S6K (70, 85kDa)
total-S6K (70, 85kDa)
GAPDH (37kDa)
Mir221/222flox/y
Mir221/222AdipoKO
B
p-AKT/total-AKT
p-TSC2/total-TSC2
p-mTOR/total-mTOR
p-S6K/total-S6K
*
Mir221/222flox/y
Mir221/222AdipoKO

Figure 5

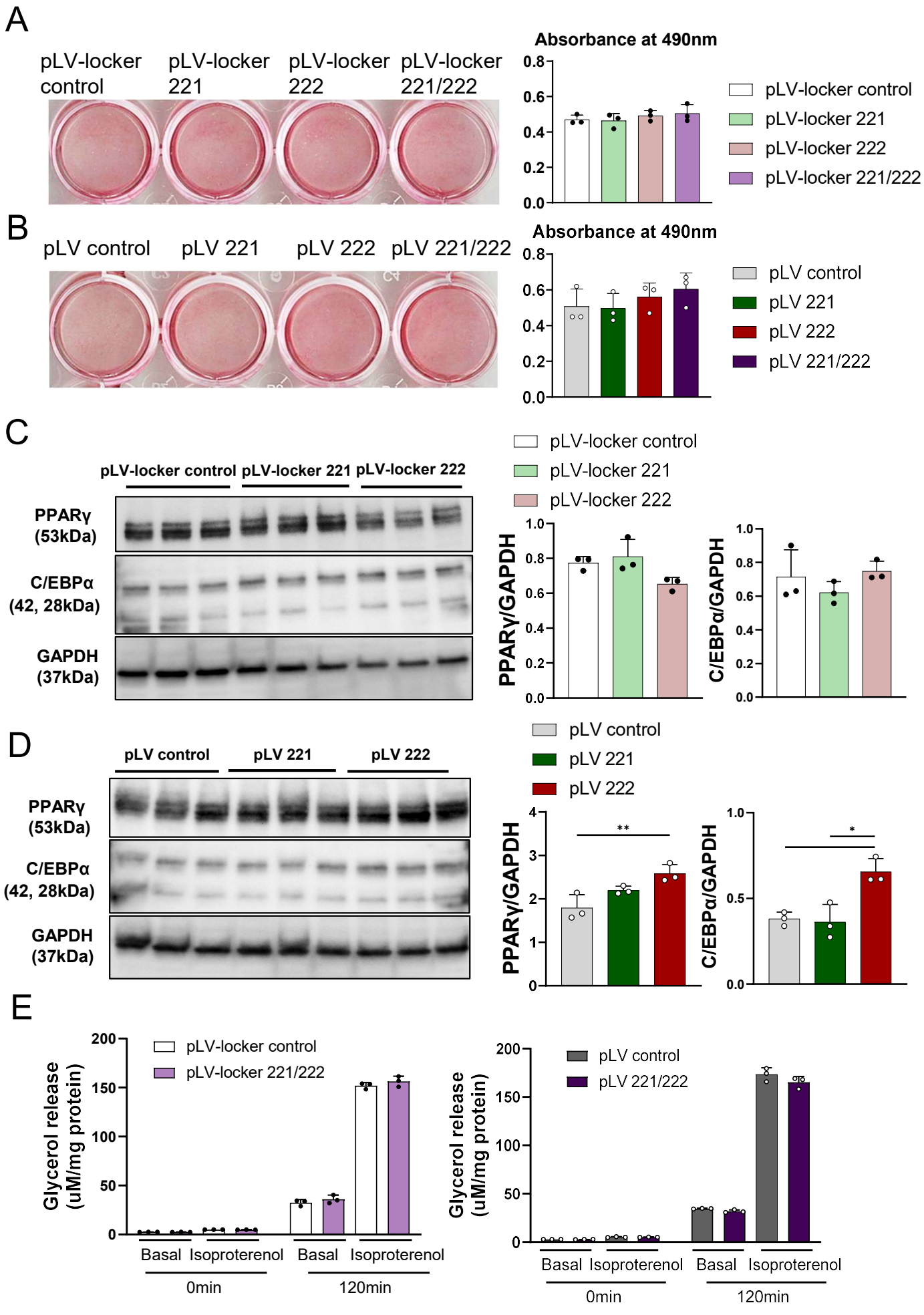
A
pLV-locker control
pLV-locker 221
pLV-locker 222
pLV-locker 221/222
Absorbance at 490nm
0.8
0.6
0.4
0.2
0.0
pLV-locker control
pLV-locker 221
pLV-locker 222
pLV-locker 221/222
B
pLV control
pLV 221
pLV 222
pLV 221/222
Absorbance at 490nm
0.8
0.6
0.4
0.2
0.0
pLV control
pLV 221
pLV 222
pLV 221/222
C
pLV-locker control
pLV-locker 221
pLV-locker 222
PPARγ (53kDa)
C/EBPα (42, 28kDa)
GAPDH (37kDa)
pLV-locker control
pLV-locker 221
pLV-locker 222
PPARγ/GAPDH
1.0
0.8
0.6
0.4
0.2
0.0
C/EBPα/GAPDH
1.0
0.8
0.6
0.4
0.2
0.0
D
pLV control
pLV 221
pLV 222
PPARγ (53kDa)
C/EBPα (42, 28kDa)
GAPDH (37kDa)
pLV control
pLV 221
pLV 222
PPARγ/GAPDH
4
3
2
1
0
**
C/EBPα/GAPDH
1.0
0.5
0.0
*
E
Glycerol release (uM/mg protein)
200
150
100
50
0
pLV-locker control
pLV-locker 221/222
Basal
Isoproterenol
Basal
Isoproterenol
0min
120min
Glycerol release (uM/mg protein)
200
150
100
50
0
pLV control
pLV 221/222
Basal
Isoproterenol
Basal
Isoproterenol
0min
120min

Supplementary Figure 1

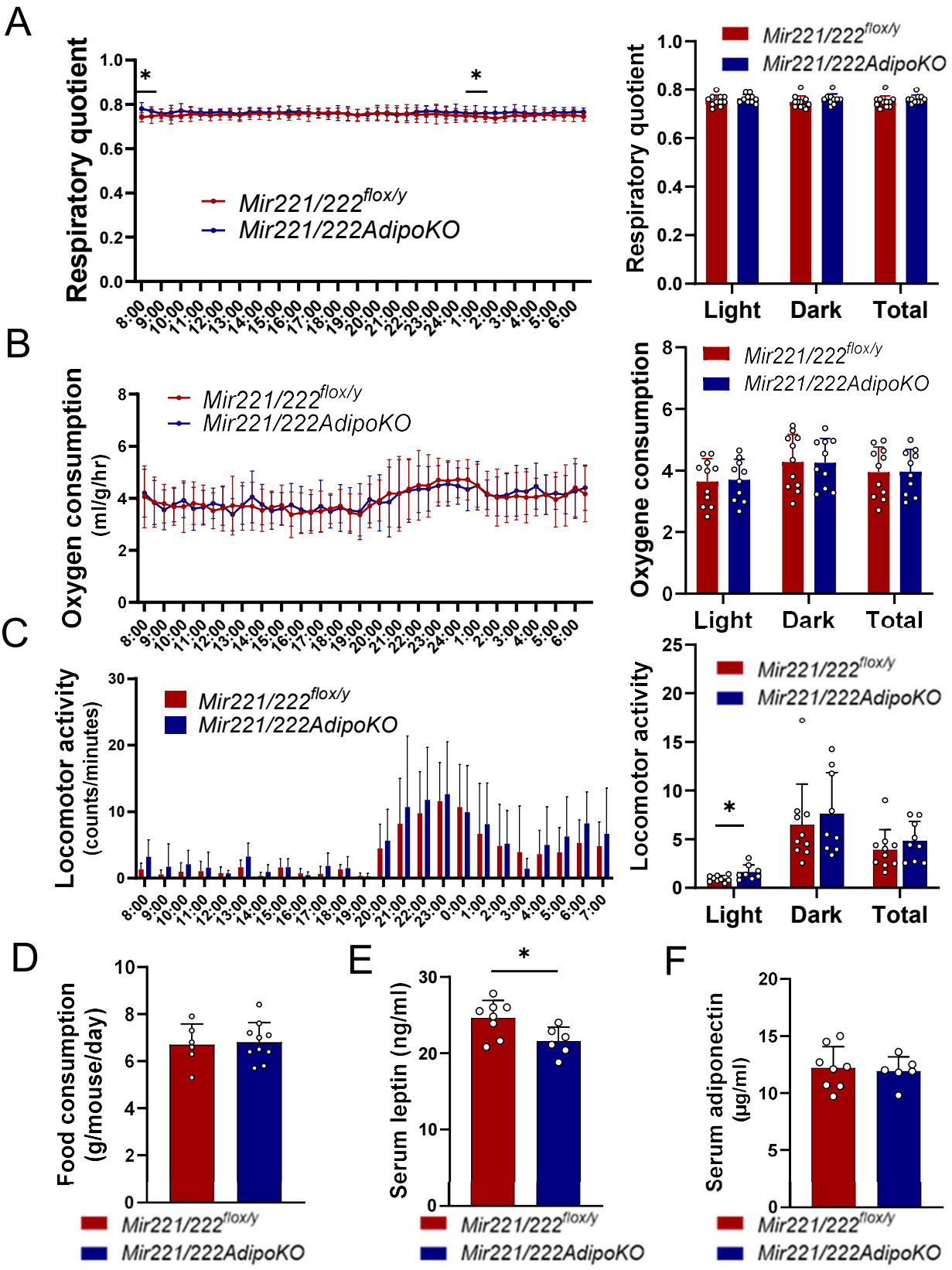

Supplementary Figure 1. Basal metabolic rate, locomotor activity and food intake. (**A and B**) Respiratory quotient (RQ) and Oxygen consumption rate in *Mir221/222*$^{flox/y}$ (n=11) and *Mir221/222AdipoKO* (n=10) mice fed with HFHS (high fat high sucrose) chow. (**C**) Locomotor activity in *Mir221/222*$^{flox/y}$ (n=10) and *Mir221/222AdipoKO* (n=9) mice fed with HFHS chow. (**D**) Food consumption in *Mir221/222*$^{flox/y}$ (n=5) and *Mir221/222AdipoKO* (n=10) mice fed with HFHS chow. (**E**) Serum leptin levels in *Mir221/222*$^{flox/y}$ (n=8) and *Mir221/222AdipoKO* (n=6) mice fed with HFHS chow. (**F**) Serum adiponectin levels in *Mir221/222*$^{flox/y}$ (n=8) and *Mir221/222AdipoKO* (n=6) mice fed with HFHS chow. Data shown as mean ± SD and analyzed by Mann-Whitney's U test (*p<0.05).

Supplementary Figure 2

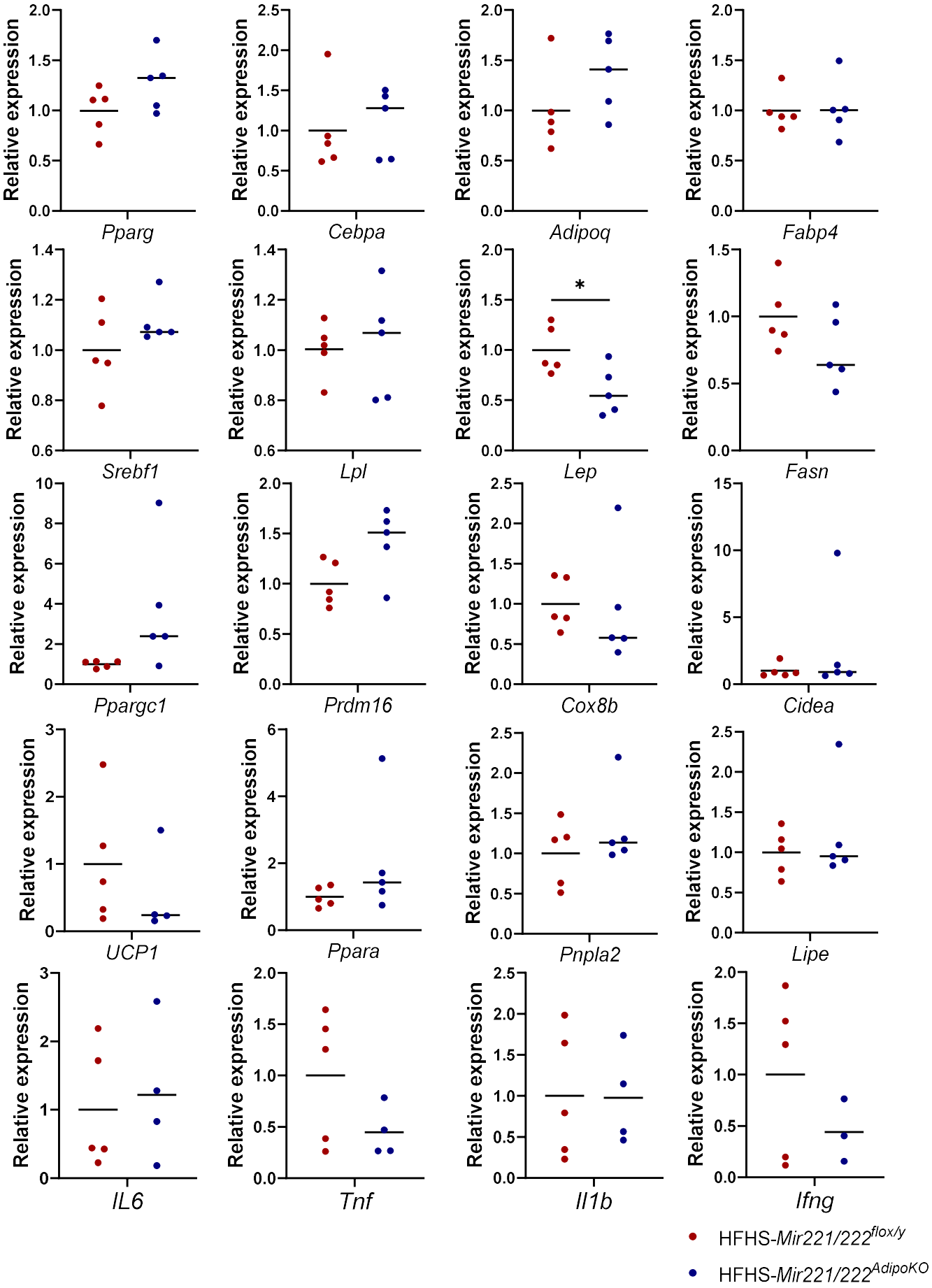

Supplementary Figure 2. mRNA expression of various genes. *Mir221/222*$^{flox/y}$ (n=5) and *Mir221/222AdipoKO* (n=5) mice fed with HFHS (high fat high sucrose) chow. Data shown as mean ± SD and analyzed by Mann-Whitney's U test (*p<0.05).

Supplementary Figure 3

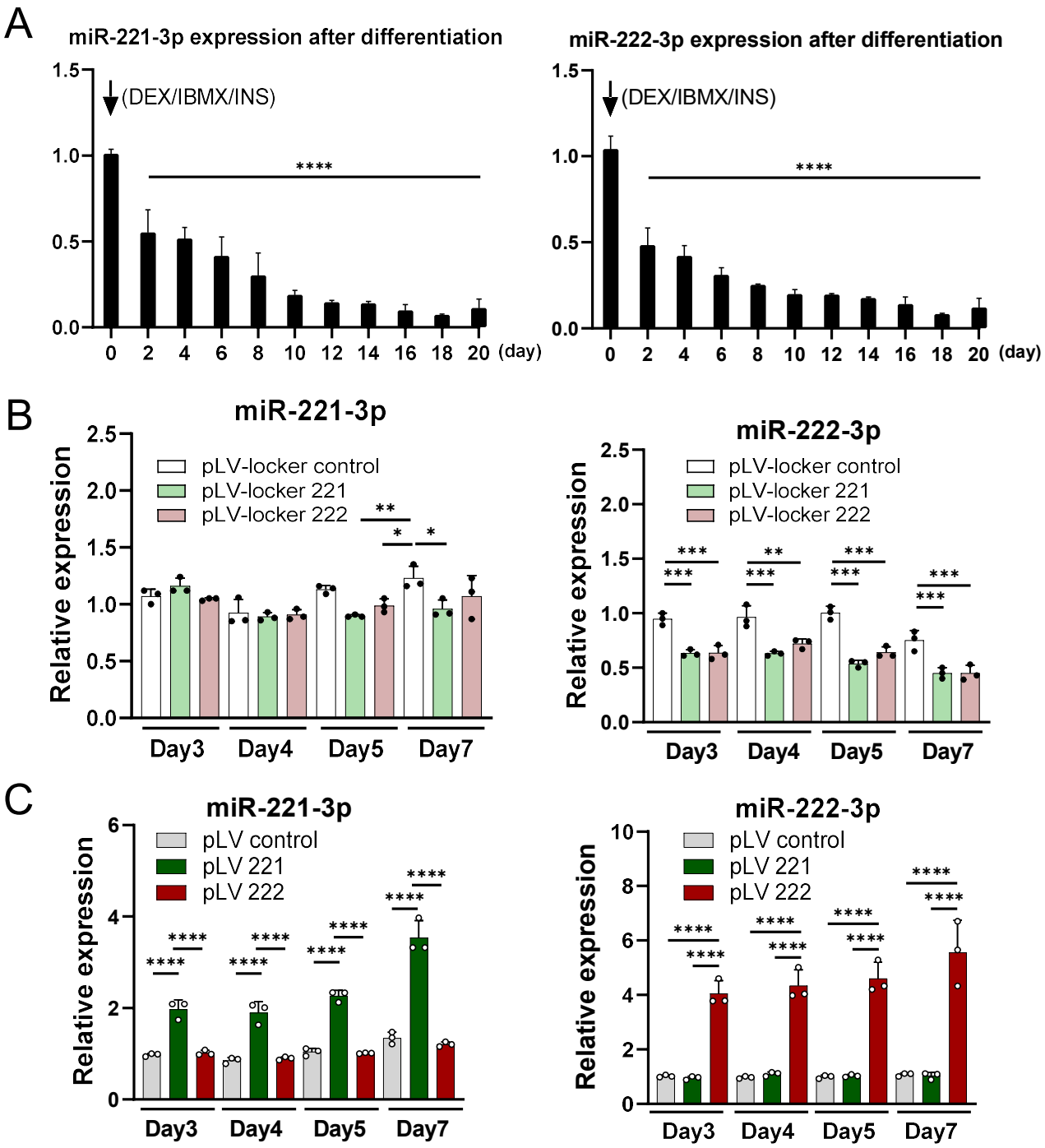

Supplementary Figure 3. Expression of miR-221-3p and miR-222-3p in 3T3-L1 cells. (**A**) Expression of miR-221-3p and miR-222-3p after the induction of adipocyte differentiation by dexamethasone, isobutylmethylxanthine, 1-methyl-3-isobutylxanthine and insulin (DEX/IBMX/INS). (n=3) (**B**) Expression of miR-221-3p and miR-222-3p in 3T3L1 cells treated with pLV-locker control, pLV-locker 221, and pLV-locker 222. (**C**) Expression of miR-221-3p and miR-222-3p in 3T3-L1 cells treated with pVL control, pLV 221, and pLV 222. Data shown as mean ± SD and analyzed one-way ANOVA with Tukey test (*p<0.05; **p<0.01; ***p<0.001; ****p<0.0001).

Supplementary Figure 4

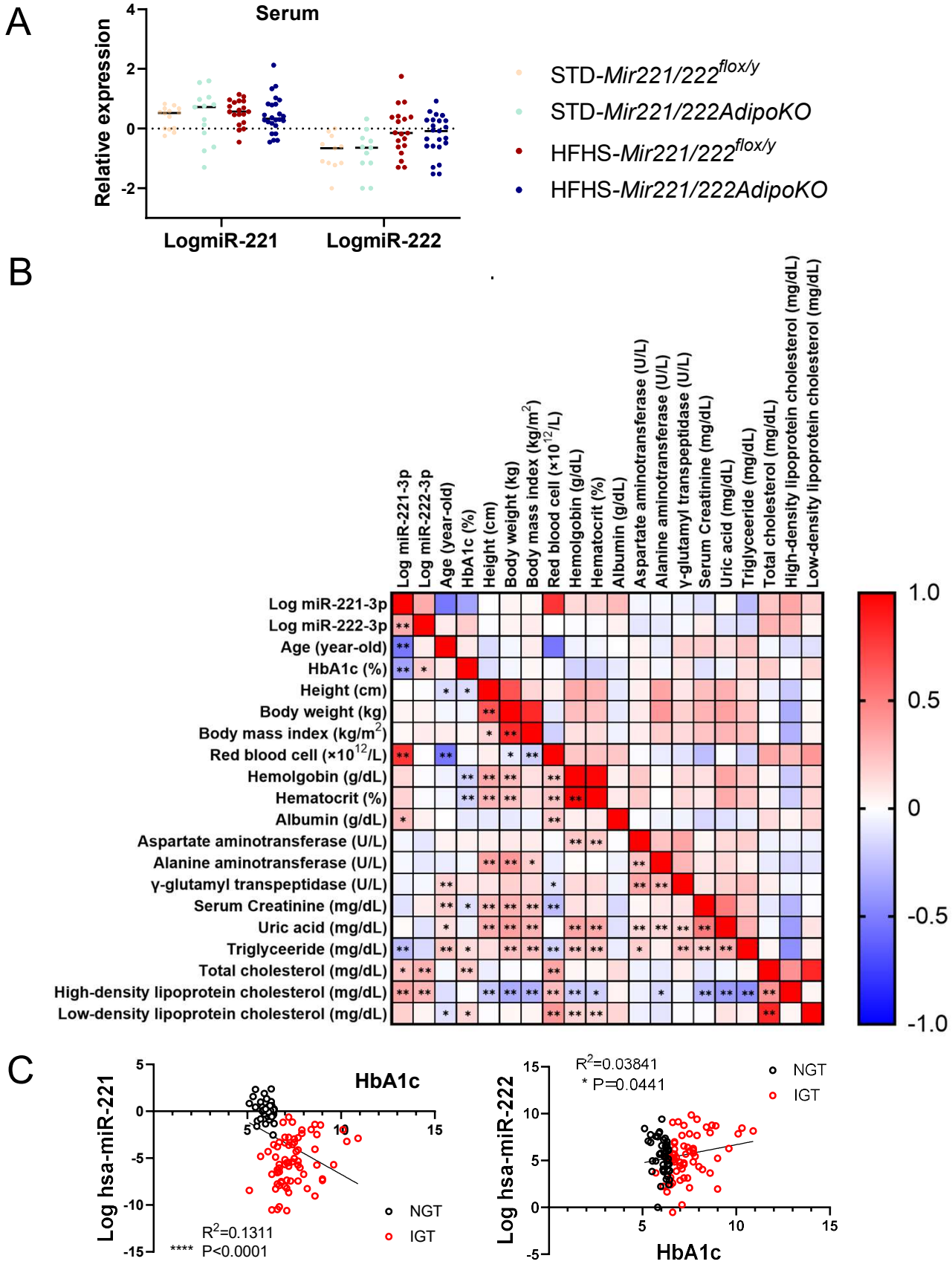

Supplementary Figure 4. Serum concentration of mir-221-3p and mir-222-3p levels in mice and human. (**A**) Serum concentrations of mir-221-3p and mir-222-3p levels in *Mir221/222*$^{flox/y}$ (n=14) and *Mir221/222AdipoKO* (n=13) mice fed with STD (standard) chow, *Mir221/222*$^{flox/y}$ (n=19) and *Mir221/222AdipoKO* (n=24) mice fed with HFHS (high fat high sucrose) chow . (**B**) Simple correlations of serum miR-221-3p and miR-222-3p levels with various clinical parameters in the subjects with normal glucose tolerance (NGT, n=45) and impaired glucose tolerance (IGT, n=69) (n=114). In correlation matrix, Spearman's rank correlation coefficient is shown. *p<0.05, **p<0.01. (**C**) Log hsa-miR-221-3p negatively correlates with HbA1c, while Log hsa-miR-222-3p positively correlates with HbA1c.

Supplementary Figure 5

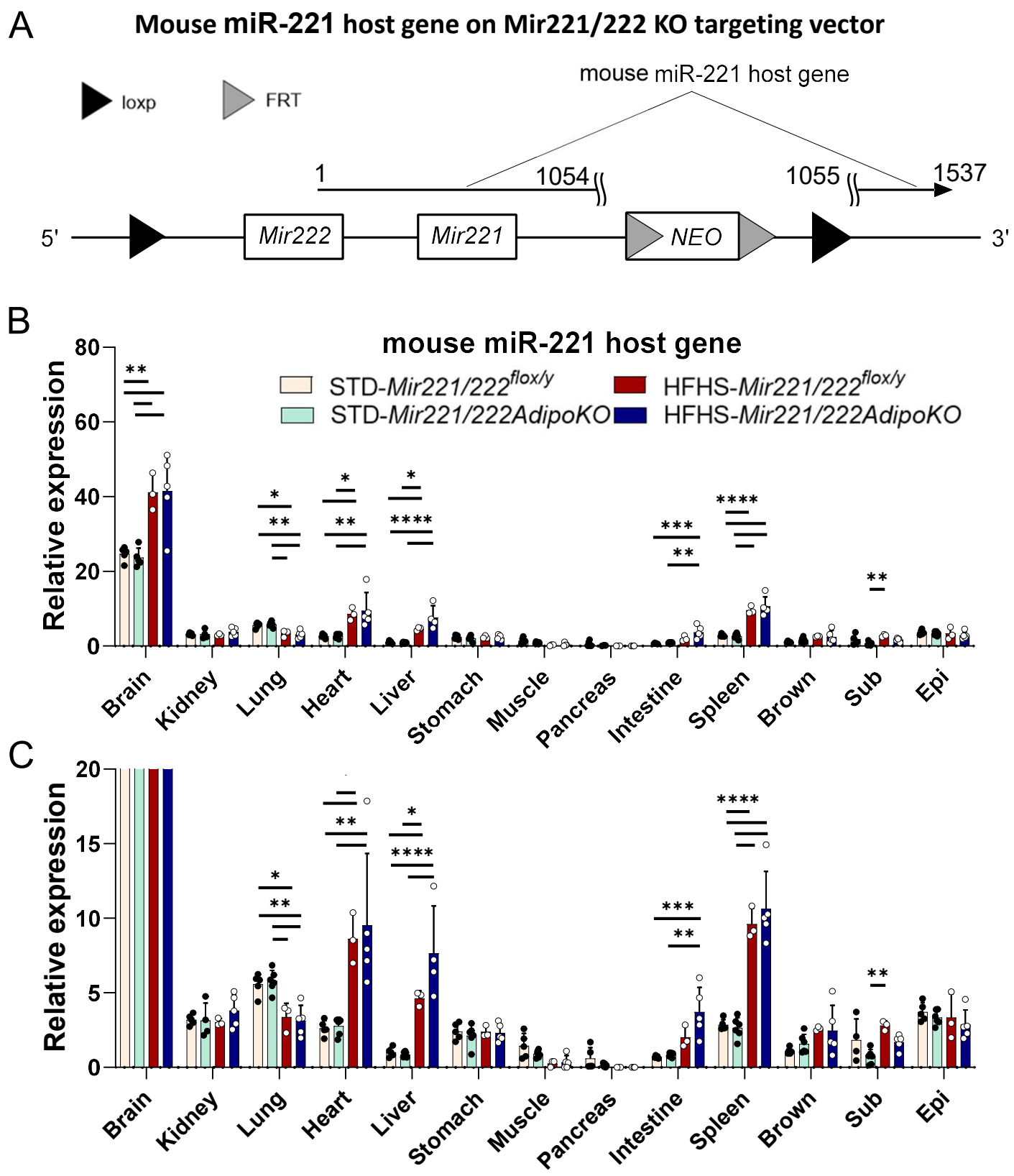

Supplementary Figure 5. Expression of miR-221 host gene (*Mir221hg*) in various tissues. (**A**) Mir221/222 KO targeting vector map and location of miR-221 host gene (*Mir221hg*). The single exon of *Mir221hg* is disrupted by NEO. (**B and C**) Expression of *Mir221hg* in various tissues in *Mir221/222*$^{flox/y}$ (n=5) and *Mir221/222AdipoKO* (n=6) mice fed with STD (standard) chow, *Mir221/222*$^{flox/y}$ (n=3) and *Mir221/222AdipoKO* (n=5) mice fed with HFHS (high fat high sucrose) chow. Whole range of relative expression (0 to 80) is shown in panel **B** and narrow range (0 to 20) in panel **C**. Data shown as mean ± SD and analyzed by one-way ANOVA with Tukey test. (*p<0.05; **p<0.01; ***p<0.001; ****p<0.0001).

Supplementary Figure 6

Uncropped images in Figure 3B

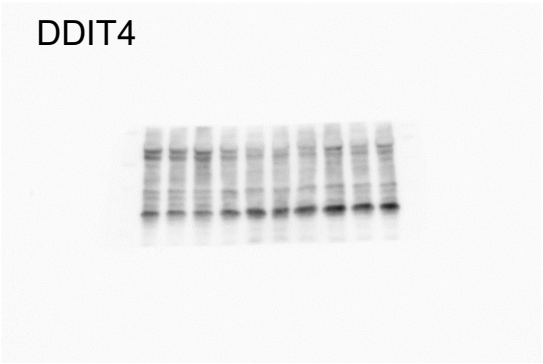

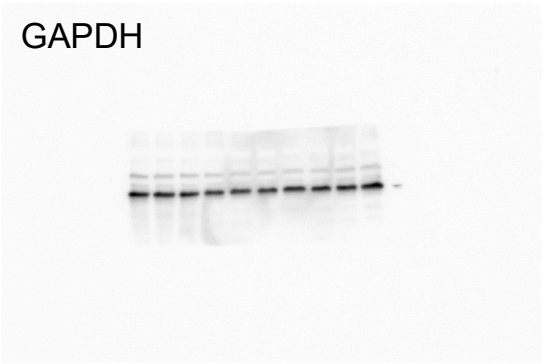

Uncropped images in Figure 4A

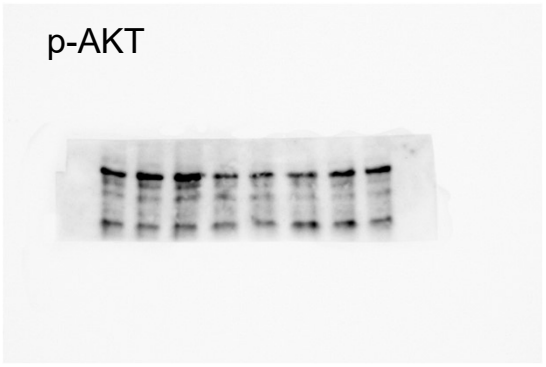

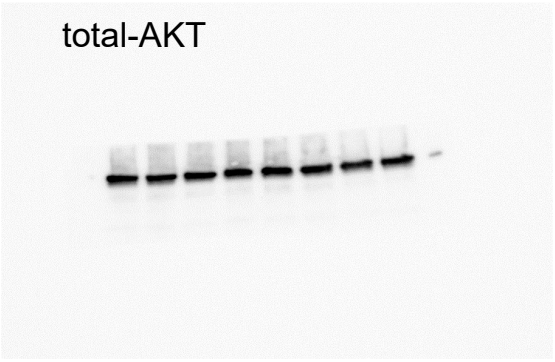

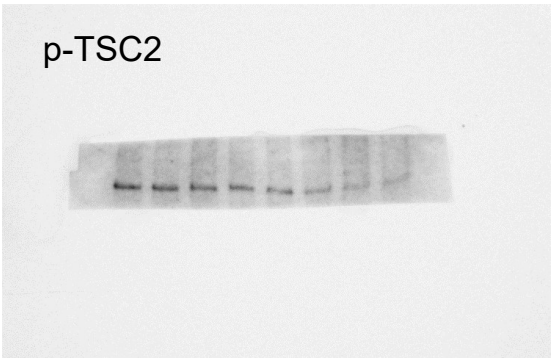

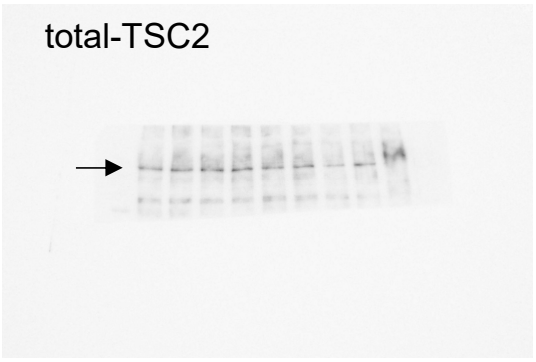

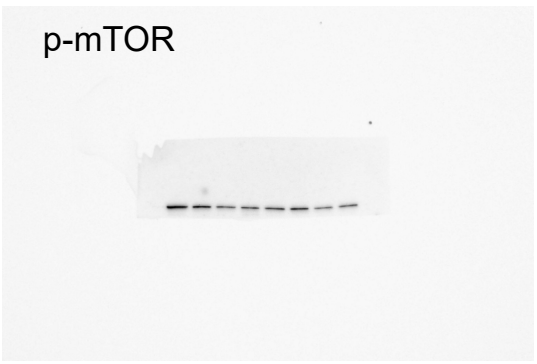

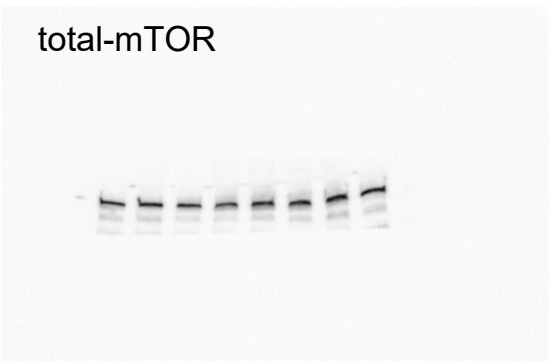

Supplementary Figure 7

Uncropped images in Figure 4A

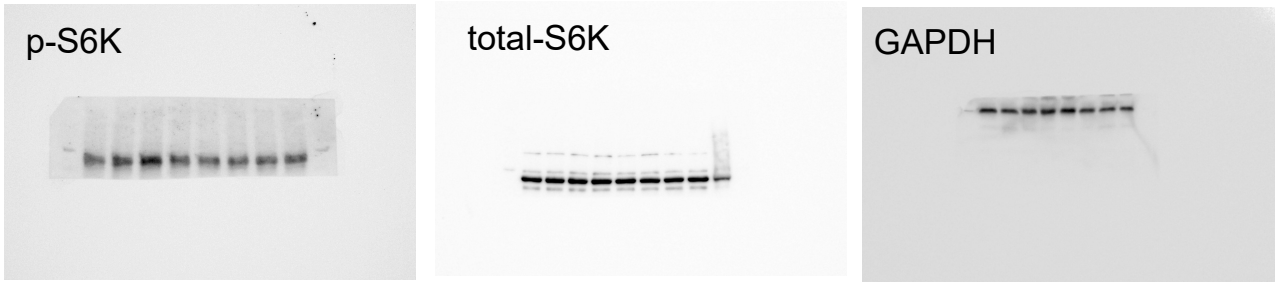

Uncropped images in Figure 5C,D

C

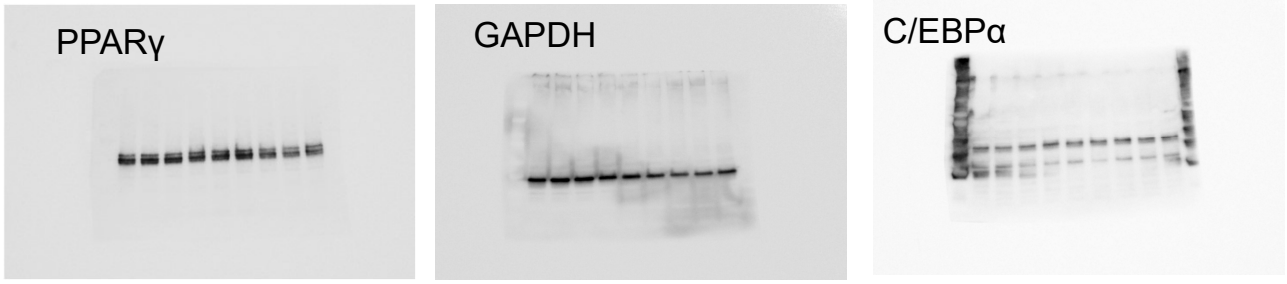

D

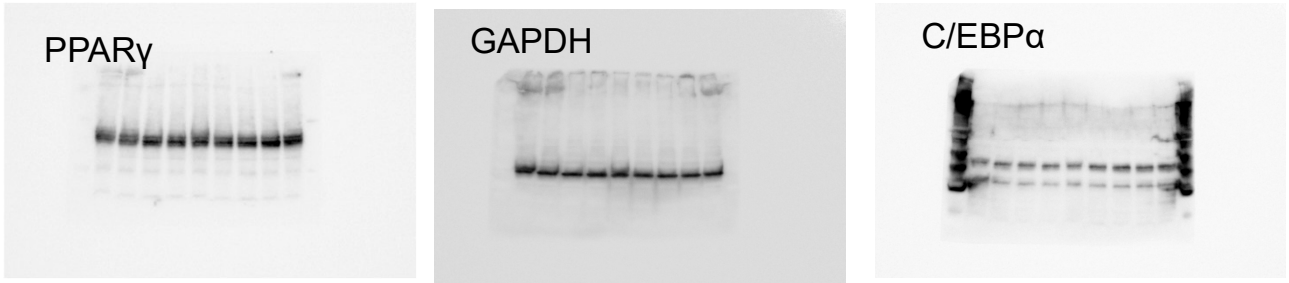

Supplementary Figure 8

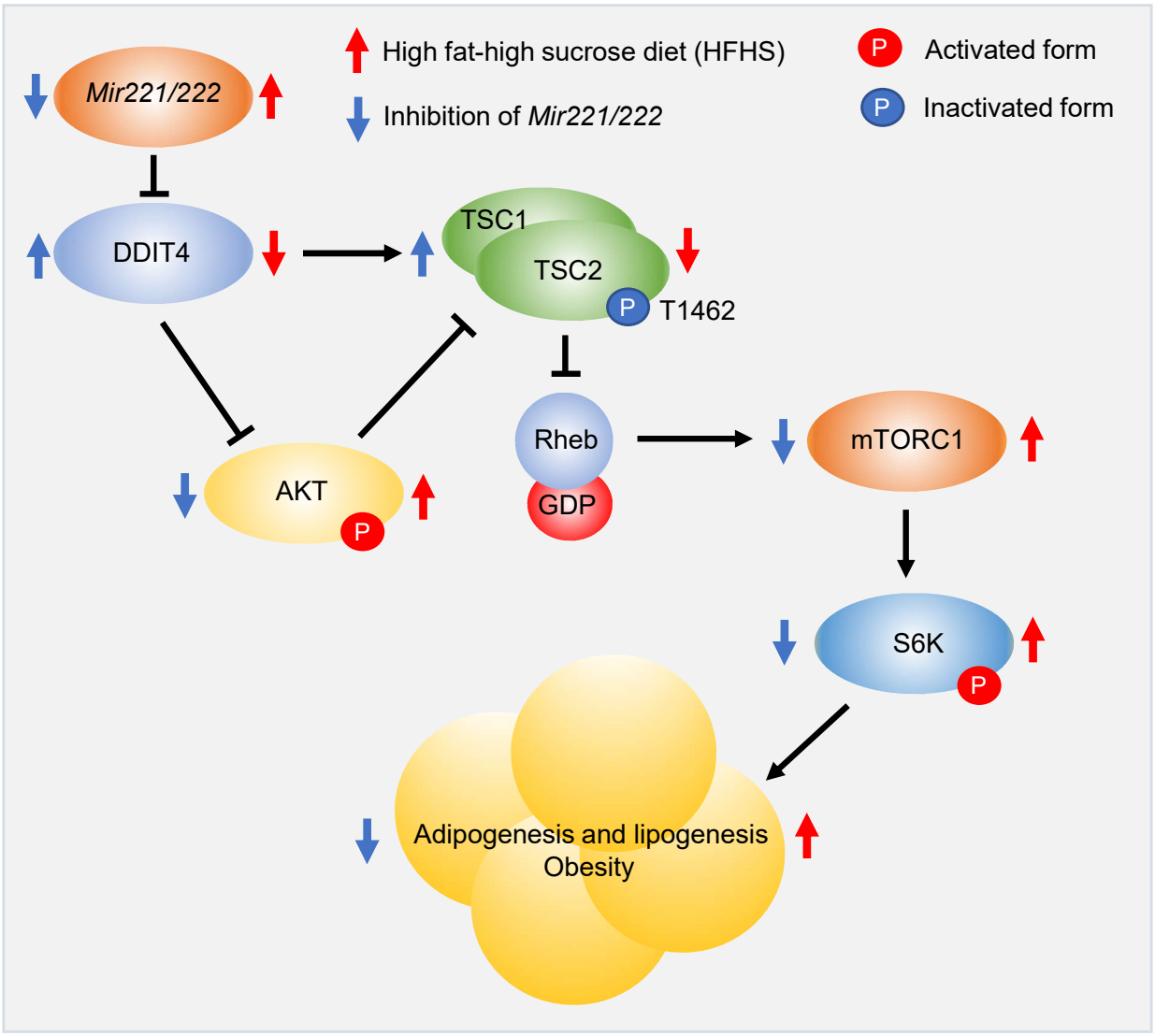

Supplementary Figure 8. Ddit4 is a direct target of miR-221-3p and miR-222-3p and it inhibits mTORC1 pathway.

Supplementary Table 1. Formulation of standard (STD) and high fat-high sucrose (HFHS) chow.

	Nutrients / 1000 g chow	STD (MF, Oriental Yeast, Japan*)	HFHS (D12331, Research Diets, New Brunswick, NJ**)
Macronutrients	Protein (g)	226.6	230
	Carbohydrate (g)	553	345
	Fat (g)	51	358.5
Carbohydrate contents	Maltodextrin (g)	0	170
	Corn starch (g)	0	0
	Sucrose (g)	0	175
		553 (as soluble nitrogen-free product from crude mixture of corn, wheat and rice bran)	
Vitamin	Vit A (IU)	12830	4000
	Vit D3 (IU)	1370	1000
	Vit E (mg)	91	50
	Vit K3 (mg)	0.4	0.5
	Vit B1 (mg)	20.5	6
	Vit B2 (mg)	11	6
	Vit B6 (mg)	8.7	7
	Vit B12 (μg)	55	10
	Biotin (μg)	270	200
	Pantothenic acid (mg)	24.5	16
	Niacin (mg)	106.1	30
	Choline (g)	1.8	0.62
	Folic acid (mg)	1.7	2
Mineral	Ca (g)	10.7	5.94
	P (g)	8.3	4.57
	Mg (g)	2.4	0.57
	Na (g)	1.9	1.14
	K (g)	9	4.11
	Fe (mg)	106	42.3
	Cu (mg)	7.8	6.86
	Zn (mg)	48.9	33.1
	Mn (mg)	48.4	67.4
	Total calories (kcal)	3590	5560

*https://www.oyc.co.jp/bio/LAD-equipment/LAD/ingredient.html and https://www.oyc.co.jp/bio/LAD-equipment/LAD/rodents.html

**https://www.eptrading.co.jp/service/researchdiets/pdf/D12328-D12331.pdf

Supplementary Table 2 RNA sequencing data sera, liver and epididymalfat tissues in C57BL/6J mice fed with standard (STD) and high fat-high sucrose chow (HFHS).

miRBase Name	miRBase Accession	LINK	s1(Serum-High fat high sucrose chow)	s2(Liver-High fat high sucrose chow)	s3 (Epididymal fat-High fat high sucrose chow)	s5 (Serum-Normal chow)	s6 (Liver-Normal chow)	s7 (Epididymal fat-Normal chow)	Total	s1/s5	s2/s6	s3/s7
mmu-mir-504	MI0005515	miRBase LINK	5	0	1,177	5	0	29	1,216	1.000	#DIV/0!	40.586
mmu-mir-703	MI0004687	miRBase LINK	1	112	13	4	170	1	301	0.250	0.659	13.000
mmu-mir-298	MI0000398	miRBase LINK	188	28	3,175	379	30	249	4,049	0.496	0.933	12.751
mmu-mir-335	MI0000817	miRBase LINK	137	2,673	110,365	54	1,504	8,778	123,511	2.537	1.777	12.573
mmu-mir-342	MI0000627	miRBase LINK	2,027	1,124	19,320	3,427	707	2,040	28,645	0.591	1.590	9.471
mmu-mir-222	MI0000710	miRBase LINK	1,039	1,763	22,488	2,231	1,578	2,759	31,858	0.466	1.117	8.151
mmu-mir-296	MI0000394	miRBase LINK	287	10	454	387	20	63	1,221	0.742	0.500	7.206
mmu-mir-211	MI0000708	miRBase LINK	17	18	7	23	9	1	75	0.739	2.000	7.000
mmu-mir-18b	MI0005483	miRBase LINK	4	3	7	7	0	1	22	0.571	#DIV/0!	7.000
mmu-mir-1193	MI0006298	miRBase LINK	0	0	26	0	1	4	31	#DIV/0!	0.000	6.500
mmu-mir-122	MI0000256	miRBase LINK	723	392,484	409	494	367,471	65	761,646	1.464	1.068	6.292
mmu-mir-669d	MI0006281	miRBase LINK	0	0	12	0	0	2	14	#DIV/0!	#DIV/0!	6.000
mmu-mir-301b	MI0004122	miRBase LINK	80	7	91	107	4	16	305	0.748	1.750	5.688
mmu-mir-221	MI0000709	miRBase LINK	7,180	6,724	38,010	9,165	7,541	6,710	75,330	0.783	0.892	5.665
mmu-mir-802	MI0004249	miRBase LINK	167	33,519	25	64	7,020	5	40,800	2.609	4.775	5.000
mmu-mir-592	MI0004127	miRBase LINK	27	66	25	24	348	6	496	1.125	0.190	4.167
mmu-mir-412	MI0001164	miRBase LINK	0	0	4	0	0	1	5	#DIV/0!	#DIV/0!	4.000
mmu-mir-494	MI0003532	miRBase LINK	4	3	252	29	5	67	360	0.138	0.600	3.761
mmu-mir-499	MI0004676	miRBase LINK	56	9	82	109	5	23	284	0.514	1.800	3.565
mmu-mir-31	MI0000579	miRBase LINK	297	8,935	189	382	11,471	55	21,329	0.777	0.779	3.436
mmu-mir-146a	MI0000170	miRBase LINK	2,113	2,851	9,532	4,266	4,742	2,822	26,326	0.495	0.601	3.378
mmu-mir-147	MI0005482	miRBase LINK	4	4	96	7	6	29	146	0.571	0.667	3.310
mmu-mir-692-1	MI0004660	miRBase LINK	3	76	16	7	63	5	170	0.429	1.206	3.200
mmu-mir-1199	MI0006307	miRBase LINK	8	8	22	9	4	7	58	0.889	2.000	3.143
mmu-mir-679	MI0004638	miRBase LINK	3	1	90	7	1	29	131	0.429	1.000	3.103
mmu-mir-190	MI0000232	miRBase LINK	1	485	713	0	325	231	1,755	#DIV/0!	1.492	3.087
mmu-mir-146b	MI0004665	miRBase LINK	663	676	20,505	1,766	859	6,707	31,176	0.375	0.787	3.057
mmu-mir-380	MI0000797	miRBase LINK	1	6	207	5	6	68	293	0.200	1.000	3.044
mmu-mir-20b	MI0003536	miRBase LINK	5	6	57	10	6	19	103	0.500	1.000	3.000
mmu-mir-684-1	MI0004647	miRBase LINK	1	3	6	0	10	2	22	#DIV/0!	0.300	3.000
mmu-mir-684-2	MI0004648	miRBase LINK	1	3	6	0	10	2	22	#DIV/0!	0.300	3.000
mmu-mir-704	MI0004688	miRBase LINK	1	2	3	2	8	1	17	0.500	0.250	3.000
mmu-mir-669e	MI0006300	miRBase LINK	0	0	3	0	0	1	4	#DIV/0!	#DIV/0!	3.000
mmu-mir-376a	MI0000793	miRBase LINK	7	7	366	0	10	132	522	#DIV/0!	0.700	2.773
mmu-mir-455	MI0004679	miRBase LINK	54	4,687	882	59	5,597	324	11,603	0.915	0.837	2.722
mmu-mir-487b	MI0003534	miRBase LINK	15	1	208	26	0	77	327	0.577	#DIV/0!	2.701
mmu-mir-496	MI0004589	miRBase LINK	2	1	262	11	6	97	379	0.182	0.167	2.701
mmu-mir-551b	MI0004131	miRBase LINK	3	116	8	1	27	3	158	3.000	4.296	2.667
mmu-mir-340	MI0000623	miRBase LINK	1,859	27,006	19,256	2,661	22,296	7,227	80,305	0.699	1.211	2.664
mmu-mir-376b	MI0001162	miRBase LINK	3	9	362	11	14	136	535	0.273	0.643	2.662
mmu-mir-370	MI0001165	miRBase LINK	7	0	53	6	0	20	86	1.167	#DIV/0!	2.650
mmu-mir-377	MI0000794	miRBase LINK	11	2	271	11	3	103	401	1.000	0.667	2.631
mmu-mir-142	MI0000167	miRBase LINK	37,026	17,590	58,187	39,676	9,631	22,754	184,864	0.933	1.826	2.557
mmu-mir-692-2	MI0004661	miRBase LINK	10	328	66	56	254	26	740	0.179	1.291	2.538
mmu-mir-433	MI0001525	miRBase LINK	21	0	191	45	2	76	335	0.467	0.000	2.513
mmu-mir-214	MI0000698	miRBase LINK	170	682	3,121	250	655	1,245	6,123	0.680	1.041	2.507
mmu-mir-543	MI0003519	miRBase LINK	0	3	102	21	3	41	170	0.000	1.000	2.488
mmu-mir-369	MI0003535	miRBase LINK	4	11	718	29	12	291	1,065	0.138	0.917	2.467
mmu-mir-155	MI0000177	miRBase LINK	123	122	1,336	251	105	542	2,479	0.490	1.162	2.465
mmu-mir-669a-2	MI0004667	miRBase LINK	15	49	439	62	41	180	786	0.242	1.195	2.439
mmu-mir-501	MI0004703	miRBase LINK	60	65	342	106	66	141	780	0.566	0.985	2.426
mmu-mir-669a-1	MI0004523	miRBase LINK	165	512	4,545	668	416	1,880	8,186	0.247	1.231	2.418
mmu-mir-411	MI0001163	miRBase LINK	136	350	35,343	272	498	14,732	51,331	0.500	0.703	2.399
mmu-mir-299	MI0000399	miRBase LINK	15	4	735	31	17	310	1,112	0.484	0.235	2.371
mmu-mir-130b	MI0000408	miRBase LINK	4,382	91	614	5,414	88	260	10,849	0.809	1.034	2.362
mmu-mir-297b	MI0004674	miRBase LINK	1	9	30	0	0	13	53	#DIV/0!	#DIV/0!	2.308
mmu-mir-136	MI0000162	miRBase LINK	182	185	8,157	428	288	3,543	12,783	0.425	0.642	2.302
mmu-mir-106a	MI0000406	miRBase LINK	3	2	16	3	1	7	32	1.000	2.000	2.286
mmu-mir-449c	MI0004645	miRBase LINK	1	0	25	0	0	11	37	#DIV/0!	#DIV/0!	2.273
mmu-mir-18a	MI0000567	miRBase LINK	754	261	410	823	214	181	2,643	0.916	1.220	2.265
mmu-mir-652	MI0004965	miRBase LINK	1,121	348	1,394	1,288	265	616	5,032	0.870	1.313	2.263
mmu-mir-9-1	MI0000720	miRBase LINK	3	25	259	9	6	115	417	0.333	4.167	2.252
mmu-mir-9-2	MI0000157	miRBase LINK	3	25	259	9	6	115	417	0.333	4.167	2.252
mmu-mir-297a-6	MI0005491	miRBase LINK	0	0	18	20	2	8	48	0.000	0.000	2.250
mmu-mir-297a-1	MI0000395	miRBase LINK	0	0	9	10	1	4	24	0.000	0.000	2.250
mmu-mir-297a-2	MI0000397	miRBase LINK	0	0	9	10	1	4	24	0.000	0.000	2.250
mmu-mir-511	MI0005554	miRBase LINK	332	663	985	683	687	439	3,789	0.486	0.965	2.244
mmu-mir-540	MI0003518	miRBase LINK	55	6	497	147	8	222	935	0.374	0.750	2.239
mmu-mir-598	MI0005556	miRBase LINK	12	162	264	5	176	118	737	2.400	0.920	2.237
mmu-mir-9-3	MI0000721	miRBase LINK	3	25	259	9	6	116	418	0.333	4.167	2.233
mmu-mir-223	MI0000703	miRBase LINK	1,534	857	7,087	2,369	671	3,189	15,707	0.648	1.277	2.222
mmu-mir-382	MI0000799	miRBase LINK	7	4	333	38	8	150	540	0.184	0.500	2.220
mmu-mir-205	MI0000248	miRBase LINK	2,127	108	71	6,337	43	32	8,718	0.336	2.512	2.219
mmu-mir-409	MI0001160	miRBase LINK	125	25	1,891	374	40	857	3,312	0.334	0.625	2.207
mmu-mir-379	MI0000796	miRBase LINK	1	10	784	11	25	356	1,187	0.091	0.400	2.202
mmu-mir-337	MI0000615	miRBase LINK	53	11	1,263	115	21	574	2,037	0.461	0.524	2.200
mmu-mir-323	MI0000592	miRBase LINK	1	1	39	14	0	18	73	0.071	#DIV/0!	2.167
mmu-mir-297c	MI0005492	miRBase LINK	0	7	26	0	0	12	45	#DIV/0!	#DIV/0!	2.167
mmu-mir-466d	MI0005546	miRBase LINK	2	4	28	11	5	13	63	0.182	0.800	2.154
mmu-mir-410	MI0001161	miRBase LINK	149	51	5,073	477	40	2,383	8,173	0.312	1.275	2.129
mmu-mir-297a-4	MI0005489	miRBase LINK	0	8	36	10	1	17	72	0.000	8.000	2.118
mmu-mir-297a-3	MI0005488	miRBase LINK	0	7	36	10	1	17	71	0.000	7.000	2.118
mmu-mir-363	MI0000765	miRBase LINK	21	5	110	71	3	52	262	0.296	1.667	2.115
mmu-mir-485	MI0003492	miRBase LINK	48	7	338	157	3	160	713	0.306	2.333	2.113
mmu-mir-34c	MI0000403	miRBase LINK	230	153	7,548	295	357	3,585	12,168	0.780	0.429	2.105
mmu-mir-141	MI0000166	miRBase LINK	273	404	88	370	272	42	1,449	0.738	1.485	2.095
mmu-mir-329	MI0000605	miRBase LINK	21	10	888	72	14	424	1,429	0.292	0.714	2.094
mmu-mir-376c	MI0003533	miRBase LINK	2	8	249	6	3	120	388	0.333	2.667	2.075
mmu-mir-541	MI0003521	miRBase LINK	769	207	15,707	1,541	288	7,593	26,105	0.499	0.719	2.069
mmu-mir-542	MI0003522	miRBase LINK	17	224	534	31	185	259	1,250	0.548	1.211	2.062
mmu-mir-467a			8	170	1,476	8	171	716	2,549	1.000	0.994	2.061
mmu-mir-434	MI0001526	miRBase LINK	2,057	403	37,349	5,758	670	18,279	64,516	0.357	0.601	2.043

mmu-mir-199a-1	MI0000241	miRBase LINK	4,296	18,270	111,847	9,449	25,278	55,294	224,434	0.455	0.723	2.023
mmu-mir-199a-2	MI0000713	miRBase LINK	4,297	18,289	111,987	9,449	25,297	55,364	224,683	0.455	0.723	2.023
mmu-mir-27b	MI0000142	miRBase LINK	22,994	253,279	390,605	29,301	245,960	193,911	1,136,050	0.785	1.030	2.014
mmu-mir-34b	MI0000404	miRBase LINK	36	11	547	20	30	273	917	1.800	0.367	2.004
mmu-mir-375	MI0000792	miRBase LINK	8,270	137	12	4,163	133	6	12,721	1.987	1.030	2.000
mmu-mir-200c	MI0000694	miRBase LINK	72	54	22	119	40	11	318	0.605	1.350	2.000
mmu-mir-466b-3	MI0005504	miRBase LINK	7	6	54	8	6	27	108	0.875	1.000	2.000
mmu-mir-539	MI0003520	miRBase LINK	2	0	14	0	0	7	23	#DIV/0!	#DIV/0!	2.000
mmu-mir-547	MI0003523	miRBase LINK	0	1	2	0	10	1	14	#DIV/0!	0.100	2.000
mmu-mir-669h	MI0006289	miRBase LINK	0	0	2	0	0	1	3	#DIV/0!	#DIV/0!	2.000
mmu-mir-199b	MI0000714	miRBase LINK	4,178	17,125	107,930	9,223	24,025	54,220	216,701	0.453	0.713	1.991
mmu-mir-181d	MI0005450	miRBase LINK	1,317	353	2,840	2,036	506	1,429	8,481	0.647	0.698	1.987
mmu-mir-674	MI0004611	miRBase LINK	417	377	1,656	623	267	836	4,176	0.669	1.412	1.981
mmu-mir-23b	MI0000141	miRBase LINK	485	8,475	16,917	745	8,883	8,549	44,054	0.651	0.954	1.979
mmu-mir-495	MI0004639	miRBase LINK	0	8	220	9	8	114	359	0.000	1.000	1.930
mmu-mir-134	MI0000160	miRBase LINK	16	5	239	101	9	124	494	0.158	0.556	1.927
mmu-mir-431	MI0001524	miRBase LINK	41	11	1,110	158	9	579	1,908	0.259	1.222	1.917
mmu-mir-466c			24	33	276	21	45	144	543	1.143	0.733	1.917
mmu-mir-669a-3	MI0004668	miRBase LINK	15	23	157	48	6	82	331	0.313	3.833	1.915
mmu-mir-181c	MI0000724	miRBase LINK	5,818	5,782	34,967	8,210	10,013	18,384	83,174	0.709	0.577	1.902
mmu-mir-32	MI0000691	miRBase LINK	22	1,000	1,235	7	656	650	3,570	3.143	1.524	1.900
mmu-mir-505	MI0004706	miRBase LINK	28	79	112	27	58	59	363	1.037	1.362	1.898
mmu-mir-15b	MI0000140	miRBase LINK	3,219	1,918	5,791	3,407	1,569	3,074	18,978	0.945	1.222	1.884
mmu-mir-466b-1	MI0005502	miRBase LINK	48	54	438	48	53	234	875	1.000	1.019	1.872
mmu-mir-466a	MI0002401	miRBase LINK	8	8	71	7	10	38	142	1.143	0.800	1.868
mmu-mir-500	MI0004702	miRBase LINK	34	141	627	74	162	337	1,375	0.459	0.870	1.861
mmu-mir-322	MI0000590	miRBase LINK	281	1,774	18,296	320	1,581	9,847	32,099	0.878	1.122	1.858
mmu-mir-450b	MI0004705	miRBase LINK	35	278	1,238	37	257	670	2,515	0.946	1.082	1.848
mmu-mir-466b-2	MI0005503	miRBase LINK	8	9	72	8	9	39	145	1.000	1.000	1.846
mmu-mir-450a-1	MI0001653	miRBase LINK	22	514	1,665	16	547	903	3,667	1.375	0.940	1.844
mmu-let-7i	MI0000138	miRBase LINK	36,717	37,261	191,131	43,314	35,448	103,687	447,558	0.848	1.051	1.843
mmu-mir-450a-2	MI0003537	miRBase LINK	22	512	1,654	17	549	901	3,655	1.294	0.933	1.836
mmu-mir-149	MI0000171	miRBase LINK	1,128	2,485	2,990	1,681	598	1,635	10,517	0.671	4.156	1.829
mmu-mir-34a	MI0000584	miRBase LINK	31	784	5,181	63	427	2,838	9,324	0.492	1.836	1.826
mmu-mir-466e	MI0005506	miRBase LINK	16	16	142	16	18	78	286	1.000	0.889	1.821
mmu-mir-300	MI0000400	miRBase LINK	65	41	2,666	179	53	1,469	4,473	0.363	0.774	1.815
mmu-mir-21	MI0000569	miRBase LINK	33,913	675,905	833,457	57,300	872,282	459,536	2,932,393	0.592	0.775	1.814
mmu-mir-362	MI0000763	miRBase LINK	19	379	709	16	348	392	1,863	1.188	1.089	1.809
mmu-mir-381	MI0000798	miRBase LINK	155	59	4,680	340	85	2,600	7,919	0.456	0.694	1.800
mmu-mir-467b	MI0004671	miRBase LINK	1	16	104	1	17	58	197	1.000	0.941	1.793
mmu-mir-15a	MI0000564	miRBase LINK	13,121	19,585	20,015	12,934	17,333	11,210	94,198	1.014	1.130	1.785
mmu-mir-181a-1	MI0000697	miRBase LINK	50,781	54,617	675,748	91,806	53,250	380,583	1,306,785	0.553	1.026	1.776
mmu-mir-181a-2	MI0000223	miRBase LINK	50,960	54,780	672,973	92,313	53,412	380,437	1,304,875	0.552	1.026	1.769
mmu-mir-148b	MI0000617	miRBase LINK	513	3,255	3,523	540	2,943	1,992	12,766	0.950	1.106	1.769
mmu-mir-182	MI0000224	miRBase LINK	1,221	16,422	1,562	1,891	12,825	888	34,809	0.646	1.280	1.759
mmu-mir-677	MI0004634	miRBase LINK	5	364	237	22	363	135	1,126	0.227	1.003	1.756
mmu-mir-127	MI0000154	miRBase LINK	1,751	714	68,083	3,850	1,120	38,800	114,318	0.455	0.638	1.755
mmu-mir-201	MI0000244	miRBase LINK	4	58	7	3	52	4	128	1.333	1.115	1.750
mmu-mir-128-2	MI0000726	miRBase LINK	2,971	452	944	4,817	322	540	10,046	0.617	1.404	1.748
mmu-mir-666	MI0004553	miRBase LINK	2	1	108	6	0	62	179	0.333	#DIV/0!	1.742
mmu-mir-17	MI0000687	miRBase LINK	1,299	1,972	2,333	1,142	1,540	1,340	9,626	1.137	1.281	1.741
mmu-mir-421	MI0005496	miRBase LINK	2,166	285	1,204	2,543	263	694	7,155	0.852	1.084	1.735
mmu-mir-7a-2	MI0000729	miRBase LINK	3	335	171	5	328	99	941	0.600	1.021	1.727
mmu-mir-24-1	MI0000231	miRBase LINK	335	2,267	13,600	604	2,923	7,887	27,616	0.555	0.776	1.724
mmu-mir-184	MI0000226	miRBase LINK	20	15	98	73	50	57	313	0.274	0.300	1.719
mmu-mir-297a-5	MI0005490	miRBase LINK	0	0	12	10	1	7	30	0.000	0.000	1.714
mmu-mir-128-1	MI0000155	miRBase LINK	3,329	596	1,171	5,477	450	688	11,711	0.608	1.324	1.702
mmu-mir-132	MI0000158	miRBase LINK	471	396	1,704	621	356	1,010	4,558	0.758	1.112	1.687
mmu-mir-126	MI0000153	miRBase LINK	13,581	210,617	507,382	15,175	201,422	301,182	1,249,359	0.895	1.046	1.685
mmu-mir-665	MI0004171	miRBase LINK	1	0	42	10	0	25	78	0.100	#DIV/0!	1.680
mmu-mir-16-1	MI0000565	miRBase LINK	270,173	109,350	189,081	274,399	112,265	113,203	1,068,471	0.985	0.974	1.670
mmu-mir-24-2	MI0000572	miRBase LINK	790	3,781	25,120	1,311	4,695	15,056	50,753	0.603	0.805	1.668
mmu-mir-341	MI0000625	miRBase LINK	25	8	662	69	5	397	1,166	0.362	1.600	1.668
mmu-mir-1-2-as			0	2	5	0	2	3	12	#DIV/0!	1.000	1.667
mmu-mir-16-2	MI0000566	miRBase LINK	270,034	108,238	187,705	274,225	111,159	112,639	1,064,000	0.985	0.974	1.666
mmu-mir-212	MI0000696	miRBase LINK	42	76	326	75	64	196	779	0.560	1.188	1.663
mmu-mir-185	MI0000227	miRBase LINK	91	1,001	765	91	901	462	3,311	1.000	1.111	1.656
mmu-mir-301a	MI0000401	miRBase LINK	1,103	1,619	4,351	1,210	1,203	2,629	12,115	0.912	1.346	1.655
mmu-mir-467c	MI0005512	miRBase LINK	1	5	43	0	4	26	79	#DIV/0!	1.250	1.654
mmu-mir-326	MI0000598	miRBase LINK	212	287	2,204	313	417	1,335	4,768	0.677	0.688	1.651
mmu-mir-668	MI0004134	miRBase LINK	27	0	224	96	2	136	485	0.281	0.000	1.647
mmu-mir-152	MI0000174	miRBase LINK	183	2,975	10,113	298	2,440	6,141	22,150	0.614	1.219	1.647
mmu-mir-452	MI0001734	miRBase LINK	0	3	36	6	4	22	71	0.000	0.750	1.636
mmu-mir-673	MI0004601	miRBase LINK	58	7	453	168	4	277	967	0.345	1.750	1.635
mmu-mir-667	MI0004196	miRBase LINK	18	1	123	51	1	76	270	0.353	1.000	1.618
mmu-mir-186	MI0000228	miRBase LINK	20,174	17,459	51,457	22,453	16,000	31,850	159,393	0.898	1.091	1.616
mmu-mir-19a	MI0000688	miRBase LINK	151	444	149	147	382	93	1,366	1.027	1.162	1.602
mmu-mir-669c	MI0004673	miRBase LINK	1	18	91	10	7	57	184	0.100	2.571	1.596
mmu-mir-700	MI0004684	miRBase LINK	27	52	258	23	72	163	595	1.174	0.722	1.583
mmu-mir-23a	MI0000571	miRBase LINK	4,046	3,914	44,281	7,353	5,152	28,227	92,973	0.550	0.760	1.569
mmu-mir-139	MI0000693	miRBase LINK	339	2,056	9,577	382	1,835	6,106	20,295	0.887	1.120	1.568
mmu-mir-27a	MI0000578	miRBase LINK	2,777	8,389	65,837	3,388	8,827	42,164	131,382	0.820	0.950	1.561
mmu-mir-19b-1	MI0000718	miRBase LINK	1,366	5,002	2,546	1,374	5,222	1,633	17,143	0.994	0.958	1.559
mmu-mir-19b-2	MI0000546	miRBase LINK	1,368	5,031	2,540	1,375	5,241	1,632	17,187	0.995	0.960	1.556
mmu-mir-7a-1	MI0000728	miRBase LINK	51	465	333	33	492	217	1,591	1.545	0.945	1.535
mmu-mir-138-2	MI0000164	miRBase LINK	271	98	1,608	488	60	1,059	3,584	0.555	1.633	1.518
mmu-mir-194-2	MI0000733	miRBase LINK	636	160,390	2,112	566	142,987	1,393	308,084	1.124	1.122	1.516
mmu-mir-338	MI0000619	miRBase LINK	58	581	1,375	64	681	910	3,669	0.906	0.853	1.511
mmu-mir-98	MI0000586	miRBase LINK	1,262	8,984	18,009	1,521	8,447	11,921	50,144	0.830	1.064	1.511
mmu-mir-689-1			1,919	2,643	2,029	2,160	2,465	1,349	12,565	0.888	1.072	1.504
mmu-mir-30b	MI0000145	miRBase LINK	13,651	52,808	70,119	16,874	43,695	46,626	243,773	0.809	1.209	1.504
mmu-mir-879	MI0005472	miRBase LINK	0	56	9	3	34	6	108	0.000	1.647	1.500
mmu-mir-669f	MI0006287	miRBase LINK	0	4	12	0	2	8	26	#DIV/0!	2.000	1.500
mmu-mir-466f-2	MI0005508	miRBase LINK	2	0	9	4	0	6	21	0.500	#DIV/0!	1.500
mmu-mir-466f-3	MI0005509	miRBase LINK	2	0	6	0	1	4	13	#DIV/0!	0.000	1.500
mmu-mir-325	MI0000597	miRBase LINK	0	0	3	0	0	2	5	#DIV/0!	#DIV/0!	1.500
mmu-mir-20a	MI0000568	miRBase LINK	239	2,168	1,656	306	1,918	1,114	7,401	0.781	1.130	1.487
mmu-mir-708	MI0004692	miRBase LINK	1	8	11,079	7	0	7,466	18,561	0.143	#DIV/0!	1.484

mmu-mir-22	MI0000570	miRBase_LINK	338,851	3,965,596	4,079,202	420,007	4,183,928	2,763,563	15,751,147	0.807	0.948	1.476
mmu-mir-188	MI0000230	miRBase_LINK	10	58	218	32	49	148	515	0.313	1.184	1.473
mmu-mir-181b-2	MI0000823	miRBase_LINK	3,670	2,242	28,133	6,614	2,261	19,128	62,048	0.555	0.992	1.471
mmu-mir-194-1	MI0000236	miRBase_LINK	646	159,842	2,109	615	142,468	1,435	307,115	1.050	1.122	1.470
mmu-mir-181b-1	MI0000723	miRBase_LINK	3,625	2,174	27,208	6,530	2,188	18,561	60,286	0.555	0.994	1.466
mmu-mir-196a-2	MI0000553	miRBase_LINK	6	4	208	15	0	142	375	0.400	#DIV/0!	1.465
mmu-mir-129-2	MI0000585	miRBase_LINK	26	17	19	32	23	13	130	0.813	0.739	1.462
mmu-mir-30e	MI0000259	miRBase_LINK	61,653	170,748	125,889	80,846	193,521	86,176	718,833	0.763	0.882	1.461
mmu-mir-672	MI0004258	miRBase_LINK	25	2	29	48	3	20	127	0.521	0.667	1.450
mmu-mir-669b	MI0004666	miRBase_LINK	0	6	29	0	0	20	55	#DIV/0!	#DIV/0!	1.450
mmu-mir-532	MI0003206	miRBase_LINK	3,030	3,678	13,418	4,082	3,515	9,271	36,994	0.742	1.046	1.447
mmu-mir-196a-1	MI0000552	miRBase_LINK	1	4	166	10	0	115	296	0.100	#DIV/0!	1.443
mmu-mir-374	MI0004125	miRBase_LINK	124	744	892	138	797	622	3,317	0.899	0.934	1.434
mmu-mir-129-1	MI0000222	miRBase_LINK	22	42	10	23	47	7	151	0.957	0.894	1.429
mmu-mir-154	MI0000176	miRBase_LINK	7	6	294	14	14	206	541	0.500	0.429	1.427
mmu-mir-497	MI0004636	miRBase_LINK	905	5,291	62,720	1,108	5,683	44,269	119,976	0.817	0.931	1.417
mmu-mir-872	MI0005549	miRBase_LINK	680	3,287	8,002	1,134	3,115	5,662	21,880	0.600	1.055	1.413
mmu-mir-30d	MI0000549	miRBase_LINK	86,140	170,538	352,452	146,223	200,896	251,104	1,207,353	0.589	0.849	1.404
mmu-mir-1197	MI0006305	miRBase_LINK	0	0	7	0	0	5	12	#DIV/0!	#DIV/0!	1.400
mmu-mir-195	MI0000237	miRBase_LINK	245	2,198	23,070	321	2,860	16,523	45,217	0.763	0.769	1.396
mmu-mir-351	MI0000643	miRBase_LINK	272	2,552	5,554	463	2,370	3,998	15,209	0.587	1.077	1.389
mmu-mir-192	MI0000551	miRBase_LINK	55,437	2,530,616	20,099	55,249	2,670,751	14,550	5,346,702	1.003	0.948	1.381
mmu-mir-744	MI0004124	miRBase_LINK	5,312	3,379	5,628	8,151	2,647	4,085	29,202	0.652	1.277	1.378
mmu-mir-574	MI0005518	miRBase_LINK	1,276	1,495	3,443	2,826	1,397	2,512	12,949	0.452	1.070	1.371
mmu-mir-467d	MI0005513	miRBase_LINK	14	27	182	19	10	133	385	0.737	2.700	1.368
mmu-mir-183	MI0000225	miRBase_LINK	128	655	75	334	426	55	1,673	0.383	1.538	1.364
mmu-mir-805			66	34,480	8,415	105	50,488	6,215	99,769	0.629	0.683	1.354
mmu-mir-101a	MI0000148	miRBase_LINK	1,277	88,769	58,100	1,312	74,119	43,132	266,709	0.973	1.198	1.347
mmu-mir-582	MI0006127	miRBase_LINK	108	360	465	268	84	346	1,631	0.403	4.286	1.344
mmu-mir-466f-1	MI0005507	miRBase_LINK	2	0	4	0	0	3	9	#DIV/0!	#DIV/0!	1.333
mmu-mir-877	MI0005553	miRBase_LINK	141	41	169	245	25	128	749	0.576	1.640	1.320
mmu-mir-491	MI0004680	miRBase_LINK	0	5	13	0	5	10	33	#DIV/0!	1.000	1.300
mmu-mir-689-2			17,105	10,236	8,756	32,701	9,330	6,780	84,908	0.523	1.097	1.291
mmu-mir-503	MI0003538	miRBase_LINK	24	67	302	41	66	234	734	0.585	1.015	1.291
mmu-let-7f-2	MI0000563	miRBase_LINK	16,610	684,828	778,838	25,149	593,665	604,641	2,703,731	0.660	1.154	1.288
mmu-mir-467e	MI0006128	miRBase_LINK	3	9	72	2	14	56	156	1.500	0.643	1.286
mmu-mir-449a	MI0001649	miRBase_LINK	16	2	45	9	2	35	109	1.778	1.000	1.286
mmu-let-7f-1	MI0000562	miRBase_LINK	11,642	621,181	731,371	17,964	543,185	572,647	2,497,990	0.648	1.144	1.277
mmu-mir-702	MI0004686	miRBase_LINK	10	10	38	19	2	30	109	0.526	5.000	1.267
mmu-mir-685			728	1,949	1,744	1,116	1,585	1,382	8,504	0.652	1.230	1.262
mmu-mir-26b	MI0000575	miRBase_LINK	4,225	87,418	89,191	4,349	85,187	70,989	341,359	0.971	1.026	1.256
mmu-mir-144	MI0000168	miRBase_LINK	1,799	4,959	6,557	2,217	2,337	5,264	23,133	0.811	2.122	1.246
mmu-let-7g	MI0000137	miRBase_LINK	24,376	121,676	109,960	28,263	143,036	88,635	515,946	0.862	0.851	1.241
mmu-mir-484	MI0003491	miRBase_LINK	4,496	1,844	4,994	5,858	1,315	4,045	22,552	0.767	1.402	1.235
mmu-mir-699			8	122	195	30	144	158	657	0.267	0.847	1.234
mmu-mir-324	MI0000595	miRBase_LINK	372	297	956	432	198	775	3,030	0.861	1.500	1.234
mmu-mir-758	MI0004129	miRBase_LINK	0	0	16	0	0	13	29	#DIV/0!	#DIV/0!	1.231
mmu-mir-423	MI0004637	miRBase_LINK	55,077	14,248	16,921	89,556	11,061	13,761	200,624	0.615	1.288	1.230
mmu-mir-493	MI0005514	miRBase_LINK	0	1	11	8	1	9	30	0.000	1.000	1.222
mmu-mir-350	MI0000640	miRBase_LINK	340	422	1,977	429	427	1,619	5,214	0.793	0.988	1.221
mmu-mir-28	MI0000690	miRBase_LINK	691	7,653	8,991	1,027	5,588	7,377	31,327	0.673	1.370	1.219
mmu-let-7e	MI0000561	miRBase_LINK	534	3,481	28,628	1,146	5,389	23,560	62,738	0.466	0.646	1.215
mmu-mir-425	MI0001447	miRBase_LINK	5,323	4,145	8,496	7,343	3,756	6,993	36,056	0.725	1.104	1.215
mmu-mir-148a	MI0000550	miRBase_LINK	10,609	903,788	326,358	11,294	998,441	270,135	2,520,625	0.939	0.905	1.208
mmu-mir-151	MI0000173	miRBase_LINK	9,486	31,203	95,030	15,283	27,328	78,781	257,111	0.621	1.142	1.206
mmu-mir-1191	MI0006296	miRBase_LINK	8	54	77	3	50	64	256	2.667	1.080	1.203
mmu-mir-451	MI0001730	miRBase_LINK	175,527	26,684	63,120	155,992	15,663	52,887	489,873	1.125	1.704	1.193
mmu-let-7a-1	MI0000556	miRBase_LINK	22,232	229,736	311,658	32,557	244,268	263,340	1,103,791	0.683	0.941	1.183
mmu-let-7a-2	MI0000557	miRBase_LINK	22,147	227,308	310,107	32,488	242,059	262,321	1,096,430	0.682	0.939	1.182
mmu-mir-191	MI0000233	miRBase_LINK	65,738	70,411	197,169	98,887	77,767	166,952	676,924	0.665	0.905	1.181
mmu-mir-361	MI0000761	miRBase_LINK	636	1,706	2,271	802	1,446	1,938	8,799	0.793	1.180	1.172
mmu-mir-29b-1	MI0000143	miRBase_LINK	74	3,496	2,779	103	3,291	2,396	12,139	0.718	1.062	1.160
mmu-let-7d	MI0000405	miRBase_LINK	19,639	51,637	74,003	28,501	42,117	64,215	280,112	0.689	1.226	1.152
mmu-mir-33	MI0000707	miRBase_LINK	40	725	244	44	431	212	1,696	0.909	1.682	1.151
mmu-mir-200b	MI0000243	miRBase_LINK	69	965	216	171	1,558	188	3,167	0.404	0.619	1.149
mmu-mir-140	MI0000165	miRBase_LINK	47,426	11,017	18,802	58,767	7,978	16,400	160,390	0.807	1.381	1.146
mmu-mir-466h	MI0005511	miRBase_LINK	1	3	16	8	3	14	45	0.125	1.000	1.143
mmu-mir-694	MI0004664	miRBase_LINK	0	5	8	6	4	7	30	0.000	1.250	1.143
mmu-mir-29b-2	MI0000712	miRBase_LINK	82	3,524	2,730	111	3,061	2,393	11,901	0.739	1.151	1.141
mmu-mir-92b	MI0005521	miRBase_LINK	382	43	341	684	119	309	1,878	0.558	0.361	1.104
mmu-let-7c-2	MI0000560	miRBase_LINK	72,776	164,719	345,608	118,692	170,389	313,353	1,185,537	0.613	0.967	1.103
mmu-let-7c-1	MI0000559	miRBase_LINK	72,525	161,513	342,882	118,216	167,212	311,496	1,173,844	0.613	0.966	1.101
mmu-mir-92a-1	MI0000719	miRBase_LINK	261,995	104,687	72,981	307,148	106,440	66,478	919,729	0.853	0.984	1.098
mmu-mir-92a-2	MI0000580	miRBase_LINK	99,452	9,614	12,718	113,997	8,089	11,624	255,494	0.872	1.189	1.094
mmu-mir-331	MI0000609	miRBase_LINK	59	313	543	66	246	497	1,724	0.894	1.272	1.093
mmu-mir-224	MI0000711	miRBase_LINK	86	57	723	145	74	664	1,749	0.593	0.770	1.089
mmu-mir-10a	MI0000685	miRBase_LINK	43,250	244,759	1,008,625	60,325	314,615	935,762	2,607,336	0.717	0.778	1.078
mmu-mir-320	MI0000704	miRBase_LINK	6,202	2,127	6,702	8,368	2,369	6,222	31,990	0.741	0.898	1.077
mmu-mir-365-2	MI0001645	miRBase_LINK	192	2,938	9,649	192	2,696	8,997	24,664	1.000	1.090	1.072
mmu-mir-1198	MI0006306	miRBase_LINK	1,567	320	489	1,670	268	456	4,770	0.938	1.194	1.072
mmu-mir-93	MI0000581	miRBase_LINK	42,293	14,738	27,822	42,227	14,053	26,003	167,136	1.002	1.049	1.070
mmu-mir-365-1	MI0000768	miRBase_LINK	184	2,901	9,541	186	2,657	8,918	24,387	0.989	1.092	1.070
mmu-mir-676	MI0005003	miRBase_LINK	3,001	1,716	5,549	4,209	1,221	5,249	20,945	0.713	1.405	1.057
mmu-mir-29c	MI0000577	miRBase_LINK	808	23,420	10,962	867	17,393	10,512	63,962	0.932	1.347	1.043
mmu-mir-204	MI0000247	miRBase_LINK	242	1	2,752	376	0	2,661	6,032	0.644	#DIV/0!	1.034
mmu-mir-100	MI0000692	miRBase_LINK	269	1,910	12,916	476	2,406	12,493	30,470	0.565	0.794	1.034
mmu-let-7b	MI0000558	miRBase_LINK	8,013	34,832	68,099	13,088	33,239	66,095	223,366	0.612	1.048	1.030
mmu-mir-101b	MI0000649	miRBase_LINK	1,894	215,325	19,259	1,459	154,713	18,731	411,381	1.298	1.392	1.028
mmu-mir-203	MI0000246	miRBase_LINK	1,701	23,074	11,688	4,293	23,155	11,380	75,291	0.396	0.997	1.027
mmu-mir-26a-2	MI0000706	miRBase_LINK	20,875	307,684	793,505	25,269	366,153	780,703	2,294,189	0.826	0.840	1.016
mmu-mir-26a-1	MI0000573	miRBase_LINK	20,871	307,545	793,290	25,267	365,994	780,582	2,293,549	0.826	0.840	1.016
mmu-mir-143	MI0000257	miRBase_LINK	26,388	278,402	2,360,422	31,475	452,685	2,327,301	5,476,673	0.838	0.615	1.014
mmu-mir-219-1	MI0000702	miRBase_LINK	77	119	62	76	112	62	508	1.013	1.063	1.000
mmu-mir-137	MI0000163	miRBase_LINK	0	273	1	0	179	1	454	#DIV/0!	1.525	1.000
mmu-mir-490	MI0005002	miRBase_LINK	99	6	8	194	16	8	331	0.510	0.375	1.000
mmu-mir-682	MI0004644	miRBase_LINK	26	76	14	33	102	14	265	0.788	0.745	1.000
mmu-mir-653	MI0005557	miRBase_LINK	4	0	2	6	1	2	15	0.667	0.000	1.000
mmu-mir-153	MI0000175	miRBase_LINK	6	1	1	0	4	1	13	#DIV/0!	0.250	1.000

mmu-mir-292	MI0000390	miRBase_LINK	0	6	1	0	0	1	8	#DIV/0!	#DIV/0!	1.000
mmu-mir-466f-4	MI0006291	miRBase_LINK	2	1	2	0	0	2	7	#DIV/0!	#DIV/0!	1.000
mmu-mir-686	MI0004650	miRBase_LINK	0	2	1	0	1	1	5	#DIV/0!	2.000	1.000
mmu-mir-693	MI0004662	miRBase_LINK	1	1	1	0	0	1	4	#DIV/0!	#DIV/0!	1.000
mmu-mir-7b	MI0000730	miRBase_LINK	0	0	2	0	0	2	4	#DIV/0!	#DIV/0!	1.000
mmu-mir-124-1	MI0000716	miRBase_LINK	0	0	1	2	0	1	4	0.000	#DIV/0!	1.000
mmu-mir-124-2	MI0000717	miRBase_LINK	0	0	1	2	0	1	4	0.000	#DIV/0!	1.000
mmu-mir-124-3	MI0000150	miRBase_LINK	0	0	1	2	0	1	4	0.000	#DIV/0!	1.000
mmu-mir-873	MI0005550	miRBase_LINK	0	1	1	0	0	1	3	#DIV/0!	#DIV/0!	1.000
mmu-mir-30c-1	MI0000547	miRBase_LINK	45,487	191,433	207,508	53,007	166,348	209,769	873,552	0.858	1.151	0.989
mmu-mir-29a	MI0000576	miRBase_LINK	10,752	77,404	98,142	13,359	82,945	99,229	381,831	0.805	0.933	0.989
mmu-mir-99b	MI0000147	miRBase_LINK	1,551	2,466	21,502	2,364	3,736	21,904	53,523	0.656	0.660	0.982
mmu-mir-200a	MI0000554	miRBase_LINK	230	718	156	332	1,377	159	2,972	0.693	0.521	0.981
mmu-mir-30c-2	MI0000548	miRBase_LINK	45,632	194,924	210,330	53,221	169,668	214,907	888,682	0.857	1.149	0.979
mmu-mir-187	MI0000229	miRBase_LINK	83	383	315	125	526	326	1,758	0.664	0.728	0.966
mmu-mir-330	MI0000607	miRBase_LINK	57	128	505	118	111	524	1,443	0.483	1.153	0.964
mmu-mir-218-1	MI0000700	miRBase_LINK	30	19	1,432	41	23	1,488	3,033	0.732	0.826	0.962
mmu-mir-218-2	MI0000701	miRBase_LINK	22	19	1,392	34	23	1,458	2,948	0.647	0.826	0.955
mmu-mir-1-1			30	3	77	38	6	81	235	0.789	0.500	0.951
mmu-mir-25	MI0000689	miRBase_LINK	195,450	19,655	47,352	192,381	19,725	49,959	524,522	1.016	0.996	0.948
mmu-mir-874	MI0005479	miRBase_LINK	46	243	85	46	114	90	624	1.000	2.132	0.944
mmu-mir-701	MI0004685	miRBase_LINK	0	0	15	0	2	16	33	#DIV/0!	0.000	0.938
mmu-mir-671	MI0004133	miRBase_LINK	149	1,253	987	220	993	1,060	4,662	0.677	1.262	0.931
mmu-mir-1-2			25	3	75	32	6	81	222	0.781	0.500	0.926
mmu-mir-615	MI0005004	miRBase_LINK	18	1	1,077	55	3	1,222	2,376	0.327	0.333	0.881
mmu-mir-10b	MI0000221	miRBase_LINK	54,948	1,404	2,277,812	74,813	2,390	2,626,307	5,037,674	0.734	0.587	0.867
mmu-mir-103-2	MI0000588	miRBase_LINK	27,499	42,040	142,351	29,023	28,914	164,768	434,595	0.947	1.454	0.864
mmu-mir-106b	MI0000407	miRBase_LINK	15,968	493	1,681	16,387	347	1,948	36,824	0.974	1.421	0.863
mmu-mir-125a	MI0000151	miRBase_LINK	4,192	10,692	72,514	6,653	16,382	84,101	194,534	0.630	0.653	0.862
mmu-mir-107	MI0000684	miRBase_LINK	21,491	29,102	18,384	21,360	16,679	21,326	128,342	1.006	1.745	0.862
mmu-mir-103-1	MI0000587	miRBase_LINK	27,496	41,808	140,803	29,020	28,764	163,598	431,489	0.947	1.453	0.861
mmu-mir-715			24	7	6	43	3	7	90	0.558	2.333	0.857
mmu-mir-138-1	MI0000722	miRBase_LINK	7	0	6	23	1	7	44	0.304	0.000	0.857
mmu-mir-130a	MI0000156	miRBase_LINK	4,735	34,984	61,132	6,012	27,528	71,682	206,073	0.788	1.271	0.853
mmu-mir-125b-2	MI0000152	miRBase_LINK	1,701	6,853	31,682	3,133	7,909	37,227	88,505	0.543	0.866	0.851
mmu-mir-145	MI0000169	miRBase_LINK	527	4,783	34,032	739	6,085	40,619	86,785	0.713	0.786	0.838
mmu-mir-190b	MI0005478	miRBase_LINK	8	37	48	14	49	58	214	0.571	0.755	0.828
mmu-mir-125b-1	MI0000725	miRBase_LINK	1,654	5,705	27,240	3,087	6,755	33,021	77,462	0.536	0.845	0.825
mmu-mir-429	MI0001642	miRBase_LINK	421	833	177	887	1,335	215	3,868	0.475	0.624	0.823
mmu-mir-193	MI0000235	miRBase_LINK	60	20,655	24,669	55	13,998	30,595	90,032	1.091	1.476	0.806
mmu-mir-30a	MI0000144	miRBase_LINK	138,290	1,092,020	1,250,491	195,513	1,174,404	1,551,606	5,402,324	0.707	0.930	0.806
mmu-mir-150	MI0000172	miRBase_LINK	36,117	2,616	40,846	54,152	1,326	50,744	185,801	0.667	1.973	0.805
mmu-mir-99a	MI0000146	miRBase_LINK	275	3,886	10,906	526	4,188	13,606	33,387	0.523	0.928	0.802
mmu-mir-339	MI0000621	miRBase_LINK	312	1,102	2,563	491	1,106	3,206	8,780	0.635	0.996	0.799
mmu-mir-216a	MI0000699	miRBase_LINK	14	11	6	9	1	8	49	1.556	11.000	0.750
mmu-mir-133b	MI0000821	miRBase_LINK	525	2	99	844	5	133	1,608	0.622	0.400	0.744
mmu-mir-344-1	MI0000630	miRBase_LINK	3	2	45	19	1	62	132	0.158	2.000	0.726
mmu-mir-344-2	MI0005495	miRBase_LINK	3	2	45	19	1	62	132	0.158	2.000	0.726
mmu-mir-328	MI0000603	miRBase_LINK	4,943	730	2,213	6,840	696	3,091	18,513	0.723	1.049	0.716
mmu-mir-210	MI0000695	miRBase_LINK	296	369	709	278	348	1,038	3,038	1.065	1.060	0.683
mmu-mir-135b	MI0000646	miRBase_LINK	0	0	4	0	0	6	10	#DIV/0!	#DIV/0!	0.667
mmu-mir-378	MI0000795	miRBase_LINK	37,243	237,812	234,917	55,688	171,521	366,144	1,103,325	0.669	1.386	0.642
mmu-mir-345	MI0000632	miRBase_LINK	202	830	660	238	935	1,106	3,971	0.849	0.888	0.597
mmu-mir-486	MI0003493	miRBase_LINK	1,715,391	31,647	92,856	2,085,838	21,114	157,644	4,104,490	0.822	1.499	0.589
mmu-mir-133a-1	MI0000159	miRBase_LINK	41,161	90	2,675	79,581	146	4,555	128,208	0.517	0.616	0.587
mmu-mir-133a-2	MI0000820	miRBase_LINK	41,106	89	2,673	79,491	146	4,553	128,058	0.517	0.610	0.587
mmu-mir-196b	MI0001151	miRBase_LINK	12	4	122	19	6	211	374	0.632	0.667	0.578
mmu-mir-208b	MI0005552	miRBase_LINK	11	0	1	35	1	2	50	0.314	0.000	0.500
mmu-mir-193b	MI0005484	miRBase_LINK	168	120	2,000	265	111	4,108	6,772	0.634	1.081	0.487
mmu-mir-217	MI0000731	miRBase_LINK	5	6	7	8	0	15	41	0.625	#DIV/0!	0.467
mmu-mir-219-2	MI0000741	miRBase_LINK	5	21	2	1	13	5	47	5.000	1.615	0.400
mmu-mir-384	MI0001146	miRBase_LINK	3	1	3	0	0	9	16	#DIV/0!	#DIV/0!	0.333
mmu-mir-670	MI0004295	miRBase_LINK	0	0	1	0	0	3	4	#DIV/0!	#DIV/0!	0.333
mmu-mir-135a-2	MI0000715	miRBase_LINK	3	0	1	3	0	4	11	1.000	#DIV/0!	0.250
mmu-mir-135a-1	MI0000161	miRBase_LINK	1	0	1	2	0	4	8	0.500	#DIV/0!	0.250
mmu-mir-483	MI0003484	miRBase_LINK	6	1	5	21	0	24	57	0.286	#DIV/0!	0.208
mmu-mir-215	MI0000974	miRBase_LINK	32,484	494	245	50,380	685	1,930	86,218	0.645	0.721	0.127
mmu-mir-871	MI0005471	miRBase_LINK	9	70	0	5	99	1	184	1.800	0.707	0.000
mmu-mir-216b	MI0004126	miRBase_LINK	37	10	0	8	3	1	59	4.625	3.333	0.000
mmu-mir-1192	MI0006297	miRBase_LINK	0	9	0	0	5	3	17	#DIV/0!	1.800	0.000
mmu-mir-206	MI0000249	miRBase_LINK	0	1	0	10	0	1	12	0.000	#DIV/0!	0.000
mmu-mir-720	MI0004678	miRBase_LINK	5	2	0	0	0	1	8	#DIV/0!	#DIV/0!	0.000
mmu-mir-713	MI0004698	miRBase_LINK	0	0	0	0	0	4	4	#DIV/0!	#DIV/0!	0.000
mmu-mir-207	MI0000250	miRBase_LINK	0	0	0	0	0	1	1	#DIV/0!	#DIV/0!	0.000

Supplementary Table 3. The comparison of global mRNA expression in Mir221/222AdipoKO and Mir221/222flox/y mice fed with standard (STD) chow.

	Sample name	Negative control
Test	STD AdipoKO 387	55.43
Control	STD flox/y 378	60.07

2Up	Ratio ≧ 2 and Expression value of test sample ≧ Negative control (average)
2Down	Ratio ≦ 0.5 and Expression value of test sample ≧ Negative control (average)

Feature ID	Normalized data				Flag			Annotation																	Keyword
Probe Set II	Expression	Expression	Ratio	Log2Ratio	解析対象 Fl	category	Ratio flag	Gene Acces	Gene Symb	Gene Descr	mRNA Acc	mRNA Sou	mRna - Des	mRNA - xhy	EntrezGene	UniGene ID	SwissProt a	Chromosom	GO Biologic	GO Biologic	GO Cellular	GO Cellular	GO Molecul	GO Molecul	miR221/222 target gene
17211066	12.07175	12.77533	0.9449267	-0.081726	0	main		NM_177722	Mcmdc2	minichromo	NM_177722	RefSeq	Mus muscu	FALSE	240697	Mm.259800	E9Q956	chr1	GO:000626	DNA replica	GO:000557	cellular_con	GO:000367	DNA bindin	○
17211305	39.99381	41.28632	0.968694	-0.045887	0	main		NM_053191	Pi15	peptidase ir	NM_053191	RefSeq	Mus muscu	FALSE	94227	Mm.442452	Q8BS03	chr1	GO:001046	negative reg	GO:000557	extracellular	GO:003041	peptidase ir	○
17211548	28.72986	30.91425	0.9293404	-0.105721	0	main		NM_133235	Khdrbs2	KH domain	NM_133235	RefSeq	Mus muscu	FALSE	170771	Mm.336594	Q9WU01	chr1	GO:000635	transcriptior	GO:000563	nucleus // r	GO:000372	RNA bindin	○
17212947	66.01734	73.47573	0.8984918	-0.154423	0	main		NM_001164	Spats2l	spermatoge	NM_001164	RefSeq	Mus muscu	FALSE	67198	Mm.159989	Q91WJ7	chr1	GO:000815	biological_p	GO:000563	nucleus // r	GO:004482	poly(A) RN/	○
17214841	450.3722	594.9557	0.7569844	-0.401664	0	main		NM_010472	Agfg1	ArfGAP witl	NM_010472	RefSeq	Mus muscu	FALSE	15463	Mm.433409	Q8K2K6	chr1	GO:000167	acrosome a	GO:000563	nucleus // c	GO:000367	DNA bindin	○
17215565	89.13591	94.91344	0.9391284	-0.090606	0	main		NM_133816	Sh3bp4	SH3-domaii	NM_133816	RefSeq	Mus muscu	FALSE	98402	Mm.170983	Q921I6	chr1	GO:000689	endocytosis	GO:000563	nucleus // c	GO:000509	GDP-dissoc	○
17216888	23.89316	26.84098	0.8901747	-0.16784	0	main		NM_172485	Thsd7b	thrombospo	NM_172485	RefSeq	Mus muscu	FALSE	210417	Mm.380518	Q6P4U0	chr1	GO:000815	biological_p	GO:001602	membrane	GO:000367	molecular_f	○
17217291	48.53498	42.96968	1.1295169	0.1757059	0	main		NM_001160	Plekha6	pleckstrin h	NM_001160	RefSeq	Mus muscu	FALSE	240753	Mm.253559	Q7TQG1	chr1	GO:000815	biological_p	GO:000557	cellular_con	GO:000367	molecular_f	○
17217854	90.1264	97.81096	0.9214346	-0.118046	0	main		ENSMUST0	Dennd1b	DENN/MAD	ENSMUST0	ENSEMBL	havana:kno	FALSE	329260	Mm.337604	Q3U1T9	chr1	GO:000681	transport //	GO:000573	cytoplasm /	GO:000508	guanyl-nucl	○
17217901	205.3408	238.968	0.8592816	-0.218797	0	main		NM_172643	Zbtb41	zinc finger a	NM_172643	RefSeq	Mus muscu	FALSE	226470	Mm.119711	Q811F1	chr1	GO:000635	transcriptior	GO:000563	nucleus	GO:000367	nucleic acid	○
17220177	28.33733	38.15434	0.7427027	-0.429143	0	main		ENSMUST0	Gm17275	predicted ge	ENSMUST0	ENSEMBL	ensembl_lir	FALSE	---	Mm.322735	P84244	chr1	GO:000633	nucleosome	GO:000078	nucleosome	GO:000367	DNA bindin	○
17220373	223.2658	264.4885	0.8441418	-0.244443	0	main		NM_173378	Trp53bp2	transformati	NM_173378	RefSeq	Mus muscu	FALSE	209456	Mm.287450	Q8CG79	chr1	GO:000691	apoptotic pr	GO:000563	nucleus // c	GO:000813	transcriptior	○
17220489	337.2852	305.6174	1.1036191	0.1422423	0	main		NM_001163	Rab3gap2	RAB3 GTPa	NM_001163	RefSeq	Mus muscu	FALSE	98732	Mm.275841	Q8BMG7	chr1	GO:004308	regulation o	GO:000573	cytoplasm /	GO:000509	GTPase act	○
17221158	18.37664	18.73044	0.981111	-0.027512	0	main		NM_001290	Mybl1	myeloblastc	NM_001290	RefSeq	Mus muscu	FALSE	17864	Mm.479	P51960	chr1	GO:000635	transcriptior	GO:000563	nucleus	GO:000367	DNA bindin	○
17222440	160.8323	235.9621	0.6816023	-0.552998	0	main		NM_019570	Rev1	REV1 homc	NM_019570	RefSeq	Mus muscu	FALSE	56210	Mm.389103	Q920Q2	chr1	GO:000626	DNA replica	GO:000563	nucleus	GO:000028	magnesium	○
17223138	87.21326	102.9134	0.8474432	-0.238811	0	main		NM_001163	Pgap1	post-GPI at	NM_001163	RefSeq	Mus muscu	FALSE	241062	Mm.103539	Q3UUQ7	chr1	GO:000650	GPI anchor	GO:000578	endoplasmi	GO:000451	nuclease ac	○
17223946	17.66826	16.0907	1.0980417	0.1349329	0	main		NM_010154	Erbb4	v-erb-a erytl	NM_010154	RefSeq	Mus muscu	FALSE	13869	Mm.442420	Q61527	chr1	GO:000175	neural crest	GO:000563	nucleus // c	GO:000016	nucleotide b	○
17225373	38.80965	27.58103	1.4071139	0.4927391	0	main		NM_010262	Gbx2	gastrulation	NM_010262	RefSeq	Mus muscu	FALSE	14472	Mm.204730	P48031	chr1	GO:000156	patterning o	GO:000563	nucleus	GO:000367	DNA bindin	○
17228426	344.0268	377.0215	0.9124859	-0.132126	0	main		NM_001039	Cep350	centrosoma	NM_001039	RefSeq	Mus muscu	FALSE	74081	Mm.260247	D3YTP2	chr1	GO:000815	biological_p	GO:000563	nucleus // c	GO:000367	molecular_f	○
17229178	183.1643	249.8483	0.733102	-0.447914	0	main		NM_009721	Atp1b1	ATPase, Na	NM_009721	RefSeq	Mus muscu	FALSE	11931	Mm.4550	P14094	chr1	GO:000166	response to	GO:000588	plasma mer	GO:000539	sodium:pota	○
17230469	56.31487	54.15099	1.0399601	0.0565282	0	main		ENSMUST0	Gm12657	predicted ge	ENSMUST0	ENSEMBL	havana:kno	FALSE	667250	Mm.449778	E0CYN1	chr1	GO:000164	osteoblast d	GO:000022	nuclear chrc	GO:000097	RNA polym	○
17230602	200.0101	210.6942	0.949291	-0.075078	0	main		NM_175127	Fbxo28	F-box protei	NM_175127	RefSeq	Mus muscu	FALSE	67948	Mm.30737	Q8BIG4	chr1	GO:000815	biological_p	GO:000557	cellular_con	GO:000367	molecular_f	○
17230668	296.3055	311.7881	0.9503426	-0.07348	0	main		NM_177389	Mia3	melanoma i	NM_177389	RefSeq	Mus muscu	FALSE	338366	Mm.41152	Q8BI84	chr1	GO:000206	chondrocyte	GO:000578	endoplasmi	GO:000367	molecular_f	○
17230760	72.25445	85.06554	0.8493974	-0.235488	0	main		NM_145515	Mark1	MAP/microt	NM_145515	RefSeq	Mus muscu	FALSE	226778	Mm.7445	Q8VHJ5	chr1	GO:000022	microtubule	GO:000573	cytoplasm /	GO:000016	nucleotide b	○
17231461	203.3791	203.6139	0.9988468	-0.001665	0	main		NM_007956	Esr1	estrogen rec	NM_007956	RefSeq	Mus muscu	FALSE	13982	Mm.9213	P19785	chr10	GO:000154	antral ovaria	GO:000563	nucleus // r	GO:000104	core promot	○
17232483	13.10851	13.23052	0.9907781	-0.013366	0	main		XR_380237	LOC102632	uncharacter	XR_380237	RefSeq	PREDICTE	FALSE	102632938	---	Q8BG92	chr10	---	---	---	---	---	---	○
17232734	146.1333	158.2847	0.9232307	-0.115237	0	main		NM_001168	Cdk19	cyclin-deper	NM_001168	RefSeq	Mus muscu	FALSE	78334	Mm.200924	Q8BWD8	chr10	GO:000646	protein phos	GO:000557	cellular_con	GO:000016	nucleotide b	○
17233437	198.2301	215.519	0.9197802	-0.120639	0	main		NM_001193	Lims1	LIM and ser	NM_001193	RefSeq	Mus muscu	FALSE	110829	Mm.57734	Q99JW4	chr10	GO:000716	cell-matrix a	GO:000588	plasma mer	GO:000551	protein bind	○
17233457	855.5234	1143.976	0.7478508	-0.419178	0	main		NM_011240	Ranbp2	RAN binding	NM_011240	RefSeq	Mus muscu	FALSE	19386	Mm.431695	Q9ERU9	chr10	GO:000645	protein foldi	GO:000563	nucleus // r	GO:000372	RNA bindin	○
17235211	232.281	400.6118	0.5798157	-0.786334	0	main		NM_021565	Midn	midnolin	NM_021565	RefSeq	Mus muscu	FALSE	59090	Mm.143813	Q3TPJ7	chr10	GO:003313	negative reg	GO:000563	nucleus // r	GO:001990	kinase bindi	○
17236182	1467.903	1672.027	0.8779182	-0.187842	0	main		NM_011595	Timp3	tissue inhibi	NM_011595	RefSeq	Mus muscu	FALSE	21859	Mm.4871	P39876	chr10	GO:001046	negative reg	GO:000557	extracellular	GO:000485	enzyme inh	○
17236439	15.10888	15.49385	0.9751534	-0.036299	0	main		NM_001128	Anks1b	ankyrin repe	NM_001128	RefSeq	Mus muscu	FALSE	77531	Mm.440605	Q8BIZ1	chr10	GO:000815	biological_p	GO:000563	nucleus // c	GO:004687	ephrin recep	○
17238449	200.7531	198.2105	1.0128278	0.0183889	0	main		NM_172790	Ankrd52	ankyrin repe	NM_172790	RefSeq	Mus muscu	FALSE	237615	Mm.440177	Q8BTI7	chr10	GO:000815	biological_p	GO:000557	cellular_con	GO:000367	molecular_f	○
17238571	267.1325	268.5456	0.994738	-0.007612	0	main		NM_028873	Dnajc14	DnaJ (Hsp4	NM_028873	RefSeq	Mus muscu	FALSE	74330	Mm.296915	Q921R4	chr10	GO:000681	transport //	GO:000578	endoplasmi	GO:000166	G-protein co	○
17239234	28.48119	24.57605	1.1589002	0.2127564	0	main		NM_001114	Grm1	glutamate re	NM_001114	RefSeq	Mus muscu	FALSE	14816	Mm.482986	P97772	chr10	GO:000018	activation of	GO:000563	nucleus // p	GO:000163	PLC activat	○
17240123	11.9302	11.32564	1.0533798	0.0750257	0	main		XM_006512	Clvs2	clavesin 2	XM_006512	RefSeq	PREDICTE	FALSE	215890	Mm.94461	Q8BG92	chr10	GO:000681	transport //	GO:000562	intracellular	GO:000521	transporter a	○
17240226	245.2886	234.4308	1.0463156	0.0653181	0	main		NM_008538	Marcks	myristoylate	NM_008538	RefSeq	Mus muscu	FALSE	17118	Mm.30059	P26645	chr10	---	---	GO:000573	cytoplasm /	GO:000377	actin bindin	○
17241032	482.7296	187.1108	2.5799131	1.3673225	0	main	2Up	NM_029083	Ddit4	DNA-damag	NM_029083	RefSeq	Mus muscu	FALSE	74747	Mm.21697	Q9D3F7	chr10	GO:000166	response to	GO:000562	intracellular	GO:007188	14-3-3 prote	○
17243509	141.4882	139.9786	1.0107845	0.0154755	0	main		NM_010914	Nfyb	nuclear tran	NM_010914	RefSeq	Mus muscu	FALSE	18045	Mm.245998	P63139	chr10	GO:000635	transcriptior	GO:000562	intracellular	GO:000367	DNA bindin	○
17245095	357.7865	384.7924	0.929817	-0.104981	0	main		NM_001037	Cnot2	CCR4-NOT	NM_001037	RefSeq	Mus muscu	FALSE	72068	Mm.351553	Q8C5L3	chr10	GO:000012	negative reg	GO:000563	nucleus // c	GO:000122	RNA polym	○
17245188	316.8773	293.1326	1.0810033	0.1123709	0	main		NM_177798	Frs2	fibroblast gr	NM_177798	RefSeq	Mus muscu	FALSE	327826	Mm.135965	Q8C180	chr10	GO:000018	activation of	GO:000573	cytoplasm /	GO:000506	transmembr	○
17245587	437.382	454.9009	0.9614885	-0.056658	0	main		NM_001163	Mon2	MON2 hom	NM_001163	RefSeq	Mus muscu	FALSE	67074	Mm.169924	Q80TL7	chr10	GO:000681	transport //	GO:000580	trans-Golgi	GO:000508	ARF guanyl	○
17246268	56.10082	51.18897	1.0959552	0.1321889	0	main		NM_011772	Ikzf4	IKAROS far	NM_011772	RefSeq	Mus muscu	FALSE	22781	Mm.358648	Q8C208	chr10	GO:000635	transcriptior	GO:000563	nucleus	GO:000367	nucleic acid	○
17247448	279.4539	315.9281	0.884549	-0.176986	0	main		ENSMUST0	Ppp3r1	protein phos	ENSMUST0	ENSEMBL	havana:kno	FALSE	19058	Mm.41840	Q63810	chr11	GO:000156	patterning o	GO:000562	intracellular	GO:000472	phosphopro	○
17247519	152.9826	168.062	0.9102748	-0.135626	0	main		NM_033523	Spred2	sprouty-rela	NM_033523	RefSeq	Mus muscu	FALSE	114716	Mm.266627	Q924S7	chr11	GO:000018	inactivation	GO:000563	nucleus // c	GO:000517	stem cell fa	○
17247533	1104.707	1084.556	1.01858	0.0265592	0	main		ENSMUST0	Rab1	RAB1, mem	ENSMUST0	ENSEMBL	havana:kno	FALSE	19324	Mm.271944	P62821	chr11	GO:000004	autophagic	GO:000013	Golgi memb	GO:000016	nucleotide b	○
17247550	335.193	423.2663	0.7919199	-0.336574	0	main		ENSMUST0	Peli1	pellino 1	ENSMUST0	ENSEMBL	havana:kno	FALSE	67245	Mm.28957	Q8C669	chr11	GO:000020	protein poly	GO:000563	nucleus	GO:000484	ubiquitin-pr	○
17248213	497.7278	864.8309	0.5755204	-0.797061	0	main		NM_001290	Cpeb4	cytoplasmic	NM_001290	RefSeq	Mus muscu	FALSE	67579	Mm.339792	Q7TN98	chr11	GO:000293	response to	GO:000563	nucleus // r	GO:000016	nucleotide b	○
17248288	106.309	143.4328	0.7411764	-0.432111	0	main		NM_177364	Sh3pxd2b	SH3 and PX	NM_177364	RefSeq	Mus muscu	FALSE	268396	Mm.227616	A2AAY5	chr11	GO:000150	skeletal syst	GO:000210	podosome	GO:001031	phosphatidy	○
17248476	946.3215	939.384	1.0073852	0.0106154	0	main		NM_145962	Pank3	pantothenat	NM_145962	RefSeq	Mus muscu	FALSE	211347	Mm.255044	Q8R2W9	chr11	GO:001593	coenzyme A	GO:000573	cytoplasm /	GO:000016	nucleotide b	○
17253307	200.6664	296.9527	0.6757521	-0.565434	0	main		NM_001024	Nufip2	nuclear frag	NM_001024	RefSeq	Mus muscu	FALSE	68564	Mm.428996	Q5F2E7	chr11	---	---	GO:000563	nucleus // c	GO:000372	RNA bindin	○
17254933	336.5393	393.6081	0.8550111	-0.225985	0	main		NM_016686	Vezf1	vascular end	NM_016686	RefSeq	Mus muscu	FALSE	22344	Mm.46628	Q5SXC3	chr11	GO:000152	angiogenesi	GO:000563	nucleus // r	GO:000367	nucleic acid	○
17255443	224.2298	225.9709	0.992295	-0.011159	0	main		NM_201609	Zfp652	zinc finger p	NM_201609	RefSeq	Mus muscu	FALSE	268469	Mm.389038	Q5DU09	chr11	GO:000635	transcriptior	GO:000563	nucleus	GO:000367	nucleic acid	○
17255727	63.1117	61.25826	1.0302562	0.0430031	0	main		NM_001081	Osbpl7	oxysterol bir	NM_001081	RefSeq	Mus muscu	FALSE	71240	Mm.190450	A2A716	chr11	GO:000681	transport //	GO:000577	autophagic	GO:001548	cholesterol	○
17255775	94.62283	106.8942	0.8852008	-0.175923	0	main		NM_138657	Socs7	suppressor	NM_138657	RefSeq	Mus muscu	FALSE	192157	Mm.34339	Q8VHQ2	chr11	GO:000828	insulin recep	GO:000563	nucleus // r	---	---	○
17255828	156.4574	181.5189	0.8619345	-0.21435	0	main		NM_139311	Mllt6	myeloid/lym	NM_139311	RefSeq	Mus muscu	FALSE	246198	Mm.23685	B1AR09	chr11	GO:000815	biological_p	GO:000557	cellular_con	GO:004687	metal ion bi	○
17256991	41.62211	38.2034	1.0894871	0.1236491	0	main		NM_001110	Adam11	a disintegrir	NM_001110	RefSeq	Mus muscu	FALSE	11488	Mm.89854	Q9R1V4	chr11	GO:000650	proteolysis	GO:001602	membrane	GO:000422	metalloendo	○
17257235	120.8629	120.3888	1.0039381	0.0056703	0	main		NM_016780	Itgb3	integrin beta	NM_016780	RefSeq	Mus muscu	FALSE	16416	Mm.87150	O54890	chr11	GO:000193	positive reg	GO:000563	nucleus // p	GO:000375	protein disu	○
17257801	83.89841	65.87026	1.2736918	0.3490162	0	main		NM_015732	Axin2	axin2	NM_015732	RefSeq	Mus muscu	FALSE	12006	Mm.71710	O88566	chr11	GO:000175	somitogene	GO:000562	intracellular	GO:000487	signal trans	○
17258789	189.1216	226.4071	0.8353166	-0.259605	0	main		NM_198022	Tnrc6c	trinucleotide	NM_198022	RefSeq	Mus muscu	FALSE	217351	Mm.40272	Q3UHC0	chr11	GO:000170	endoderm fo	GO:000557	cellular_con	GO:000016	nucleotide b	○
17261289	51.45292	45.55436	1.129484	0.1756638	0	main		NM_146016	Eml6	echinoderm	NM_146016	RefSeq	Mus muscu	FALSE	237711	Mm.445271	Q5SQM0	chr11	GO:000815	biological_p	GO:000573	cytoplasm /	GO:000367	molecular_f	○
17261896	27.95826	24.7414	1.1300193	0.1763474	0	main		NM_010250	Gabra1	gamma-ami	NM_010250	RefSeq	Mus muscu	FALSE	14394	Mm.439668	P62812	chr11	GO:000681	transport //	GO:000588	plasma mer	GO:000489	GABA-A re	○
17262055	57.27368	56.09911	1.0209374	0.0298944	0	main		NM_172524	Nipal4	NIPA-like do	NM_172524	RefSeq	Mus muscu	FALSE	214112	Mm.225253	Q8BZF2	chr11	GO:000681	transport //	GO:001602	membrane	GO:001509	magnesium	○
17262964	29.18693	28.15368	1.0367004	0.051999	0	main		NM_001029	Fat2	FAT tumor s	NM_001029	RefSeq	Mus muscu	FALSE	245827	Mm.339363	Q5F226	chr11	GO:000715	cell adhesio	GO:000563	nucleus // p	GO:000550	calcium ion	○
17266264	685.7847	808.1497	0.8485862	-0.236867	0	main		NM_144825	Taok1	TAO kinase	NM_144825	RefSeq	Mus muscu	FALSE	216965	Mm.340436	Q5F2E8	chr11	GO:000016	MAPK casc	GO:000573	cytoplasm /	GO:000016	nucleotide b	○
17266498	277.0902	313.5163	0.8838143	-0.178185	0	main		NM_008702	Nlk	nemo like ki	NM_008702	RefSeq	Mus muscu	FALSE	18099	Mm.9001	O54949	chr11	GO:000016	MAPK casc	GO:000563	nucleus // c	GO:000016	nucleotide b	○
17266534	125.6685	102.0037	1.2319994	0.3010016	0	main		NM_013571	Ksr1	kinase supp	NM_013571	RefSeq	Mus muscu	FALSE	16706	Mm.4745	Q61097	chr11	GO:000646	protein phos	GO:000573	cytoplasm /	GO:000467	protein kina	○
17267632	101.8389	105.6088	0.9643032	-0.052441	0	main		NM_019505	Dgke	diacylglycer	NM_019505	RefSeq	Mus muscu	FALSE	56077	Mm.153695	Q9R1C6	chr11	GO:000720	protein kina	GO:000573	cytoplasm /	GO:000016	nucleotide b	○
17270621	274.41	276.8301	0.9912578	-0.012668	0	main		NM_001081	Kansl1	KAT8 regula	NM_001081	RefSeq	Mus muscu	FALSE	76719	Mm.136418	Q80TG1	chr11	GO:001656	chromatin m	GO:000012	histone acet	GO:004399	histone acet	○
17272095	85.95374	96.8969	0.8870639	-0.17289	0	main		NM_008211	H3f3b	H3 histone,	NM_008211	RefSeq	Mus muscu	FALSE	15081	Mm.371563	P84244	chr11	GO:000164	osteoblast d	GO:000022	nuclear chrc	GO:000097	RNA polym	○
17272530	1212.562	1443.771	0.8398576	-0.251783	0	main		NM_011358	Srsf2	serine/argin	NM_011358	RefSeq	Mus muscu	FALSE	20382	Mm.21841	Q62093	chr11	GO:000639	mRNA proc	GO:000563	nucleus // r	GO:000016	nucleotide b	○
17273819	271.2213	307.9908	0.8806149	-0.183417	0	main		NM_001099	Atad2b	ATPase fan	NM_001099	RefSeq	Mus muscu	FALSE	320817	Mm.210966	E9Q166	chr12	GO:000815	biological_p	GO:000563	nucleus	GO:000016	nucleotide b	○
17277017	40.16175	37.5067	1.0707887	0.0986738	0	main		XM_006516	Rgs6	regulator of	XM_006516	RefSeq	PREDICTE	FALSE	50779	Mm.153013	Q9Z2H2	chr12	GO:000716	signal trans	GO:000573	cytoplasm /	GO:000487	signal trans	○
17277177	50.57738	48.52398	1.0423172	0.0597944	0	main		NM_028821	Dnal1	dynein, axor	NM_028821	RefSeq	Mus muscu	FALSE	105000	Mm.101525	Q05A62	chr12	GO:000815	biological_p	GO:000557	cellular_con	GO:000367	molecular_f	○
17277387	96.99457	250.5789	0.387082	-1.369289	0	main	2Down	ENSMUST0	Fos	FBJ osteosa	ENSMUST0	ENSEMBL	havana:puta	FALSE	14281	Mm.246513	P01101	chr12	GO:000635	regulation o	GO:000563	nucleus // r	GO:000097	RNA polym	○
17277521	61.92524	58.45456	1.059374	0.083212	0	main		NM_177354	Vash1	vasohibin 1	NM_177354	RefSeq	Mus muscu	FALSE	238328	Mm.216101	Q8C1W1	chr12	GO:000152	angiogenesi	GO:000557	extracellular	GO:000367	molecular_f	○
17279210	384.4613	385.0033	0.9985922	-0.002032	0	main		NM_001025	Klc1	kinesin light	NM_001025	RefSeq	Mus muscu	FALSE	16593	Mm.278357	O88447	chr12	GO:000688	intracellular	GO:000562	intracellular	GO:000377	microtubule	○
17280913	217.6443	167.5096	1.2992945	0.3777285	0	main		NM_021361	Nova1	neuro-oncol	NM_021361	RefSeq	Mus muscu	FALSE	664883	Mm.247195	Q9JKN6	chr12	GO:000039	mRNA splic	GO:000563	nucleus // r	GO:000372	RNA bindin	○
17281228	370.9284	432.9735	0.8567	-0.223138	0	main		NM_001003	Ralgapa1	Ral GTPase	NM_001003	RefSeq	Mus muscu	FALSE	56784	Mm.292180	Q6GYP7	chr12	GO:000635	regulation o	GO:000563	nucleus // c	GO:000509	GTPase act	○
17284839	53.44313	54.55101	0.9796909	-0.029601	0	main		NM_177290	Itgb8	integrin beta	NM_177290	RefSeq	Mus muscu	FALSE	320910	Mm.217000	Q0VBD0	chr12	GO:000157	ganglioside	GO:001602	membrane	GO:000510	receptor bin	○
17286595	478.4573	444.4544	1.0765048	0.1063548	0	main		NM_001039	Rreb1	ras responsi	NM_001039	RefSeq	Mus muscu	FALSE	68750	Mm.491109	Q3UH06	chr13	GO:000635	transcriptior	GO:000563	nucleus // c	GO:000367	nucleic acid	○
17286962	353.1282	611.6155	0.5773696	-0.792433	0	main		NM_153789	Mylip	myosin regu	NM_153789	RefSeq	Mus muscu	FALSE	218203	Mm.212855	Q8BM54	chr13	GO:000692	cellular com	GO:000562	intracellular	GO:000484	ubiquitin-pr	○
17286998	34.79554	32.43024	1.072935	0.1015627	0	main		NM_001081	Rbm24	RNA binding	NM_001081	RefSeq	Mus muscu	FALSE	666794	Mm.38269	D3Z4I3	chr13	GO:001083	regulation o	GO:000563	nucleus // c	GO:000016	nucleotide b	○
17287144	42.57329	46.63666	0.9128718	-0.131516	0	main		AK029314	Tes3-ps	testis derive	AK029314	GenBank H	Mus muscu	FALSE	54339	Mm.441473	Q9QZ73	chr13	---	---	GO:000015	ubiquitin lig	---	---	○
17289196	81.04126	62.01216	1.3068608	0.3861055	0	main		NM_172589	Lhfpl2	lipoma HMG	NM_172589	RefSeq	Mus muscu	FALSE	218454	Mm.316553	Q8BGA2	chr13	GO:000815	biological_p	GO:001602	membrane	GO:000367	molecular_f	○
17289824	219.6841	404.4613	0.5431523	-0.880571	0	main		NM_172593	Mier3	mesoderm i	NM_172593	RefSeq	Mus muscu	FALSE	218613	Mm.31012	Q3UHF3	chr13	GO:000635	transcriptior	GO:000563	nucleus // c	GO:000367	DNA bindin	○
17290121	469.8768	534.5063	0.8790856	-0.185924	0	main		XM_006517	Paip1	polyadenyla	XM_006517	RefSeq	PREDICTE	FALSE	218693	Mm.490243	Q8VE62	chr13	GO:000641	regulation o	GO:000573	cytoplasm /	GO:000372	RNA bindin	○
17290363	133.7339	158.4648	0.8439344	-0.244797	0	main		NM_001039	Wdr37	WD repeat	NM_001039	RefSeq	Mus muscu	FALSE	207615	Mm.284654	Q8CBE3	chr13	GO:000815	biological_p	GO:000557	cellular_con	GO:000367	molecular_f	○
17290815	230.501	241.5116	0.9544096	-0.067319	0	main		NM_019491	Rala	v-ral simian	NM_019491	RefSeq	Mus muscu	FALSE	56044	Mm.27348	P63321	chr13	GO:000091	cytokinesis	GO:000588	plasma mer	GO:000016	nucleotide b	○
17292174	353.9647	314.4709	1.1255881	0.170679	0	main		NM_001199	Atxn1	ataxin 1	NM_001199	RefSeq	Mus muscu	FALSE	20238	Mm.342683	P54254	chr13	GO:000635	transcriptior	GO:000563	nucleus // r	GO:000367	DNA bindin	○
17292346	420.8883	423.4393	0.9939755	-0.008718	0	main		NM_011078	Phf2	PHD finger	NM_011078	RefSeq	Mus muscu	FALSE	18676	Mm.486213	Q9WTU0	chr13	GO:000635	transcriptior	GO:000563	nucleus // r	GO:000090	sulfonate di	○
17292732	163.3297	170.0451	0.9605081	-0.05813	0	main		NM_001146	Rnf44	ring finger p	NM_001146	RefSeq	Mus muscu	FALSE	105239	Mm.25366	Q3UHJ8	chr13	GO:000815	biological_p	GO:000557	cellular_con	GO:000827	zinc ion bin	○
17292759	60.33015	42.76512	1.4107326	0.4964446	0	main		NM_033610	Sncb	synuclein, b	NM_033610	RefSeq	Mus muscu	FALSE	104069	Mm.200843	Q91ZZ3	chr13	GO:000726	synaptic tra	GO:000563	nucleus // c	GO:000550	calcium ion	○
17293085	262.4058	273.2763	0.9602216	-0.058561	0	main		NM_029872	Hnrnpa0	heterogene	NM_029872	RefSeq	Mus muscu	FALSE	77134	Mm.490274	Q9CX86	chr13	GO:000695	inflammator	GO:000563	nucleus // r	GO:000016	nucleotide b	○
17296142	452.3061	591.9007	0.7641588	-0.388056	0	main		NM_001122	Gpbp1	GC-rich pro	NM_001122	RefSeq	Mus muscu	FALSE	73274	Mm.57286	Q6NXH3	chr13	GO:000635	transcriptior	GO:000563	nucleus // r	GO:000367	DNA bindin	○
17297359	237.8828	225.8601	1.0532307	0.0748215	0	main		NM_001113	Thrb	thyroid horn	NM_001113	RefSeq	Mus muscu	FALSE	21834	Mm.32563	P37242	chr14	GO:000012	negative reg	GO:000079	nuclear chrc	GO:000367	DNA bindin	○
17297913	798.386	821.9045	0.9713854	-0.041884	0	main		NM_007479	Arf4	ADP-ribosyl	NM_007479	RefSeq	Mus muscu	FALSE	11843	Mm.297768	P61750	chr14	GO:000647	protein ADF	GO:000562	intracellular	GO:000016	nucleotide b	○
17299217	41.16053	50.95481	0.807785	-0.307957	0	main		NM_019637	Styx	serine/threo	NM_019637	RefSeq	Mus muscu	FALSE	56291	Mm.202561	Q60969	chr14	GO:000647	protein depl	GO:000573	cytoplasm /	GO:000472	phosphopro	○
17299316	125.4103	157.564	0.7959324	-0.329282	0	main		NM_080843	Socs4	suppressor	NM_080843	RefSeq	Mus muscu	FALSE	67296	Mm.425886	Q91ZA6	chr14	GO:000717	negative reg	GO:000557	cellular_con	GO:000367	molecular_f	○
17300292	241.691	235.6604	1.0255902	0.0364544	0	main		NM_022993	Lrp10	low-density	NM_022993	RefSeq	Mus muscu	FALSE	65107	Mm.472719	Q7TQH7	chr14	GO:000662	lipid metabo	GO:001602	integral con	GO:000504	low-density	○
17300860	397.176	446.2243	0.8900815	-0.167991	0	main		NM_029498	Zmym2	zinc finger,	NM_029498	RefSeq	Mus muscu	FALSE	76007	Mm.31417	Q9CU65	chr14	GO:000635	transcriptior	GO:000563	nucleus // F	GO:000551	protein bind	○
17301225	27.95084	27.66383	1.0103749	0.0148907	0	main		NM_177628	Fam167a	family with s	NM_177628	RefSeq	Mus muscu	FALSE	219148	Mm.37882	Q6P1G6	chr14	GO:000815	biological_p	GO:000557	cellular_con	GO:000367	molecular_f	○
17301849	35.85318	40.01425	0.8960103	-0.158413	0	main		ENSMUST0	Gm16549	predicted ge	ENSMUST0	ENSEMBL	havana:kno	FALSE	---	---	Q8BX90	chr14	---	---	---	---	---	---	○
17302600	51.29952	50.52592	1.015311	0.0219216	0	main		NM_198865	Slitrk5	SLIT and NT	NM_198865	RefSeq	Mus muscu	FALSE	75409	Mm.235097	Q810B7	chr14	GO:000726	synaptic tra	GO:001602	membrane	GO:000367	molecular_f	○
17303941	188.5184	193.7652	0.9729219	-0.039604	0	main		NM_018829	Ap3m1	adaptor-rela	NM_018829	RefSeq	Mus muscu	FALSE	55946	Mm.376269	Q9JKC8	chr14	GO:000681	transport //	GO:000562	intracellular	---	---	○
17305662	534.8237	595.9213	0.8974737	-0.156058	0	main		NM_146054	Fermt2	fermitin fam	NM_146054	RefSeq	Mus muscu	FALSE	218952	Mm.210018	Q8CIB5	chr14	GO:000715	cell adhesio	GO:000172	stress fiber	GO:000554	phosphatidy	○
17306230	218.8448	207.4168	1.0550968	0.0773754	0	main		NM_201637	Chd8	chromodom	NM_201637	RefSeq	Mus muscu	FALSE	67772	Mm.289934	Q09XV5	chr14	GO:000170	in utero eml	GO:000563	nucleus // r	GO:000016	nucleotide b	○
17307709	205.5327	205.0916	1.0021507	0.0030995	0	main		XM_006518	Hmbox1	homeobox c	XM_006518	RefSeq	PREDICTE	FALSE	219150	Mm.344074	Q8BJA3	chr14	GO:000635	transcriptior	GO:000563	nucleus // c	GO:000367	DNA bindin	○
17307935	136.4849	173.6408	0.7860186	-0.347365	0	main		NM_028032	Ppp2r2a	protein phos	NM_028032	RefSeq	Mus muscu	FALSE	71978	Mm.273997	Q6P1F6	chr14	GO:000647	protein depl	GO:000015	protein phos	GO:000472	protein serir	○
17308132	228.4169	245.1689	0.9316716	-0.102107	0	main		NM_026331	Slc25a37	solute carrie	NM_026331	RefSeq	Mus muscu	FALSE	67712	Mm.293635	Q920G8	chr14	GO:000681	transport //	GO:000573	mitochondri	GO:000538	iron ion tran	○
17308165	98.43435	82.31371	1.1958439	0.2580291	0	main		ENSMUST0	Gm21464	predicted ge	ENSMUST0	ENSEMBL	havana:kno	FALSE	100862085	Mm.291443	Q920G8	chr14	GO:000681	transport //	GO:000573	mitochondri	GO:000538	iron ion tran	○
17308525	716.1914	788.4019	0.908409	-0.138586	0	main		NM_207636	Fndc3a	fibronectin t	NM_207636	RefSeq	Mus muscu	FALSE	319448	Mm.205421	Q8BX90	chr14	GO:000728	spermatid d	GO:000166	acrosomal v	GO:004482	poly(A) RN/	○
17309774	29.8855	29.32752	1.0190258	0.0271906	0	main		NM_010201	Fgf14	fibroblast gr	NM_010201	RefSeq	Mus muscu	FALSE	14169	Mm.206362	P70379	chr14	GO:000725	JNK cascac	GO:000557	extracellular	GO:000510	receptor bin	○
17310872	260.9909	311.0828	0.8389757	-0.253299	0	main		NM_008304	Sdc2	syndecan 2	NM_008304	RefSeq	Mus muscu	FALSE	15529	Mm.234266	P43407	chr15	GO:000739	nervous sys	GO:001602	membrane	GO:000551	protein bind	○
17311272	122.2655	118.9235	1.0281021	0.0399835	0	main		NM_011766	Zfpm2	zinc finger p	NM_011766	RefSeq	Mus muscu	FALSE	22762	Mm.39496	Q8CCH7	chr15	GO:000012	negative reg	GO:000563	nucleus // r	GO:000107	nucleic acid	○
17314421	22.20171	20.39221	1.0887349	0.1226527	0	main		NM_001164	Pdzrn4	PDZ domaii	NM_001164	RefSeq	Mus muscu	FALSE	239618	Mm.309826	B9EKP7	chr15	GO:000815	biological_p	GO:000557	cellular_con	GO:004687	metal ion bi	○
17315500	29.13863	25.73942	1.1320624	0.1789535	0	main		NM_010462	Hoxc10	homeobox C	NM_010462	RefSeq	Mus muscu	FALSE	209448	Mm.31665	P31257	chr15	GO:000150	skeletal syst	GO:000563	nucleus // c	GO:000367	DNA bindin	○
17315810	561.6248	705.8835	0.7956338	-0.329823	0	main		NM_027707	Nipbl	Nipped-B ho	NM_027707	RefSeq	Mus muscu	FALSE	71175	Mm.240329	Q6KCD5	chr15	GO:000012	negative reg	GO:000563	nucleus // S	GO:000368	chromatin b	○
17316845	56.43475	58.41259	0.9661402	-0.049696	0	main		NM_001285	Sybu	syntabulin (	NM_001285	RefSeq	Mus muscu	FALSE	319613	Mm.207715	Q8BHS8	chr15	GO:006117	regulation o	GO:000579	Golgi appar	GO:000801	microtubule	○
17316956	166.2788	193.3805	0.859853	-0.217838	0	main		ENSMUST0	Trps1	trichorhinop	ENSMUST0	ENSEMBL	havana:puta	FALSE	83925	Mm.30466	Q8BZ62	chr15	GO:000012	negative reg	GO:000563	nucleus // r	GO:000367	DNA bindin	○
17316977	27.25347	27.01605	1.0087881	0.0126232	0	main		NR_035444	Mir1907	microRNA 1	NR_035444	RefSeq	Mus muscu	FALSE	100316685	---	Q925H1	chr15	---	---	---	---	---	---	○
17319299	277.1267	309.8194	0.8944782	-0.160882	0	main		NM_001205	Sun2	Sad1 and U	NM_001205	RefSeq	Mus muscu	FALSE	223697	Mm.202715	Q8BJS4	chr15	GO:000699	nuclear env	GO:000078	nuclear chrc	GO:000551	protein bind	○
17320583	240.7783	216.8393	1.1103997	0.1510791	0	main		NM_001033	Cpne8	copine VIII	NM_001033	RefSeq	Mus muscu	FALSE	66871	Mm.290991	Q9DC53	chr15	GO:000815	biological_p	GO:007006	extracellular	GO:000367	molecular_f	○
17322261	533.8728	431.9658	1.2359145	0.305579	0	main		ENSMUST0	Atf7	activating tr	ENSMUST0	ENSEMBL	ensembl:kn	FALSE	---	---	Q7TNN1	chr15	---	---	---	---	---	---	○
17322263	648.076	591.0241	1.0965306	0.132946	0	main		NM_146065	Atf7	activating tr	NM_146065	RefSeq	Mus muscu	FALSE	223922	Mm.208714	Q8R0S1	chr15	GO:000635	regulation o	GO:003439	nuclear peri	GO:000813	transcriptior	○
17322359	111.1243	104.1711	1.0667479	0.0932192	0	main		NM_013866	Zfp385a	zinc finger p	NM_013866	RefSeq	Mus muscu	FALSE	29813	Mm.14099	Q8VD12	chr15	GO:000635	transcriptior	GO:000079	nuclear chrc	GO:000203	p53 binding	○
17322950	96.59696	85.33616	1.1319581	0.1788206	0	main		NM_028964	Snx29	sorting nexi	NM_028964	RefSeq	Mus muscu	FALSE	74478	Mm.325831	Q9D3S3	chr16	GO:000815	biological_p	GO:000587	kinesin com	GO:003509	phosphatidy	○
17323465	169.8339	180.2454	0.9422371	-0.085838	0	main		NM_023348	Snap29	synaptosom	NM_023348	RefSeq	Mus muscu	FALSE	67474	Mm.271992	Q9ERB0	chr16	GO:000004	autophagic	GO:000573	cytoplasm /	GO:001990	syntaxin bin	○
17327445	13.71385	13.26748	1.0336439	0.0477393	0	main		ENSMUST0	Dennd1b	DENN/MAD	ENSMUST0	ENSEMBL	ensembl_lir	FALSE	329260	Mm.337604	Q3U1T9	chr16	GO:000681	transport //	GO:000573	cytoplasm /	GO:000508	guanyl-nucl	○
17327465	364.8452	528.1785	0.6907612	-0.533741	0	main		NM_011809	Ets2	E26 avian le	NM_011809	RefSeq	Mus muscu	FALSE	23872	Mm.290207	P15037	chr16	GO:000635	transcriptior	GO:000563	nucleus // r	GO:000097	RNA polym	○
17327482	43.9964	51.22802	0.8588347	-0.219548	0	main		ENSMUST0	Gm15342	predicted ge	ENSMUST0	ENSEMBL	havana:kno	FALSE	---	Mm.399491	Q921C3	chr16	---	---	---	---	---	---	○
17328104	50.50248	60.51356	0.8345647	-0.260904	0	main		NM_001271	Socs1	suppressor	NM_001271	RefSeq	Mus muscu	FALSE	12703	Mm.130	O35716	chr16	GO:000193	regulation o	GO:000562	intracellular	GO:000515	insulin-like	○
17329258	111.7554	118.6727	0.9417111	-0.086644	0	main		ENSMUST0	Igf2bp2	insulin-like	ENSMUST0	ENSEMBL	havana:kno	FALSE	319765	Mm.489442	Q5SF07	chr16	GO:000641	regulation o	GO:000563	nucleus // c	GO:000016	nucleotide b	○
17331418	112.1973	145.4918	0.7711589	-0.3749	0	main		NM_028059	Zfp654	zinc finger p	NM_028059	RefSeq	Mus muscu	FALSE	72020	Mm.25960	Q9DAU9	chr16	GO:000635	transcriptior	GO:000563	nucleus	GO:000367	DNA bindin	○
17332395	195.937	251.0268	0.7805422	-0.357452	0	main		NM_001103	Brwd1	bromodoma	NM_001103	RefSeq	Mus muscu	FALSE	93871	Mm.240871	Q921C3	chr16	GO:000635	transcriptior	GO:000563	nucleus // r	GO:000551	protein bind	○
17332628	187.4104	191.0261	0.9810722	-0.027569	0	main		NM_174847	C2cd2	C2 calcium-	NM_174847	RefSeq	Mus muscu	FALSE	207781	Mm.1465	E9Q3C1	chr16	GO:000815	biological_p	GO:000563	nucleus // c	GO:000367	molecular_f	○
17334241	226.1623	237.5832	0.9519288	-0.071074	0	main		NM_001080	Rnps1	ribonucleic a	NM_001080	RefSeq	Mus muscu	FALSE	19826	Mm.1951	Q99M28	chr17	GO:000018	nuclear-tran	GO:000563	nucleus // c	GO:000016	nucleotide b	○
17335550	106.4903	101.6232	1.0478936	0.0674922	0	main		NM_198647	Tbc1d22b	TBC1 doma	NM_198647	RefSeq	Mus muscu	FALSE	381085	Mm.328934	Q6PAT2	chr17	GO:000815	biological_p	GO:000557	cellular_con	GO:000367	molecular_f	○
17338460	37.94201	36.53804	1.0384249	0.0543969	0	main		NM_027452	Lrfn2	leucine rich	NM_027452	RefSeq	Mus muscu	FALSE	70530	Mm.133607	Q80TG9	chr17	---	---	GO:000588	plasma mer	GO:000551	protein bind	○
17338521	126.3513	96.95976	1.3031313	0.3819825	0	main		NM_013880	Plcl2	phospholipa	NM_013880	RefSeq	Mus muscu	FALSE	224860	Mm.217362	Q8K394	chr17	GO:000232	B cell prolife	GO:000573	cytoplasm	GO:000443	phosphatidy	○
17339973	201.6805	217.6629	0.9265727	-0.110024	0	main		NM_134117	Pkdcc	protein kina	NM_134117	RefSeq	Mus muscu	FALSE	106522	Mm.311974	Q5RJI4	chr17	GO:000150	skeletal syst	GO:000579	Golgi appar	GO:000016	nucleotide b	○
17340323	264.9203	303.9398	0.871621	-0.198227	0	main		NM_180974	Foxn2	forkhead bo	NM_180974	RefSeq	Mus muscu	FALSE	14236	Mm.112824	D3Z6Z3	chr17	GO:000635	transcriptior	GO:000563	nucleus // i	GO:000367	DNA bindin	○
17340756	1251.231	1358.052	0.9213425	-0.118191	0	main		NM_001159	Qk	quaking	NM_001159	RefSeq	Mus muscu	FALSE	19317	Mm.384135	Q9QYS9	chr17	GO:000157	vasculogene	GO:000563	nucleus // c	GO:000372	RNA bindin	○
17345038	640.0774	811.4113	0.7888446	-0.342187	0	main		NM_009847	Cd2ap	CD2-associ	NM_009847	RefSeq	Mus muscu	TRUE	12488	Mm.218637	Q9JLQ0	chr17	GO:000704	cell cycle //	GO:000172	ruffle // cyto	GO:000517	vascular en	○
17345134	31.97208	31.27957	1.0221394	0.0315919	0	main		NM_001146	Runx2	runt related	NM_001146	RefSeq	Mus muscu	TRUE	12393	Mm.391013	Q08775	chr17	GO:000150	skeletal syst	GO:000079	nuclear chrc	GO:000097	RNA polym	○
17347680	536.5801	931.9779	0.5757434	-0.796502	0	main		NM_001001	Zfp36l2	zinc finger p	NM_001001	RefSeq	Mus muscu	TRUE	12193	Mm.259321	P23949	chr17	GO:000028	nuclear-tran	GO:000563	nucleus // c	GO:000367	DNA bindin	○
17348238	208.3686	276.0688	0.7547705	-0.40589	0	main		NM_001278	Rab18	RAB18, me	NM_001278	RefSeq	Mus muscu	TRUE	19330	Mm.132802	P35293	chr18	GO:000681	transport //	GO:000562	intracellular	GO:000016	nucleotide b	○
17348591	19.65303	19.43399	1.011271	0.0161696	0	main		NM_001042	Cabyr	calcium-bin	NM_001042	RefSeq	Mus muscu	TRUE	71132	Mm.179740	Q9D424	chr18	GO:001972	calcium-me	GO:000562	intracellular	GO:000550	calcium ion	○
17349243	326.1957	371.9801	0.8769171	-0.189488	0	main		NM_011946	Map3k2	mitogen-act	NM_011946	RefSeq	Mus muscu	TRUE	26405	Mm.211762	Q61083	chr18	GO:000016	MAPK casc	GO:000563	nucleus // c	GO:000016	nucleotide b	○
17349572	238.104	254.2783	0.9363913	-0.094816	0	main		NM_026420	Paip2	polyadenyla	NM_026420	RefSeq	Mus muscu	TRUE	67869	Mm.126534	Q9D6V8	chr18	GO:000641	regulation o	GO:000573	cytoplasm /	GO:000090	translation r	○
17349671	412.55	469.3047	0.8790664	-0.185956	0	main		NM_175375	Ankhd1	ankyrin repe	NM_175375	RefSeq	Mus muscu	TRUE	108857	Mm.482287	E9PUR0	chr18	GO:000815	biological_p	---	---	GO:004482	poly(A) RN/	○
17349713	402.2929	385.6921	1.0430416	0.0607967	0	main		ENSMUST0	Ankhd1	ankyrin repe	ENSMUST0	ENSEMBL	havana:puta	TRUE	108857	Mm.482287	F6RUI8	chr18	GO:000815	biological_p	---	---	GO:004482	poly(A) RN/	○
17349807	78.50404	74.36163	1.0557063	0.0782085	0	main		NM_001003	Pcdhac1	protocadher	NM_001003	RefSeq	Mus muscu	TRUE	353236	Mm.308500	O88689	chr18	GO:000715	cell adhesio	GO:000588	plasma mer	GO:000550	calcium ion	○
17350011	618.4423	691.2709	0.8946454	-0.160612	0	main		NM_022996	Ndfip1	Nedd4 fami	NM_022996	RefSeq	Mus muscu	TRUE	65113	Mm.102496	Q8R0W6	chr18	GO:000276	regulation o	GO:000557	extracellular	GO:000487	signal trans	○
17351594	433.9506	416.0981	1.0429045	0.0606071	0	main		NM_001083	Tcf4	transcriptior	NM_001083	RefSeq	Mus muscu	TRUE	21413	Mm.4269	Q60722	chr18	GO:000012	negative reg	GO:000563	nucleus // r	GO:000097	RNA polym	○
17352212	81.81394	94.76816	0.8633062	-0.212056	0	main		NM_146090	Zadh2	zinc binding	NM_146090	RefSeq	Mus muscu	TRUE	225791	Mm.147052	Q8BGC4	chr18	GO:005511	oxidation-re	GO:000573	mitochondri	GO:000827	zinc ion bin	○

17519967	58.33921	63.36783	0.920644	-0.119285	0	main		NM_011162	Tpbg	trophoblast	NM_011622	RefSeq	Mus muscu	TRUE	21983	Mm.20864	Q9Z0L0	chr9	---	---	GO:000573	cytoplasm	---	---							
17520815	472.654	686.8726	0.6881247	-0.539258	0	main		NM_001110	Msl2	male-specifi	NM_001110	RefSeq	Mus muscu	TRUE	77853	Mm.326206	Q69ZF8	chr9	GO:004398	histone H4-	GO:007248	MSL compl	GO:000827	zinc ion bin							
17522848	192.6177	257.2575	0.748735	-0.417473	0	main		NM_001048	Azi2	5-azacytidin	NM_001048	RefSeq	Mus muscu	TRUE	27215	Mm.92705	Q9QYP6	chr9	GO:000027	mitotic cell	GO:000573	cytoplasm	GO:000551	protein bind							
17523081	65.08034	40.75385	1.5969127	0.6752854	0	main		NM_007399	Acvr2b	activin rece	NM_007399	RefSeq	Mus muscu	TRUE	11481	Mm.390239	P27040	chr9	GO:000150	skeletal sys	GO:000562	cell // cytop	GO:000016	nucleotide b							
17526130	354.3606	396.8731	0.8928814	-0.16346	0	main		NM_007616	Cbl	Casitas B-lin	NM_007616	RefSeq	Mus muscu	TRUE	12402	Mm.266871	P22682	chr9	GO:000716	cell surface	GO:000563	nucleus // c	GO:000178	phosphotyro							
17528714	242.9754	249.4519	0.9740371	-0.037951	0	main		NM_001255	Tcf12	transcriptior	NM_001255	RefSeq	Mus muscu	TRUE	21406	Mm.171615	Q61286	chr9	GO:000635	transcriptior	GO:000563	nucleus // t	GO:000367	DNA bindin							
17529713	466.7708	529.5917	0.8813786	-0.182166	0	main		NM_001114	U2surp	U2 snRNP-a	NM_001114	RefSeq	Mus muscu	TRUE	67958	Mm.292742	Q6NV83	chr9	GO:000639	RNA proces	GO:000563	nucleus // r	GO:000016	nucleotide b							
17530930	54.65099	59.80752	0.9137812	-0.130079	0	main		NM_001042	Sema3b	sema doma	NM_001042	RefSeq	Mus muscu	TRUE	20347	Mm.4083	Q62177	chr9	GO:000727	multicellular	GO:000557	extracellular	GO:000487	receptor act							
17530955	979.2015	842.2397	1.1626162	0.2173749	0	main		NM_008138	Gnai2	guanine nuc	NM_008138	RefSeq	Mus muscu	TRUE	14678	Mm.196464	P08752	chr9	GO:000018	activation of	GO:000563	nucleus // c	GO:000016	nucleotide b							
17531734	32.60688	28.00312	1.1644017	0.2195888	0	main		NM_016852	Stac	src homolog	NM_016852	RefSeq	Mus muscu	TRUE	20840	Mm.1414	P97306	chr9	GO:003460	cellular resp	GO:000573	cytoplasm	GO:004687	metal ion bi							
17533416	664.2457	858.501	0.7737273	-0.370103	0	main		NM_010028	Ddx3x	DEAD/H (A	NM_010028	RefSeq	Mus muscu	TRUE	13205	Mm.289662	Q62167	chrX	GO:000237	immune sys	GO:000563	nucleus // c	GO:000016	nucleotide b							
17535208	564.8925	546.4041	1.0338365	0.048008	0	main		NM_001129	Fmr1	fragile X mr	NM_001129	RefSeq	Mus muscu	TRUE	14265	Mm.3451	P35922	chrX	GO:000681	transport	// GO:000563	nucleus // c	GO:000372	RNA bindin							
17535241	106.2006	151.5649	0.7006939	-0.513144	0	main		ENSMUST(	Styx	serine/threo	ENSMUST(	ENSEMBL	havana:kno	TRUE	56291	Mm.202561	Q60969	chrX	GO:000647	protein dept	GO:000573	cytoplasm	GO:000472	phosphopro							
17538018	15.7973	16.62154	0.9504113	-0.073376	0	main		NM_013724	Nrk	Nik related l	NM_013724	RefSeq	Mus muscu	TRUE	27206	Mm.482319	Q9R0G8	chrX	GO:000646	protein phos	GO:000573	cytoplasm	GO:000016	nucleotide b							
17538395	11.10096	10.32762	1.0748808	0.1041766	0	main		NM_001033	Zcchc16	zinc finger,	NM_001033	RefSeq	Mus muscu	TRUE	619287	Mm.387961	Q3URY0	chrX	GO:000815	biological_p	GO:000557	cellular_con	GO:000367	nucleic acid							
17538658	27.22501	22.67239	1.2008002	0.2639961	0	main		NM_001271	Wnk3	WNK lysine	NM_001271	RefSeq	Mus muscu	TRUE	279561	Mm.441474	Q80XP9	chrX	GO:000646	protein phos	GO:000573	cytoplasm	GO:000016	nucleotide b							
17539828	28.17557	25.36139	1.1109632	0.151811	0	main		NM_019461	Usp27x	ubiquitin sp	NM_019461	RefSeq	Mus muscu	TRUE	54651	Mm.483107	Q8CEG8	chrX	GO:000650	proteolysis	GO:000557	cellular_con	GO:000823	peptidase ac							
17541343	22.6035	20.20307	1.1188151	0.1619716	0	main		NM_001298	Smarca1	SWI/SNF re	NM_001298	RefSeq	Mus muscu	TRUE	93761	Mm.229151	Q6PGB8	chrX	GO:000073	DNA strand	GO:000079	nuclear chr	GO:000016	nucleotide b							
17543840	13.13452	12.28752	1.0689317	0.0961697	0	main		NM_001107	C77370	expressed s	NM_001107	RefSeq	Mus muscu	TRUE	245555	Mm.381907	Q5DTT1	chrX	GO:000008	mitotic S ph	GO:000563	nucleus // c	GO:000388	DNA-directe							
17544102	52.66202	66.44284	0.7925913	-0.335351	0	main		ENSMUST(	Brwd3	bromodoma	ENSMUST(	ENSEMBL	ensembl_ha	TRUE	382236	Mm.426127	A2AHJ4	chrX	GO:000701	cytoskeletor	GO:000557	cellular_con	GO:000551	protein bind							
17544939	251.5343	267.6529	0.939778	-0.089608	0	main		NM_001107	Tsc22d3	TSC22 dom	NM_001107	RefSeq	Mus muscu	TRUE	14605	Mm.22216	Q9Z2S7	chrX	GO:000012	negative reg	GO:000563	nucleus // c	GO:000370	sequence-sp							
17545078	69.16832	93.64679	0.7386086	-0.437118	0	main		NM_019490	Ammecr1	Alport syndr	NM_019490	RefSeq	Mus muscu	TRUE	56068	Mm.143724	Q9JHT5	chrX	GO:000815	biological_p	GO:000557	cellular_con	GO:000367	molecular_f							
17545618	50.85996	41.40395	1.2283842	0.2967619	0	main		XM_006528	Ptchd1	patched dor	XM_006528	RefSeq	PREDICTE	TRUE	211612	Mm.218811	Q14B62	chrX	GO:000722	smoothened	GO:000588	plasma mer	GO:000815	hedgehog re							
17545629	13.46382	15.85833	0.8490062	-0.236153	0	main		NM_011077	Phex	phosphate r	NM_011077	RefSeq	Mus muscu	TRUE	18675	Mm.2529	P70669	chrX	GO:000650	proteolysis	GO:000578	endoplasmi	GO:000422	metalloendo							
17546834	749.3524	1081.035	0.6931805	-0.528697	0	main		NM_012008	Ddx3y	DEAD (Asp	NM_012008	RefSeq	Mus muscu	TRUE	26900	Mm.302938	Q62095	chrY	GO:000620	ATP catabo	GO:000563	nucleus // c	GO:000016	nucleotide b							
17547616	663.494	810.2198	0.8189062	-0.28823	0	main		---	---	---	X91866	GenBank	M.musculus	TRUE	---	---	P84244	chr11	GO:000633	nucleosome	GO:000078	nucleosome	GO:000367	DNA bindin							
17547837	95.57313	88.08841	1.0849683	0.1176529	0	main		ENSMUST(	Gm21464	predicted ge	ENSMUST(	ENSEMBL	havana:kno	TRUE	100862085	Mm.291443	Q920G8	chr14	GO:000681	transport	// GO:000573	mitochondri	GO:000538	iron ion tran							
17547846	99.60606	94.7348	1.05142	0.072339	0	main		ENSMUST(	Gm21464	predicted ge	ENSMUST(	ENSEMBL	havana:kno	TRUE	100862085	Mm.291443	Q920G8	chr14	GO:000681	transport	// GO:000573	mitochondri	GO:000538	iron ion tran							
17548283	1204.558	1613.575	0.746515	-0.421757	0	main		NM_008211	H3f3b	H3 histone,	NM_008211	RefSeq	Mus muscu	TRUE	15081	Mm.371563	P84244	chr3	GO:000164	osteoblast d	GO:000022	nuclear chr	GO:000097	RNA polym							
17548518	1303.143	1200.466	1.085531	0.1184009	0	main		NM_001081	Gm12657	predicted ge	NM_001081	RefSeq	Mus muscu	TRUE	667250	Mm.449778	P84244	chr6	---	---	---	---	---	---							
17548946	1054.596	1431.395	0.736761	-0.440731	0	main		NM_008211	H3f3b	H3 histone,	NM_008211	RefSeq	Mus muscu	TRUE	15081	Mm.371563	P84244	chr1	GO:000164	osteoblast d	GO:000022	nuclear chr	GO:000097	RNA polym							

Supplementary Table 4. The comparison of global mRNA expression in Mir221/222AdipoKO and Mir221/222flox/y mice fed with high fat-high sucrose (HFHS) chow.

	Sample name	Negative control
Test	HFHS AdipoKO 384	52.80
Control	HFHS flox/y 388	50.46

2Up	Ratio ≧ 2 and Expression value of test sample ≧ Negative control (average)
2Down	Ratio ≦ 0.5 and Expression value of test sample ≧ Negative control (average)

Feature ID	Normalized data				Flag			Annotation																	Keyword
Probe Set II	Expression	Expression	Ratio	Log2Ratio	解析対象 Fl	category	Ratio flag	Gene Acces	Gene Symb	Gene Descr	mRNA Acce	mRNA Sou	mRna - Des	mRNA - xhy	EntrezGene	UniGene ID	SwissProt a	Chromosom	GO Biologic	GO Biologic	GO Cellular	GO Cellular	GO Molecul	GO Molecul	miR221/222 target gene
17211066	13.61456	10.85042	1.2547496	0.3273995	0	main		NM_17772	Mcmdc2	minichromo	NM_17772	RefSeq	Mus muscu	FALSE	240697	Mm.25980	E9Q956	chr1	GO:000626	DNA replica	GO:000557	cellular_con	GO:000367	DNA bindin	O
17211305	51.30147	47.63595	1.0769486	0.1069494	0	main		NM_05319	Pi15	peptidase ir	NM_05319	RefSeq	Mus muscu	FALSE	94227	Mm.44245	Q8BS03	chr1	GO:001046	negative reg	GO:000557	extracellular	GO:003041	peptidase ir	O
17211548	27.61715	28.53265	0.967914	-0.047049	0	main		NM_13323	Khdrbs2	KH domain	NM_13323	RefSeq	Mus muscu	FALSE	170771	Mm.336594	Q9WU01	chr1	GO:000635	transcription	GO:000563	nucleus // r	GO:000372	RNA bindin	O
17212947	68.2433	75.26522	0.9067043	-0.141296	0	main		NM_00116	Spats2l	spermatoge	NM_00116	RefSeq	Mus muscu	FALSE	67198	Mm.15998	Q91WJ7	chr1	GO:000815	biological_p	GO:000563	nucleus // r	GO:004482	poly(A) RN	O
17214841	646.7574	470.1974	1.3755019	0.4599581	0	main		NM_01047	Agfg1	ArfGAP witl	NM_01047	RefSeq	Mus muscu	FALSE	15463	Mm.43340	Q8K2K6	chr1	GO:000167	acrosome a	GO:000563	nucleus //	GO:000367	DNA bindin	O
17215565	94.51138	90.34522	1.0461138	0.0650398	0	main		NM_13381	Sh3bp4	SH3-domai	NM_13381	RefSeq	Mus muscu	FALSE	98402	Mm.17098	Q921I6	chr1	GO:000689	endocytosis	GO:000563	nucleus //	GO:000509	GDP-dissoc	O
17216888	27.64335	24.47034	1.1296676	0.1758983	0	main		NM_17248	Thsd7b	thrombospo	NM_17248	RefSeq	Mus muscu	FALSE	210417	Mm.38051	Q6P4U0	chr1	GO:000815	biological_p	GO:001602	membrane	GO:000367	molecular_f	O
17217291	41.8703	51.58801	0.8116285	-0.301109	0	main		NM_00116	Plekha6	pleckstrin h	NM_00116	RefSeq	Mus muscu	FALSE	240753	Mm.25355	Q7TQG1	chr1	GO:000815	biological_p	GO:000557	cellular_con	GO:000367	molecular_f	O
17217854	97.77634	92.4662	1.0574279	0.0805593	0	main		ENSMUST	Dennd1b	DENN/MAD	ENSMUST	ENSEMBL	havana:kno	FALSE	329260	Mm.337604	Q3U1T9	chr1	GO:000681	transport //	GO:000573	cytoplasm	GO:000508	guanyl-nucl	O
17217901	197.4886	215.3279	0.9171529	-0.124766	0	main		NM_17264	Zbtb41	zinc finger	NM_17264	RefSeq	Mus muscu	FALSE	226470	Mm.119711	Q811F1	chr1	GO:000635	transcription	GO:000563	nucleus	GO:000367	nucleic acid	O
17220177	38.61103	25.35535	1.5227962	0.6067229	0	main		ENSMUST	Gm17275	predicted ge	ENSMUST	ENSEMBL	ensembl_lir	FALSE	---	Mm.32273	P84244	chr1	GO:000633	nucleosome	GO:000078	nucleosome	GO:000367	DNA bindin	O
17220373	233.1286	197.5178	1.1802916	0.2391433	0	main		NM_17337	Trp53bp2	transformati	NM_17337	RefSeq	Mus muscu	FALSE	209456	Mm.28745	Q8CG79	chr1	GO:000691	apoptotic pr	GO:000563	nucleus //	GO:000813	transcription	O
17220489	275.2593	256.9431	1.071285	0.0993424	0	main		NM_00116	Rab3gap2	RAB3 GTPa	NM_00116	RefSeq	Mus muscu	FALSE	98732	Mm.275841	Q8BMG7	chr1	GO:004308	regulation o	GO:000573	cytoplasm	GO:000509	GTPase act	O
17221158	17.12076	15.44752	1.1083177	0.1483715	0	main		NM_00129	Mybl1	myeloblasto	NM_00129	RefSeq	Mus muscu	FALSE	17864	Mm.479	P51960	chr1	GO:000635	transcription	GO:000563	nucleus	GO:000367	DNA bindin	O
17222440	135.0569	128.7281	1.0491641	0.0692403	0	main		NM_01957	Rev1	REV1 homo	NM_01957	RefSeq	Mus muscu	FALSE	56210	Mm.38910	Q920Q2	chr1	GO:000626	DNA replica	GO:000563	nucleus	GO:000028	magnesium	O
17223138	68.90113	81.77136	0.8426071	-0.247068	0	main		NM_00116	Pgap1	post-GPI at	NM_00116	RefSeq	Mus muscu	FALSE	241062	Mm.10353	Q3UUQ7	chr1	GO:000650	GPI anchor	GO:000578	endoplasmi	GO:000451	nuclease ac	O
17223946	18.81731	15.54949	1.2101561	0.2751931	0	main		NM_01015	Erbb4	v-erb-a erytl	NM_01015	RefSeq	Mus muscu	FALSE	13869	Mm.44242	Q61527	chr1	GO:000175	neural crest	GO:000563	nucleus //	GO:000016	nucleotide b	O
17225373	35.51353	43.87009	0.8095158	-0.304869	0	main		NM_01026	Gbx2	gastrulation	NM_01026	RefSeq	Mus muscu	FALSE	14472	Mm.20473	P48031	chr1	GO:000156	patterning o	GO:000563	nucleus	GO:000367	DNA bindin	O
17228426	276.9101	309.3543	0.8951228	-0.159842	0	main		NM_00103	Cep350	centrosoma	NM_00103	RefSeq	Mus muscu	FALSE	74081	Mm.260247	D3YTP2	chr1	GO:000815	biological_p	GO:000563	nucleus //	GO:000367	molecular_f	O
17229178	132.5691	234.3915	0.5655883	-0.822176	0	main		NM_00972	Atp1b1	ATPase, Na	NM_00972	RefSeq	Mus muscu	FALSE	11931	Mm.4550	P14094	chr1	GO:000166	response to	GO:000588	plasma mer	GO:000539	sodium:pota	O
17230469	57.44956	64.60298	0.8892711	-0.169305	0	main		ENSMUST	Gm12657	predicted ge	ENSMUST	ENSEMBL	havana:kno	FALSE	667250	Mm.44977	E0CYN1	chr1	GO:000164	osteoblast d	GO:000022	nuclear chro	GO:000097	RNA polym	O
17230602	156.8367	168.3848	0.9314184	-0.102499	0	main		NM_17512	Fbxo28	F-box protei	NM_17512	RefSeq	Mus muscu	FALSE	67948	Mm.30737	Q8BIG4	chr1	GO:000815	biological_p	GO:000557	cellular_con	GO:000367	molecular_f	O
17230668	249.5798	283.7418	0.8796018	-0.185078	0	main		NM_17738	Mia3	melanoma i	NM_17738	RefSeq	Mus muscu	FALSE	338366	Mm.41152	Q8BI84	chr1	GO:000206	chondrocyte	GO:000578	endoplasmi	GO:000367	molecular_f	O
17230760	73.05361	51.96034	1.4059494	0.4915447	0	main		NM_14551	Mark1	MAP/microt	NM_14551	RefSeq	Mus muscu	FALSE	226778	Mm.7445	Q8VHJ5	chr1	GO:000022	microtubule	GO:000573	cytoplasm	GO:000016	nucleotide b	O
17231461	208.4178	215.5273	0.9670135	-0.048392	0	main		NM_00795	Esr1	estrogen rec	NM_00795	RefSeq	Mus muscu	FALSE	13982	Mm.9213 /	P19785	chr10	GO:000154	antral ovaria	GO:000563	nucleus // r	GO:000104	core promot	O
17232483	14.57383	15.28952	0.9531908	-0.069163	0	main		XR_380237	LOC10263	uncharacter	XR_380237	RefSeq	PREDICTE	FALSE	102632938	---	Q8BG92	chr10	---	---	---	---	---	---	O
17232734	147.3443	169.2554	0.8705442	-0.200011	0	main		NM_00116	Cdk19	cyclin-deper	NM_00116	RefSeq	Mus muscu	FALSE	78334	Mm.200924	Q8BWD8	chr10	GO:000646	protein phos	GO:000557	cellular_con	GO:000016	nucleotide b	O
17233437	211.5285	198.1677	1.0674217	0.0941302	0	main		NM_00119	Lims1	LIM and ser	NM_00119	RefSeq	Mus muscu	FALSE	110829	Mm.57734	Q99JW4	chr10	GO:000716	cell-matrix a	GO:000588	plasma mer	GO:000551	protein bind	O
17233457	817.5409	663.1248	1.2328613	0.3020105	0	main		NM_01124	Ranbp2	RAN binding	NM_01124	RefSeq	Mus muscu	FALSE	19386	Mm.43169	Q9ERU9	chr10	GO:000645	protein foldi	GO:000563	nucleus // r	GO:000372	RNA bindin	O
17235211	278.3539	219.8713	1.2659856	0.340261	0	main		NM_02156	Midn	midnolin	NM_02156	RefSeq	Mus muscu	FALSE	59090	Mm.14381	Q3TPJ7	chr10	GO:003313	negative reg	GO:000563	nucleus // r	GO:001990	kinase bindi	O
17236182	1561.97	1261.031	1.2386452	0.308763	0	main		NM_01159	Timp3	tissue inhibi	NM_01159	RefSeq	Mus muscu	FALSE	21859	Mm.4871	P39876	chr10	GO:001046	negative reg	GO:000557	extracellular	GO:000485	enzyme inh	O
17236439	15.89399	16.5119	0.9625779	-0.055025	0	main		NM_00112	Anks1b	ankyrin repe	NM_00112	RefSeq	Mus muscu	FALSE	77531	Mm.44060	Q8BIZ1	chr10	GO:000815	biological_p	GO:000563	nucleus //	GO:004687	ephrin recep	O
17238449	209.311	193.3304	1.0826595	0.1145796	0	main		NM_17279	Ankrd52	ankyrin repe	NM_17279	RefSeq	Mus muscu	FALSE	237615	Mm.440177	Q8BTI7	chr10	GO:000815	biological_p	GO:000557	cellular_con	GO:000367	molecular_f	O
17238571	271.1223	297.3772	0.9117118	-0.13335	0	main		NM_02887	Dnajc14	DnaJ (Hsp4	NM_02887	RefSeq	Mus muscu	FALSE	74330	Mm.29691	Q921R4	chr10	GO:000681	transport //	GO:000578	endoplasmi	GO:000166	G-protein co	O
17239234	31.84827	28.0104	1.1370159	0.1852524	0	main		NM_00111	Grm1	glutamate re	NM_00111	RefSeq	Mus muscu	FALSE	14816	Mm.48298	P97772	chr10	GO:000018	activation of	GO:000563	nucleus // p	GO:000163	PLC activat	O
17240123	12.5492	11.87797	1.0565105	0.0793071	0	main		XM_00651	Clvs2	clavesin 2	XM_00651	RefSeq	PREDICTE	FALSE	215890	Mm.94461	Q8BG92	chr10	GO:000681	transport //	GO:000562	intracellular	GO:000521	transporter	O
17240226	274.3249	378.1627	0.725415	-0.463121	0	main		NM_00853	Marcks	myristoylate	NM_00853	RefSeq	Mus muscu	FALSE	17118	Mm.30059	P26645	chr10	---	---	GO:000573	cytoplasm	GO:000377	actin bindin	O
17241032	383.8727	201.7627	1.902595	0.9279685	0	main		NM_02908	Ddit4	DNA-damag	NM_02908	RefSeq	Mus muscu	FALSE	74747	Mm.21697	Q9D3F7	chr10	GO:000166	response to	GO:000562	intracellular	GO:007188	14-3-3 prote	O
17243509	91.19772	82.39014	1.1069009	0.1465261	0	main		NM_01091	Nfyb	nuclear tran	NM_01091	RefSeq	Mus muscu	FALSE	18045	Mm.24599	P63139	chr10	GO:000635	transcription	GO:000562	intracellular	GO:000367	DNA bindin	O
17245095	322.7195	322.5288	1.0005913	0.0008528	0	main		NM_00103	Cnot2	CCR4-NOT	NM_00103	RefSeq	Mus muscu	FALSE	72068	Mm.35155	Q8C5L3	chr10	GO:000012	negative reg	GO:000563	nucleus //	GO:000122	RNA polym	O
17245188	235.5322	245.1456	0.9607849	-0.057715	0	main		NM_17779	Frs2	fibroblast gr	NM_17779	RefSeq	Mus muscu	FALSE	327826	Mm.13596	Q8C180	chr10	GO:000018	activation of	GO:000573	cytoplasm	GO:000506	transmembr	O
17245587	403.3884	439.5294	0.9177734	-0.12379	0	main		NM_00116	Mon2	MON2 hom	NM_00116	RefSeq	Mus muscu	FALSE	67074	Mm.169924	Q80TL7	chr10	GO:000681	transport //	GO:000580	trans-Golgi	GO:000508	ARF guanyl	O
17246268	53.70585	48.08744	1.1168374	0.1594191	0	main		NM_01177	Ikzf4	IKAROS fan	NM_01177	RefSeq	Mus muscu	FALSE	22781	Mm.35864	Q8C208	chr10	GO:000635	transcription	GO:000563	nucleus	GO:000367	nucleic acid	O
17247448	276.1858	286.4043	0.9643214	-0.052414	0	main		ENSMUST	Ppp3r1	protein phos	ENSMUST	ENSEMBL	havana:kno	FALSE	19058	Mm.41840	Q63810	chr11	GO:000156	patterning o	GO:000562	intracellular	GO:000472	phosphopro	O
17247519	145.4549	177.3747	0.8200431	-0.286228	0	main		NM_03352	Spred2	sprouty-rela	NM_03352	RefSeq	Mus muscu	FALSE	114716	Mm.266627	Q924S7	chr11	GO:000018	inactivation	GO:000563	nucleus //	GO:000517	stem cell fa	O
17247533	1021.62	1017.681	1.0038706	0.0055733	0	main		ENSMUST	Rab1	RAB1, mem	ENSMUST	ENSEMBL	havana:kno	FALSE	19324	Mm.271944	P62821	chr11	GO:000004	autophagic	GO:000013	Golgi memb	GO:000016	nucleotide b	O
17247550	393.5545	413.364	0.9520773	-0.070849	0	main		ENSMUST	Peli1	pellino 1	ENSMUST	ENSEMBL	havana:kno	FALSE	67245	Mm.28957	Q8C669	chr11	GO:000020	protein poly	GO:000563	nucleus	GO:000484	ubiquitin-pr	O
17248213	448.3499	433.511	1.0342296	0.0485565	0	main		NM_00129	Cpeb4	cytoplasmic	NM_00129	RefSeq	Mus muscu	FALSE	67579	Mm.339792	Q7TN98	chr11	GO:000293	response to	GO:000563	nucleus // r	GO:000016	nucleotide b	O
17248288	156.112	127.1214	1.2280544	0.2963745	0	main		NM_17736	Sh3pxd2b	SH3 and PX	NM_17736	RefSeq	Mus muscu	FALSE	268396	Mm.22761	A2AAY5	chr11	GO:000150	skeletal syst	GO:000210	podosome	GO:001031	phosphatidy	O
17248476	955.1849	1037.724	0.9204614	-0.119571	0	main		NM_14596	Pank3	pantothenat	NM_14596	RefSeq	Mus muscu	FALSE	211347	Mm.255044	Q8R2W9	chr11	GO:001593	coenzyme A	GO:000573	cytoplasm	GO:000016	nucleotide b	O
17253307	193.5559	210.5211	0.9194133	-0.121215	0	main		NM_00102	Nufip2	nuclear frag	NM_00102	RefSeq	Mus muscu	FALSE	68564	Mm.42899	Q5F2E7	chr11	---	---	GO:000563	nucleus //	GO:000372	RNA bindin	O
17254933	312.357	283.0973	1.1033556	0.1418979	0	main		NM_01668	Vezf1	vascular end	NM_01668	RefSeq	Mus muscu	FALSE	22344	Mm.46628	Q5SXC3	chr11	GO:000152	angiogenesi	GO:000563	nucleus // r	GO:000367	nucleic acid	O
17255443	204.2556	257.5068	0.7932047	-0.334235	0	main		NM_20160	Zfp652	zinc finger p	NM_20160	RefSeq	Mus muscu	FALSE	268469	Mm.38903	Q5DU09	chr11	GO:000635	transcription	GO:000563	nucleus	GO:000367	nucleic acid	O
17255727	71.14986	75.58215	0.941358	-0.087185	0	main		NM_00108	Osbpl7	oxysterol bir	NM_00108	RefSeq	Mus muscu	FALSE	71240	Mm.19045	A2A716	chr11	GO:000681	transport //	GO:000577	autophagic	GO:001548	cholesterol	O
17255775	84.22844	78.28211	1.0759603	0.1056248	0	main		NM_13865	Socs7	suppressor	NM_13865	RefSeq	Mus muscu	FALSE	192157	Mm.34339	Q8VHQ2	chr11	GO:000828	insulin rece	GO:000563	nucleus // r	---	---	O
17255828	146.9251	163.7507	0.8972487	-0.15642	0	main		NM_13931	Mllt6	myeloid/lym	NM_13931	RefSeq	Mus muscu	FALSE	246198	Mm.23685	B1AR09	chr11	GO:000815	biological_p	GO:000557	cellular_con	GO:004687	metal ion bi	O
17256991	46.31411	44.79544	1.0339023	0.0480999	0	main		NM_00111	Adam11	a disintegrin	NM_00111	RefSeq	Mus muscu	FALSE	11488	Mm.89854	Q9R1V4	chr11	GO:000650	proteolysis	GO:001602	membrane	GO:000422	metalloendo	O
17257235	120.8584	112.4936	1.074358	0.1034748	0	main		NM_01678	Itgb3	integrin beta	NM_01678	RefSeq	Mus muscu	FALSE	16416	Mm.87150	O54890	chr11	GO:000193	positive reg	GO:000563	nucleus // p	GO:000375	protein disu	O
17257801	61.82838	72.32794	0.854834	-0.226284	0	main		NM_01573	Axin2	axin2	NM_01573	RefSeq	Mus muscu	FALSE	12006	Mm.71710	O88566	chr11	GO:000175	somitogene	GO:000562	intracellular	GO:000487	signal trans	O
17258789	176.7436	174.3007	1.0140154	0.0200796	0	main		NM_19802	Tnrc6c	trinucleotide	NM_19802	RefSeq	Mus muscu	FALSE	217351	Mm.40272	Q3UHC0	chr11	GO:000170	endoderm f	GO:000557	cellular_con	GO:000016	nucleotide b	O
17261289	50.959	53.34941	0.9551933	-0.066135	0	main		NM_14601	Eml6	echinoderm	NM_14601	RefSeq	Mus muscu	FALSE	237711	Mm.445271	Q5SQM0	chr11	GO:000815	biological_p	GO:000573	cytoplasm	GO:000367	molecular_f	O
17261896	28.72132	26.70852	1.0753617	0.104822	0	main		NM_01025	Gabra1	gamma-ami	NM_01025	RefSeq	Mus muscu	FALSE	14394	Mm.43966	P62812	chr11	GO:000681	transport //	GO:000588	plasma mer	GO:000489	GABA-A re	O
17262055	60.9169	49.51683	1.2302262	0.2989236	0	main		NM_17252	Nipal4	NIPA-like d	NM_17252	RefSeq	Mus muscu	FALSE	214112	Mm.22525	Q8BZF2	chr11	GO:000681	transport //	GO:001602	membrane	GO:001509	magnesium	O
17262964	32.02223	31.10429	1.0295117	0.0419602	0	main		NM_00102	Fat2	FAT tumor	NM_00102	RefSeq	Mus muscu	FALSE	245827	Mm.33936	Q5F226	chr11	GO:000715	cell adhesio	GO:000563	nucleus // p	GO:000550	calcium ion	O
17266264	723.2512	647.6657	1.1167045	0.1592475	0	main		NM_14482	Taok1	TAO kinase	NM_14482	RefSeq	Mus muscu	FALSE	216965	Mm.34043	Q5F2E8	chr11	GO:000016	MAPK casc	GO:000573	cytoplasm	GO:000016	nucleotide b	O
17266498	232.3093	243.4246	0.9543378	-0.067428	0	main		NM_00870	Nlk	nemo like ki	NM_00870	RefSeq	Mus muscu	FALSE	18099	Mm.9001	O54949	chr11	GO:000016	MAPK casc	GO:000563	nucleus //	GO:000016	nucleotide b	O
17266534	93.77359	109.636	0.8553175	-0.225468	0	main		NM_01357	Ksr1	kinase supp	NM_01357	RefSeq	Mus muscu	FALSE	16706	Mm.4745	Q61097	chr11	GO:000646	protein phos	GO:000573	cytoplasm	GO:000467	protein kina	O
17267632	78.75014	101.3317	0.7771521	-0.363731	0	main		NM_01950	Dgke	diacylglycer	NM_01950	RefSeq	Mus muscu	FALSE	56077	Mm.15369	Q9R1C6	chr11	GO:000720	protein kina	GO:000573	cytoplasm	GO:000016	nucleotide b	O
17270621	249.5549	236.9771	1.053076	0.0746096	0	main		NM_00108	Kansl1	KAT8 regula	NM_00108	RefSeq	Mus muscu	FALSE	76719	Mm.13641	Q80TG1	chr11	GO:001656	chromatin m	GO:000012	histone acet	GO:004399	histone acet	O
17272095	76.51385	64.37485	1.1885674	0.2492238	0	main		NM_00821	H3f3b	H3 histone,	NM_00821	RefSeq	Mus muscu	FALSE	15081	Mm.37156	P84244	chr11	GO:000164	osteoblast d	GO:000022	nuclear chro	GO:000097	RNA polym	O
17272530	1123.532	986.7911	1.1385713	0.1872246	0	main		NM_01135	Srsf2	serine/argin	NM_01135	RefSeq	Mus muscu	FALSE	20382	Mm.21841	Q62093	chr11	GO:000639	mRNA proc	GO:000563	nucleus // r	GO:000016	nucleotide b	O
17273819	249.6144	248.0828	1.0061737	0.0088794	0	main		NM_00109	Atad2b	ATPase fam	NM_00109	RefSeq	Mus muscu	FALSE	320817	Mm.21096	E9Q166	chr12	GO:000815	biological_p	GO:000563	nucleus	GO:000016	nucleotide b	O
17277017	39.39758	39.7174	0.9919476	-0.011664	0	main		XM_00651	Rgs6	regulator of	XM_00651	RefSeq	PREDICTE	FALSE	50779	Mm.15301	Q9Z2H2	chr12	GO:000716	signal trans	GO:000573	cytoplasm	GO:000487	signal trans	O
17277177	46.78327	52.09187	0.8980916	-0.155066	0	main		NM_02882	Dnal1	dynein, axor	NM_02882	RefSeq	Mus muscu	FALSE	105000	Mm.10152	Q05A62	chr12	GO:000815	biological_p	GO:000557	cellular_con	GO:000367	molecular_f	O
17277387	173.6935	115.658	1.5017854	0.5866787	0	main		ENSMUST	Fos	FBJ osteosa	ENSMUST	ENSEMBL	havana:puta	FALSE	14281	Mm.24651	P01101	chr12	GO:000635	regulation o	GO:000563	nucleus // r	GO:000097	RNA polym	O
17277521	71.07616	74.09139	0.9593039	-0.05994	0	main		NM_17735	Vash1	vasohibin 1	NM_17735	RefSeq	Mus muscu	FALSE	238328	Mm.216101	Q8C1W1	chr12	GO:000152	angiogenesi	GO:000557	extracellular	GO:000367	molecular_f	O
17279210	330.2432	355.8349	0.9280798	-0.107679	0	main		NM_00102	Klc1	kinesin light	NM_00102	RefSeq	Mus muscu	FALSE	16593	Mm.278357	O88447	chr12	GO:000688	intracellular	GO:000562	intracellular	GO:000377	microtubule	O
17280913	105.5651	210.4908	0.5015188	-0.995624	0	main		NM_02136	Nova1	neuro-oncol	NM_02136	RefSeq	Mus muscu	FALSE	664883	Mm.24719	Q9JKN6	chr12	GO:000039	mRNA splic	GO:000563	nucleus // r	GO:000372	RNA bindin	O
17281228	392.2571	388.6653	1.0092414	0.0132713	0	main		NM_00100	Ralgapa1	Ral GTPase	NM_00100	RefSeq	Mus muscu	FALSE	56784	Mm.29218	Q6GYP7	chr12	GO:000635	regulation o	GO:000563	nucleus //	GO:000509	GTPase act	O
17284839	71.05316	51.56115	1.3780368	0.4626144	0	main		NM_17729	Itgb8	integrin beta	NM_17729	RefSeq	Mus muscu	FALSE	320910	Mm.21700	Q0VBD0	chr12	GO:000157	ganglioside	GO:001602	membrane	GO:000510	receptor bin	O
17286595	351.2864	342.7743	1.024833	0.0353888	0	main		NM_00103	Rreb1	ras responsi	NM_00103	RefSeq	Mus muscu	FALSE	68750	Mm.49110	Q3UH06	chr13	GO:000635	transcription	GO:000563	nucleus //	GO:000367	nucleic acid	O
17286962	584.5587	470.676	1.2419556	0.3126136	0	main		NM_15378	Mylip	myosin regu	NM_15378	RefSeq	Mus muscu	FALSE	218203	Mm.21285	Q8BM54	chr13	GO:000692	cellular com	GO:000562	intracellular	GO:000484	ubiquitin-pr	O
17286998	41.44395	38.23375	1.0839625	0.1163148	0	main		NM_00108	Rbm24	RNA binding	NM_00108	RefSeq	Mus muscu	FALSE	666794	Mm.38269	D3Z4I3	chr13	GO:001083	regulation o	GO:000563	nucleus //	GO:000016	nucleotide b	O
17287144	44.87271	44.78688	1.0019164	0.0027621	0	main		AK029314	Tes3-ps	testis derive	AK029314	GenBank H	Mus muscu	FALSE	54339	Mm.44147	Q9QZ73	chr13	---	---	GO:000015	ubiquitin lig	---	---	O
17289196	65.10943	82.20768	0.7920115	-0.336407	0	main		NM_17258	Lhfpl2	lipoma HMG	NM_17258	RefSeq	Mus muscu	FALSE	218454	Mm.31655	Q8BGA2	chr13	GO:000815	biological_p	GO:001602	membrane	GO:000367	molecular_f	O
17289824	240.8311	189.1224	1.2734139	0.3487015	0	main		NM_17259	Mier3	mesoderm i	NM_17259	RefSeq	Mus muscu	FALSE	218613	Mm.31012	Q3UHF3	chr13	GO:000635	transcription	GO:000563	nucleus //	GO:000367	DNA bindin	O
17290121	390.8395	383.4963	1.019148	0.0273636	0	main		XM_00651	Paip1	polyadenyla	XM_00651	RefSeq	PREDICTE	FALSE	218693	Mm.49024	Q8VE62	chr13	GO:000641	regulation o	GO:000573	cytoplasm	GO:000372	RNA bindin	O
17290363	129.0872	155.3877	0.8307427	-0.267526	0	main		NM_00103	Wdr37	WD repeat	NM_00103	RefSeq	Mus muscu	FALSE	207615	Mm.284654	Q8CBE3	chr13	GO:000815	biological_p	GO:000557	cellular_con	GO:000367	molecular_f	O
17290815	252.3634	262.2838	0.9621768	-0.055626	0	main		NM_01949	Rala	v-ral simian	NM_01949	RefSeq	Mus muscu	FALSE	56044	Mm.27348	P63321	chr13	GO:000091	cytokinesis	GO:000588	plasma mer	GO:000016	nucleotide b	O
17292174	427.9402	355.5998	1.2034321	0.2671547	0	main		NM_00119	Atxn1	ataxin 1	NM_00119	RefSeq	Mus muscu	FALSE	20238	Mm.34268	P54254	chr13	GO:000635	transcription	GO:000563	nucleus // r	GO:000367	DNA bindin	O
17292346	402.3347	339.4914	1.1851101	0.2450211	0	main		NM_01107	Phf2	PHD finger	NM_01107	RefSeq	Mus muscu	FALSE	18676	Mm.48621	Q9WTU0	chr13	GO:000635	transcription	GO:000563	nucleus // r	GO:000090	sulfonate di	O
17292732	168.7932	156.933	1.0755749	0.105108	0	main		NM_00114	Rnf44	ring finger p	NM_00114	RefSeq	Mus muscu	FALSE	105239	Mm.25366	Q3UHJ8	chr13	GO:000815	biological_p	GO:000557	cellular_con	GO:000827	zinc ion bin	O
17292759	63.40198	61.13007	1.0371652	0.0526457	0	main		NM_03361	Sncb	synuclein, b	NM_03361	RefSeq	Mus muscu	FALSE	104069	Mm.20084	Q91ZZ3	chr13	GO:000726	synaptic tra	GO:000563	nucleus //	GO:000550	calcium ion	O
17293085	233.8683	204.4518	1.1438799	0.1939356	0	main		NM_02987	Hnrnpa0	heterogene	NM_02987	RefSeq	Mus muscu	FALSE	77134	Mm.490274	Q9CX86	chr13	GO:000695	inflammator	GO:000563	nucleus // r	GO:000016	nucleotide b	O
17296142	381.684	370.2949	1.0307568	0.043704	0	main		NM_00112	Gpbp1	GC-rich pro	NM_00112	RefSeq	Mus muscu	FALSE	73274	Mm.57286	Q6NXH3	chr13	GO:000635	transcription	GO:000563	nucleus // r	GO:000367	DNA bindin	O
17297359	213.4073	237.9575	0.8968295	-0.157094	0	main		NM_00111	Thrb	thyroid horm	NM_00111	RefSeq	Mus muscu	FALSE	21834	Mm.32563	P37242	chr14	GO:000012	negative reg	GO:000079	nuclear chro	GO:000367	DNA bindin	O
17297913	963.4631	898.0315	1.0728611	0.1014634	0	main		NM_00747	Arf4	ADP-ribosyl	NM_00747	RefSeq	Mus muscu	FALSE	11843	Mm.29776	P61750	chr14	GO:000647	protein ADP	GO:000562	intracellular	GO:000016	nucleotide b	O
17299217	42.56583	44.12502	0.9646643	-0.051901	0	main		NM_01963	Styx	serine/threo	NM_01963	RefSeq	Mus muscu	FALSE	56291	Mm.202561	Q60969	chr14	GO:000647	protein dept	GO:000573	cytoplasm	GO:000472	phosphopro	O
17299316	131.3514	127.8254	1.0275845	0.039257	0	main		NM_08084	Socs4	suppressor	NM_08084	RefSeq	Mus muscu	FALSE	67296	Mm.42588	Q91ZA6	chr14	GO:000717	negative reg	GO:000557	cellular_con	GO:000367	molecular_f	O
17300292	293.0891	297.1501	0.9863335	-0.019853	0	main		NM_02299	Lrp10	low-density	NM_02299	RefSeq	Mus muscu	FALSE	65107	Mm.47271	Q7TQH7	chr14	GO:000662	lipid metabo	GO:001602	integral com	GO:000504	low-density	O
17300860	269.8	355.2199	0.7595295	-0.396822	0	main		NM_02949	Zmym2	zinc finger,	NM_02949	RefSeq	Mus muscu	FALSE	76007	Mm.31417	Q9CU65	chr14	GO:000635	transcription	GO:000563	nucleus //	GO:000551	protein bind	O
17301225	37.67636	33.48871	1.1250466	0.1699848	0	main		NM_17762	Fam167a	family with	NM_17762	RefSeq	Mus muscu	FALSE	219148	Mm.37882	Q6P1G6	chr14	GO:000815	biological_p	GO:000557	cellular_con	GO:000367	molecular_f	O
17301849	37.49914	30.26217	1.2391425	0.3093421	0	main		ENSMUST	Gm16549	predicted ge	ENSMUST	ENSEMBL	havana:kno	FALSE	---	---	Q8BX90	chr14	---	---	---	---	---	---	O
17302600	42.95873	45.80589	0.9378429	-0.092582	0	main		NM_19886	Slitrk5	SLIT and N	NM_19886	RefSeq	Mus muscu	FALSE	75409	Mm.23509	Q810B7	chr14	GO:000726	synaptic tra	GO:001602	membrane	GO:000367	molecular_f	O
17303941	242.0922	218.0668	1.1101745	0.1507865	0	main		NM_01882	Ap3m1	adaptor-rela	NM_01882	RefSeq	Mus muscu	FALSE	55946	Mm.37626	Q9JKC8	chr14	GO:000681	transport //	GO:000562	intracellular	---	---	O
17305662	638.4142	520.9209	1.2255492	0.2934284	0	main		NM_14605	Fermt2	fermitin fam	NM_14605	RefSeq	Mus muscu	FALSE	218952	Mm.21001	Q8CIB5	chr14	GO:000715	cell adhesio	GO:000172	stress fiber	GO:000554	phosphatidy	O
17306230	211.2961	188.8597	1.1187993	0.1619513	0	main		NM_20163	Chd8	chromodom	NM_20163	RefSeq	Mus muscu	FALSE	67772	Mm.28993	Q09XV5	chr14	GO:000170	in utero eml	GO:000563	nucleus // r	GO:000016	nucleotide b	O
17307709	207.4294	212.3038	0.9770404	-0.03351	0	main		XM_00651	Hmbox1	homeobox c	XM_00651	RefSeq	PREDICTE	FALSE	219150	Mm.344074	Q8BJA3	chr14	GO:000635	transcription	GO:000563	nucleus //	GO:000367	DNA bindin	O
17307935	156.1966	103.3587	1.511209	0.5957032	0	main		NM_02803	Ppp2r2a	protein phos	NM_02803	RefSeq	Mus muscu	FALSE	71978	Mm.273997	Q6P1F6	chr14	GO:000647	protein dept	GO:000015	protein phos	GO:000472	protein serir	O
17308132	178.5929	217.3462	0.8216978	-0.28332	0	main		NM_02633	Slc25a37	solute carrie	NM_02633	RefSeq	Mus muscu	FALSE	67712	Mm.29363	Q920G8	chr14	GO:000681	transport //	GO:000573	mitochondri	GO:000538	iron ion tran	O
17308165	77.65087	85.0218	0.9133054	-0.130831	0	main		ENSMUST	Gm21464	predicted ge	ENSMUST	ENSEMBL	havana:kno	FALSE	100862085	Mm.29144	Q920G8	chr14	GO:000681	transport //	GO:000573	mitochondri	GO:000538	iron ion tran	O
17308525	581.114	657.1865	0.8842452	-0.177482	0	main		NM_20763	Fndc3a	fibronectin t	NM_20763	RefSeq	Mus muscu	FALSE	319448	Mm.205421	Q8BX90	chr14	GO:000728	spermatid d	GO:000166	acrosomal v	GO:004482	poly(A) RN	O
17309774	28.23562	26.01733	1.085262	0.1180434	0	main		NM_01020	Fgf14	fibroblast gr	NM_01020	RefSeq	Mus muscu	FALSE	14169	Mm.206362	P70379	chr14	GO:000725	JNK cascac	GO:000557	extracellular	GO:000510	receptor bin	O
17310872	299.957	381.6093	0.7860317	-0.347341	0	main		NM_00830	Sdc2	syndecan 2	NM_00830	RefSeq	Mus muscu	FALSE	15529	Mm.23426	P43407	chr15	GO:000739	nervous sys	GO:001602	membrane	GO:000551	protein bind	O
17311272	108.4189	117.3688	0.9237455	-0.114433	0	main		NM_01176	Zfpm2	zinc finger p	NM_01176	RefSeq	Mus muscu	FALSE	22762	Mm.39496	Q8CCH7	chr15	GO:000012	negative reg	GO:000563	nucleus // r	GO:000107	nucleic acid	O
17314421	24.96736	18.83454	1.3256156	0.4066625	0	main		NM_00116	Pdzrn4	PDZ domain	NM_00116	RefSeq	Mus muscu	FALSE	239618	Mm.30982	B9EKP7	chr15	GO:000815	biological_p	GO:000557	cellular_con	GO:004687	metal ion bi	O
17315500	31.22255	31.42917	0.9934259	-0.009516	0	main		NM_01046	Hoxc10	homeobox C	NM_01046	RefSeq	Mus muscu	FALSE	209448	Mm.31665	P31257	chr15	GO:000150	skeletal syst	GO:000563	nucleus //	GO:000367	DNA bindin	O
17315810	520.3255	532.1091	0.9778549	-0.032308	0	main		NM_02770	Nipbl	Nipped-B h	NM_02770	RefSeq	Mus muscu	FALSE	71175	Mm.24032	Q6KCD5	chr15	GO:000012	negative reg	GO:000563	nucleus //	GO:000368	chromatin b	O
17316845	76.38311	65.56257	1.1650414	0.2203813	0	main		NM_00128	Sybu	syntabulin (	NM_00128	RefSeq	Mus muscu	FALSE	319613	Mm.20771	Q8BHS8	chr15	GO:006117	regulation o	GO:000579	Golgi appar	GO:000801	microtubule	O
17316956	107.144	168.1638	0.6371407	-0.650316	0	main		ENSMUST	Trps1	trichorhinop	ENSMUST	ENSEMBL	havana:puta	FALSE	83925	Mm.30466	Q8BZ62	chr15	GO:000012	negative reg	GO:000563	nucleus // r	GO:000367	DNA bindin	O
17316977	23.65247	26.61115	0.888818	-0.17004	0	main		NR_035444	Mir1907	microRNA	NR_035444	RefSeq	Mus muscu	FALSE	100316685	---	Q925H1	chr15	---	---	---	---	---	---	O
17319299	292.7424	252.4587	1.1595655	0.2135843	0	main		NM_00120	Sun2	Sad1 and U	NM_00120	RefSeq	Mus muscu	FALSE	223697	Mm.20271	Q8BJS4	chr15	GO:000699	nuclear env	GO:000078	nuclear chro	GO:000551	protein bind	O
17320583	249.4114	187.5397	1.3299125	0.4113314	0	main		NM_00103	Cpne8	copine VIII	NM_00103	RefSeq	Mus muscu	FALSE	66871	Mm.290991	Q9DC53	chr15	GO:000815	biological_p	GO:007006	extracellular	GO:000367	molecular_f	O
17322261	414.385	459.7737	0.9012803	-0.149952	0	main		ENSMUST	Atf7	activating tr	ENSMUST	ENSEMBL	ensembl:kn	FALSE	---	---	Q7TNN1	chr15	---	---	---	---	---	---	O
17322263	534.1051	542.6584	0.9842382	-0.022921	0	main		NM_14606	Atf7	activating tr	NM_14606	RefSeq	Mus muscu	FALSE	223922	Mm.208714	Q8R0S1	chr15	GO:000635	regulation o	GO:003439	nuclear peri	GO:000813	transcription	O
17322359	109.2495	141.1824	0.7738181	-0.369934	0	main		NM_01386	Zfp385a	zinc finger p	NM_01386	RefSeq	Mus muscu	FALSE	29813	Mm.14099	Q8VD12	chr15	GO:000635	transcription	GO:000079	nuclear chro	GO:000203	p53 binding	O
17322950	59.93401	92.95651	0.6447532	-0.633181	0	main		NM_02896	Snx29	sorting nexi	NM_02896	RefSeq	Mus muscu	FALSE	74478	Mm.325831	Q9D3S3	chr16	GO:000815	biological_p	GO:000587	kinesin com	GO:003509	phosphatidy	O
17323465	156.8344	159.4473	0.9836128	-0.023838	0	main		NM_02334	Snap29	synaptosom	NM_02334	RefSeq	Mus muscu	FALSE	67474	Mm.27199	Q9ERB0	chr16	GO:000004	autophagic	GO:000573	cytoplasm	GO:001990	syntaxin bin	O
17327445	15.62372	15.47195	1.0098094	0.014083	0	main		ENSMUST	Dennd1b	DENN/MAD	ENSMUST	ENSEMBL	ensembl_lir	FALSE	329260	Mm.337604	Q3U1T9	chr16	GO:000681	transport //	GO:000573	cytoplasm	GO:000508	guanyl-nucl	O
17327465	406.857	309.0158	1.316622	0.3968412	0	main		NM_01180	Ets2	E26 avian le	NM_01180	RefSeq	Mus muscu	FALSE	23872	Mm.29020	P15037	chr16	GO:000635	transcription	GO:000563	nucleus // r	GO:000097	RNA polym	O
17327482	56.39662	50.936	1.1072055	0.146923	0	main		ENSMUST	Gm15342	predicted ge	ENSMUST	ENSEMBL	havana:kno	FALSE	---	Mm.399491	Q921C3	chr16	---	---	---	---	---	---	O
17328104	64.66173	55.21127	1.171169	0.2279493	0	main		NM_00127	Socs1	suppressor	NM_00127	RefSeq	Mus muscu	FALSE	12703	Mm.130	O35716	chr16	GO:000193	regulation o	GO:000562	intracellular	GO:000515	insulin-like	O
17329258	233.6214	92.12485	2.5359216	1.3425102	0	main	2Up	ENSMUST	Igf2bp2	insulin-like	ENSMUST	ENSEMBL	havana:kno	FALSE	319765	Mm.48944	Q5SF07	chr16	GO:000641	regulation o	GO:000563	nucleus //	GO:000016	nucleotide b	O
17331418	73.65264	76.68375	0.9604726	-0.058184	0	main		NM_02805	Zfp654	zinc finger p	NM_02805	RefSeq	Mus muscu	FALSE	72020	Mm.25960	Q9DAU9	chr16	GO:000635	transcription	GO:000563	nucleus	GO:000367	DNA bindin	O
17332395	162.9478	170.6023	0.9551325	-0.066227	0	main		NM_00110	Brwd1	bromodoma	NM_00110	RefSeq	Mus muscu	FALSE	93871	Mm.240871	Q921C3	chr16	GO:000635	transcription	GO:000563	nucleus // r	GO:000551	protein bind	O
17332628	172.1137	194.4698	0.8850408	-0.176184	0	main		NM_17484	C2cd2	C2 calcium-	NM_17484	RefSeq	Mus muscu	FALSE	207781	Mm.1465	E9Q3C1	chr16	GO:000815	biological_p	GO:000563	nucleus //	GO:000367	molecular_f	O
17334241	225.2325	188.232	1.1965686	0.2589031	0	main		NM_00108	Rnps1	ribonucleic	NM_00108	RefSeq	Mus muscu	FALSE	19826	Mm.1951	Q99M28	chr17	GO:000018	nuclear-tran	GO:000563	nucleus //	GO:000016	nucleotide b	O
17335550	124.2128	114.5701	1.0841642	0.1165833	0	main		NM_19864	Tbc1d22b	TBC1 doma	NM_19864	RefSeq	Mus muscu	FALSE	381085	Mm.32893	Q6PAT2	chr17	GO:000815	biological_p	GO:000557	cellular_con	GO:000367	molecular_f	O
17338460	46.39688	43.92234	1.056339	0.0790729	0	main		NM_02745	Lrfn2	leucine rich	NM_02745	RefSeq	Mus muscu	FALSE	70530	Mm.13360	Q80TG9	chr17	---	---	GO:000588	plasma mer	GO:000551	protein bind	O
17338521	52.51792	83.08208	0.6321209	-0.661728	0	main		NM_01388	Plcl2	phospholipa	NM_01388	RefSeq	Mus muscu	FALSE	224860	Mm.217362	Q8K394	chr17	GO:000232	B cell prolife	GO:000573	cytoplasm	GO:000443	phosphatidy	O
17339973	149.0461	174.6721	0.8532908	-0.228891	0	main		NM_13411	Pkdcc	protein kina	NM_13411	RefSeq	Mus muscu	FALSE	106522	Mm.311974	Q5RJI4	chr17	GO:000150	skeletal syst	GO:000579	Golgi appar	GO:000016	nucleotide b	O
17340323	262.6019	217.4165	1.2078288	0.2724159	0	main		NM_18097	Foxn2	forkhead bo	NM_18097	RefSeq	Mus muscu	FALSE	14236	Mm.112824	D3Z6Z3	chr17	GO:000635	transcription	GO:000563	nucleus // i	GO:000367	DNA bindin	O
17340756	1234.498	1248.215	0.9890107	-0.015942	0	main		NM_00115	Qk	quaking	NM_00115	RefSeq	Mus muscu	FALSE	19317	Mm.38413	Q9QYS9	chr17	GO:000157	vasculogene	GO:000563	nucleus //	GO:000372	RNA bindin	O
17345038	607.5766	647.5317	0.9382963	-0.091885	0	main		NM_00984	Cd2ap	CD2-associ	NM_00984	RefSeq	Mus muscu	TRUE	12488	Mm.21863	Q9JLQ0	chr17	GO:000704	cell cycle //	GO:000172	ruffle // cyt	GO:000517	vascular en	O
17345134	40.50004	41.16046	0.983955	-0.023336	0	main		NM_00114	Runx2	runt related	NM_00114	RefSeq	Mus muscu	TRUE	12393	Mm.39101	Q08775	chr17	GO:000150	skeletal syst	GO:000079	nuclear chro	GO:000097	RNA polym	O
17347680	515.8293	490.6622	1.0512921	0.0721636	0	main		NM_00100	Zfp36l2	zinc finger p	NM_00100	RefSeq	Mus muscu	TRUE	12193	Mm.259321	P23949	chr17	GO:000028	nuclear-tran	GO:000563	nucleus //	GO:000367	DNA bindin	O
17348238	193.7463	200.9488	0.9641575	-0.052659	0	main		NM_00127	Rab18	RAB18, me	NM_00127	RefSeq	Mus muscu	TRUE	19330	Mm.132802	P35293	chr18	GO:000681	transport //	GO:000562	intracellular	GO:000016	nucleotide b	O
17348591	18.44108	17.7663	1.0379809	0.0537799	0	main		NM_00104	Cabyr	calcium-bin	NM_00104	RefSeq	Mus muscu	TRUE	71132	Mm.17974	Q9D424	chr18	GO:001972	calcium-me	GO:000562	intracellular	GO:000550	calcium ion	O
17349243	268.5541	289.953	0.9261987	-0.110606	0	main		NM_01194	Map3k2	mitogen-act	NM_01194	RefSeq	Mus muscu	TRUE	26405	Mm.211762	Q61083	chr18	GO:000016	MAPK casc	GO:000563	nucleus //	GO:000016	nucleotide b	O
17349572	230.8831	242.5387	0.9519433	-0.071052	0	main		NM_02642	Paip2	polyadenyla	NM_02642	RefSeq	Mus muscu	TRUE	67869	Mm.126534	Q9D6V8	chr18	GO:000641	regulation o	GO:000573	cytoplasm	GO:000090	translation r	O
17349671	316.1422	299.7853	1.054562	0.076644	0	main		NM_17537	Ankhd1	ankyrin repe	NM_17537	RefSeq	Mus muscu	TRUE	108857	Mm.482287	E9PUR0	chr18	GO:000815	biological_p	---	---	GO:004482	poly(A) RN	O
17349713	278.5127	288.4999	0.9653823	-0.050828	0	main		ENSMUST	Ankhd1	ankyrin repe	ENSMUST	ENSEMBL	havana:puta	TRUE	108857	Mm.482287	F6RUI8	chr18	GO:000815	biological_p	---	---	GO:004482	poly(A) RN	O
17349807	69.84968	73.48066	0.9505859	-0.073111	0	main		NM_00100	Pcdhac1	protocadher	NM_00100	RefSeq	Mus muscu	TRUE	353236	Mm.30850	O88689	chr18	GO:000715	cell adhesio	GO:000588	plasma mer	GO:000550	calcium ion	O
17350011	688.7121	698.5485	0.9859188	-0.020459	0	main		NM_02299	Ndfip1	Nedd4 famil	NM_02299	RefSeq	Mus muscu	TRUE	65113	Mm.10249	Q8R0W6	chr18	GO:000276	regulation o	GO:000557	extracellular	GO:000487	signal trans	O
17351594	402.0595	440.16	0.9134394	-0.130619	0	main		NM_00108	Tcf4	transcription	NM_00108	RefSeq	Mus muscu	TRUE	21413	Mm.4269	Q60722	chr18	GO:000012	negative reg	GO:000563	nucleus // r	GO:000097	RNA polym	O
17352212	70.08739	100.4986	0.6973967	-0.519949	0	main		NM_14609	Zadh2	zinc binding	NM_14609	RefSeq	Mus muscu	TRUE	225791	Mm.14705	Q8BGC4	chr18	GO:005511	oxidation-re	GO:000573	mitochondri	GO:000827	zinc ion bin	O

17519967	66.36326	77.80013	0.8529968	-0.229388	0	main		NM_011162	Tpbg	trophoblast	NM_011622	RefSeq	Mus muscu	TRUE	21983	Mm.20864	Q92L0	chr9	---	---	GO:000573	cytoplasm	---	---								
17520815	372.401	381.8084	0.9753609	-0.035992	0	main		NM_001110	Msl2	male-specifi	NM_001100	RefSeq	Mus muscu	TRUE	77853	Mm.326206	Q69ZF8	chr9	GO:004398	histone H4-	GO:007248	MSL compl	GO:000827	zinc ion bin								
17522848	200.9076	205.7395	0.9765145	-0.034287	0	main		NM_001104	Azi2	5-azacytidin	NM_001104	RefSeq	Mus muscu	TRUE	27215	Mm.92705	Q9QYP6	chr9	GO:000027	mitotic cell	GO:000573	cytoplasm	GO:000551	protein bind								
17523081	63.08196	70.94463	0.8891717	-0.169466	0	main		NM_007399	Acvr2b	activin rece	NM_007399	RefSeq	Mus muscu	TRUE	11481	Mm.390239	P27040	chr9	GO:000150	skeletal sys	GO:000562	cell // cytop	GO:000016	nucleotide b								
17526130	363.0498	339.0828	1.0706819	0.0985299	0	main		NM_007611	Cbl	Casitas B-lin	NM_007611	RefSeq	Mus muscu	TRUE	12402	Mm.266871	P22682	chr9	GO:000716	cell surface	GO:000563	nucleus // c	GO:000178	phosphotyro								
17528714	257.718	235.3805	1.0948995	0.1307985	0	main		NM_001255	Tcf12	transcriptior	NM_001252	RefSeq	Mus muscu	TRUE	21406	Mm.171615	Q61286	chr9	GO:000635	transcriptior	GO:000563	nucleus // t	GO:000367	DNA bindin								
17529713	385.1018	331.4807	1.1617624	0.216315	0	main		NM_001114	U2surp	U2 snRNP-a	NM_001114	RefSeq	Mus muscu	TRUE	67958	Mm.292742	Q6NV83	chr9	GO:000639	RNA proces	GO:000563	nucleus // r	GO:000016	nucleotide b								
17530930	60.10501	64.3563	0.9339414	-0.098596	0	main		NM_001042	Sema3b	sema domai	NM_001042	RefSeq	Mus muscu	TRUE	20347	Mm.4083	Q62177	chr9	GO:000727	multicellular	GO:000557	extracellular	GO:000487	receptor act								
17530955	1003.845	986.2798	1.0178096	0.0254676	0	main		NM_008138	Gnai2	guanine nuc	NM_008138	RefSeq	Mus muscu	TRUE	14678	Mm.196464	P08752	chr9	GO:000018	activation of	GO:000563	nucleus // c	GO:000016	nucleotide b								
17531734	32.55711	28.70505	1.1341945	0.1816681	0	main		NM_016852	Stac	src homolog	NM_016852	RefSeq	Mus muscu	TRUE	20840	Mm.1414	P97306	chr9	GO:003460	cellular resp	GO:000573	cytoplasm	GO:004687	metal ion bi								
17533416	688.9457	512.7594	1.3436042	0.4261082	0	main		NM_010028	Ddx3x	DEAD/H (A	NM_010028	RefSeq	Mus muscu	TRUE	13205	Mm.289662	Q62167	chrX	GO:000237	immune sys	GO:000563	nucleus // c	GO:000016	nucleotide b								
17535208	861.1144	1145.401	0.7518017	-0.411576	0	main		NM_001290	Fmr1	fragile X me	NM_001290	RefSeq	Mus muscu	TRUE	14265	Mm.3451	P35922	chrX	GO:000681	transport //	GO:000563	nucleus // c	GO:000372	RNA bindin								
17535241	113.162	124.9131	0.9059258	-0.142535	0	main		ENSMUST(	Styx	serine/threo	ENSMUST(	ENSEMBL	havana:kno	TRUE	56291	Mm.202561	Q60969	chrX	GO:000647	protein dept	GO:000573	cytoplasm	GO:000472	phosphopro								
17538018	18.69999	16.33215	1.1449803	0.1953228	0	main		NM_013724	Nrk	Nik related l	NM_013724	RefSeq	Mus muscu	TRUE	27206	Mm.482319	Q9R0G8	chrX	GO:000646	protein phos	GO:000573	cytoplasm	GO:000016	nucleotide b								
17538395	10.53644	9.817351	1.0732467	0.1019818	0	main		NM_001033	Zcchc16	zinc finger,	NM_001033	RefSeq	Mus muscu	TRUE	619287	Mm.387961	Q3URY0	chrX	GO:000815	biological_p	GO:000557	cellular_con	GO:000367	nucleic acid								
17538658	22.98368	24.19338	0.9499987	-0.074003	0	main		NM_001271	Wnk3	WNK lysine	NM_001271	RefSeq	Mus muscu	TRUE	279561	Mm.441474	Q80XP9	chrX	GO:000646	protein phos	GO:000573	cytoplasm	GO:000016	nucleotide b								
17539828	29.07195	24.83115	1.1707855	0.2274768	0	main		NM_019461	Usp27x	ubiquitin sp	NM_019461	RefSeq	Mus muscu	TRUE	54651	Mm.483107	Q8CEG8	chrX	GO:000650	proteolysis	GO:000557	cellular_con	GO:000823	peptidase ac								
17541343	28.04365	21.40388	1.3102146	0.3898031	0	main		NM_001290	Smarca1	SWI/SNF re	NM_001290	RefSeq	Mus muscu	TRUE	93761	Mm.229151	Q6PGB8	chrX	GO:000073	DNA strand	GO:000079	nuclear chr	GO:000016	nucleotide b								
17543840	12.0706	12.03887	1.0026356	0.0037974	0	main		NM_001107	C77370	expressed s	NM_001107	RefSeq	Mus muscu	TRUE	245555	Mm.381907	Q5DTT1	chrX	GO:000008	mitotic S ph	GO:000563	nucleus // c	GO:000388	DNA-directe								
17544102	56.45731	56.45731	1	0	0	main		ENSMUST(	Brwd3	bromodoma	ENSMUST(	ENSEMBL	ensembl_ha	TRUE	382236	Mm.426127	A2AHJ4	chrX	GO:000701	cytoskeletor	GO:000557	cellular_con	GO:000551	protein bind								
17544939	299.5348	360.4171	0.8310782	-0.266944	0	main		NM_001107	Tsc22d3	TSC22 dom	NM_001107	RefSeq	Mus muscu	TRUE	14605	Mm.22216	Q9Z2S7	chrX	GO:000012	negative reg	GO:000563	nucleus // c	GO:000370	sequence-sp								
17545078	88.37831	95.12606	0.9290652	-0.106148	0	main		NM_019490	Ammecr1	Alport syndr	NM_019490	RefSeq	Mus muscu	TRUE	56068	Mm.143724	Q9JHT5	chrX	GO:000815	biological_p	GO:000557	cellular_con	GO:000367	molecular_f								
17545618	47.19572	57.85563	0.8157498	-0.293801	0	main		XM_006528	Ptchd1	patched dor	XM_006528	RefSeq	PREDICTE	TRUE	211612	Mm.218811	Q14B62	chrX	GO:000722	smoothened	GO:000588	plasma mer	GO:000815	hedgehog re								
17545629	11.86074	13.29709	0.8919801	-0.164917	0	main		NM_011077	Phex	phosphate r	NM_011077	RefSeq	Mus muscu	TRUE	18675	Mm.2529	P70669	chrX	GO:000650	proteolysis	GO:000578	endoplasmi	GO:000422	metalloendo								
17546834	642.2186	541.8898	1.1851461	0.245065	0	main		NM_012008	Ddx3y	DEAD (Asp	NM_012008	RefSeq	Mus muscu	TRUE	26900	Mm.302938	Q62095	chrY	GO:000620	ATP catabo	GO:000563	nucleus // c	GO:000016	nucleotide b								
17547616	821.7177	769.094	1.068423	0.0954829	0	main		---	H3F3A	---	X91866	GenBank	M.musculus	TRUE	---	---	P84244	chr11	GO:000633	nucleosome	GO:000078	nucleosome	GO:000367	DNA bindin								
17547837	96.34195	85.62926	1.1251055	0.1700603	0	main		ENSMUST(	Gm21464	predicted ge	ENSMUST(	ENSEMBL	havana:kno	TRUE	100862085	Mm.291443	Q920G8	chr14	GO:000681	transport //	GO:000573	mitochondri	GO:000538	iron ion tran								
17547846	101.3808	92.70303	1.0936083	0.1290961	0	main		ENSMUST(	Gm21464	predicted ge	ENSMUST(	ENSEMBL	havana:kno	TRUE	100862085	Mm.291443	Q920G8	chr14	GO:000681	transport //	GO:000573	mitochondri	GO:000538	iron ion tran								
17548283	1129.61	948.6991	1.1906937	0.2518023	0	main		NM_008211	H3f3b	H3 histone,	NM_008211	RefSeq	Mus muscu	TRUE	15081	Mm.371563	P84244	chr3	GO:000164	osteoblast d	GO:000022	nuclear chr	GO:000097	RNA polym								
17548518	1145.085	1182.456	0.9683954	-0.046332	0	main		NM_001081	Gm12657	predicted ge	NM_001081	RefSeq	Mus muscu	TRUE	667250	Mm.449778	P84244	chr6	---	---	---	---	---	---								
17548946	993.8382	826.8755	1.20192	0.2653409	0	main		NM_008211	H3f3b	H3 histone,	NM_008211	RefSeq	Mus muscu	TRUE	15081	Mm.371563	P84244	chr1	GO:000164	osteoblast d	GO:000022	nuclear chr	GO:000097	RNA polym								

Supplementary Table 5. The comparison of global mRNA expression in *Mir221/222flox/y* mice fed with high fat-high sucrose (HFHS) and standard (STD) chow.

	Sample name	Negative control
Test	HFHS flox/y 388	50.46
Control	STD flox/y 378	60.07

2Up	Ratio ≧ 2 and Expression value of test sample ≧ Negative control (average)
2Down	Ratio ≦ 0.5 and Expression value of test sample ≧ Negative control (average)

Feature ID	Normalized data				Flag			Annotation																	Keyword
Probe Set I	Expression	Expression	Ratio	Log2Ratio	解析対象 Fl	category	Ratio flag	Gene Acces	Gene Symb	Gene Descr	mRNA Acc	mRNA Sou	mRna - Des	mRNA - xhy	EntrezGene	UniGene ID	SwissProt a	Chromosom	GO Biologic	GO Biologic	GO Cellular	GO Cellular	GO Molecul	GO Molecul	miR221/222 target gene
17211066	10.85042	12.77533	0.849326	-0.23561	0	main		NM_17772	Mcmdc2	minichromo	NM_17772	RefSeq	Mus muscu	FALSE	240697	Mm.25980	E9Q956	chr1	GO:000626	DNA replica	GO:000557	cellular_con	GO:000367	DNA bindin	○
17211305	47.63595	41.28632	1.153795	0.2063869	0	main		NM_05319	Pi15	peptidase ir	NM_05319	RefSeq	Mus muscu	FALSE	94227	Mm.442452	Q8BS03	chr1	GO:001046	negative reg	GO:000557	extracellular	GO:003041	peptidase ir	○
17211548	28.53265	30.91425	0.9229611	-0.115658	0	main		NM_13323	Khdrbs2	KH domain	NM_13323	RefSeq	Mus muscu	FALSE	170771	Mm.336594	Q9WU01	chr1	GO:000635	transcriptior	GO:000563	nucleus // r	GO:000372	RNA bindin	○
17212947	75.26522	73.47573	1.0243548	0.0347156	0	main		NM_00116	Spats2l	spermatoge	NM_00116	RefSeq	Mus muscu	FALSE	67198	Mm.15998	Q91WJ7	chr1	GO:000815	biological_p	GO:000563	nucleus // r	GO:004482	poly(A) RN	○
17214841	470.1974	594.9557	0.7903066	-0.339516	0	main		NM_01047	Agfg1	ArfGAP witl	NM_01047	RefSeq	Mus muscu	FALSE	15463	Mm.43340	Q8K2K6	chr1	GO:000167	acrosome a	GO:000563	nucleus // c	GO:000367	DNA bindin	○
17215565	90.34522	94.91344	0.9518696	-0.071164	0	main		NM_13381	Sh3bp4	SH3-domai	NM_13381	RefSeq	Mus muscu	FALSE	98402	Mm.17098	Q921I6	chr1	GO:000689	endocytosis	GO:000563	nucleus // c	GO:000509	GDP-dissoc	○
17216888	24.47034	26.84098	0.9116783	-0.133403	0	main		NM_17248	Thsd7b	thrombospo	NM_17248	RefSeq	Mus muscu	FALSE	210417	Mm.38051	Q6P4U0	chr1	GO:000815	biological_p	GO:001602	membrane	GO:000367	molecular_f	○
17217291	51.58801	42.96968	1.2005677	0.2637168	0	main		NM_00116	Plekha6	pleckstrin h	NM_00116	RefSeq	Mus muscu	FALSE	240753	Mm.25355	Q7TQG1	chr1	GO:000815	biological_p	GO:000557	cellular_con	GO:000367	molecular_f	○
17217854	92.4662	97.81096	0.9453562	-0.08107	0	main		ENSMUST	Dennd1b	DENN/MAD	ENSMUST	ENSEMBL	havana:kno	FALSE	329260	Mm.337604	Q3U1T9	chr1	GO:000681	transport //	GO:000573	cytoplasm ,	GO:000508	guanyl-nucl	○
17217901	215.3279	238.968	0.9010742	-0.150282	0	main		NM_17264	Zbtb41	zinc finger a	NM_17264	RefSeq	Mus muscu	FALSE	226470	Mm.119711	Q811F1	chr1	GO:000635	transcriptior	GO:000563	nucleus	GO:000367	nucleic acid	○
17220177	25.35535	38.15434	0.6645469	-0.589557	0	main		ENSMUST	Gm17275	predicted ge	ENSMUST	ENSEMBL	ensembl_lir	FALSE	---	Mm.32273	P84244	chr1	GO:000633	nucleosome	GO:000078	nucleosome	GO:000367	DNA bindin	○
17220373	197.5178	264.4885	0.7467916	-0.421222	0	main		NM_17337	Trp53bp2	transformati	NM_17337	RefSeq	Mus muscu	FALSE	209456	Mm.28745	Q8CG79	chr1	GO:000691	apoptotic pr	GO:000563	nucleus // c	GO:000813	transcriptior	○
17220489	256.9431	305.6174	0.8407345	-0.250278	0	main		NM_00116	Rab3gap2	RAB3 GTPa	NM_00116	RefSeq	Mus muscu	FALSE	98732	Mm.275841	Q8BMG7	chr1	GO:004308	regulation o	GO:000573	cytoplasm ,	GO:000509	GTPase act	○
17221158	15.44752	18.73044	0.8247281	-0.27801	0	main		NM_00129	Mybl1	myeloblasto	NM_00129	RefSeq	Mus muscu	FALSE	17864	Mm.479	P51960	chr1	GO:000635	transcriptior	GO:000563	nucleus	GO:000367	DNA bindin	○
17222440	128.7281	235.9621	0.5455457	-0.874228	0	main		NM_01957	Rev1	REV1 homo	NM_01957	RefSeq	Mus muscu	FALSE	56210	Mm.38910	Q920Q2	chr1	GO:000626	DNA replica	GO:000563	nucleus	GO:000028	magnesium	○
17223138	81.77136	102.9134	0.7945648	-0.331763	0	main		NM_00116	Pgap1	post-GPI att	NM_00116	RefSeq	Mus muscu	FALSE	241062	Mm.10353	Q3UUQ7	chr1	GO:000650	GPI anchor	GO:000578	endoplasmi	GO:000451	nuclease ac	○
17223946	15.54949	16.0907	0.966365	-0.04936	0	main		NM_01015	Erbb4	v-erb-a erytl	NM_01015	RefSeq	Mus muscu	FALSE	13869	Mm.44242	Q61527	chr1	GO:000175	neural crest	GO:000563	nucleus // c	GO:000016	nucleotide b	○
17225373	43.87009	27.58103	1.5905893	0.6695613	0	main		NM_01026	Gbx2	gastrulation	NM_01026	RefSeq	Mus muscu	FALSE	14472	Mm.20473	P48031	chr1	GO:000156	patterning o	GO:000563	nucleus	GO:000367	DNA bindin	○
17228426	309.3543	377.0215	0.8205216	-0.285387	0	main		NM_00103	Cep350	centrosoma	NM_00103	RefSeq	Mus muscu	FALSE	74081	Mm.260247	D3YTP2	chr1	GO:000815	biological_p	GO:000563	nucleus // c	GO:000367	molecular_f	○
17229178	234.3915	249.8483	0.9381353	-0.092132	0	main		NM_009721	Atp1b1	ATPase, Na	NM_009721	RefSeq	Mus muscu	FALSE	11931	Mm.4550	P14094	chr1	GO:000166	response to	GO:000588	plasma mer	GO:000539	sodium:pota	○
17230469	64.60298	54.15099	1.1930157	0.254613	0	main		ENSMUST	Gm12657 /	predicted ge	ENSMUST	ENSEMBL	havana:kno	FALSE	667250	Mm.44977	E0CYN1	chr1	GO:000164	osteoblast d	GO:000022	nuclear chrc	GO:000097	RNA polym	○
17230602	168.3848	210.6942	0.7991905	-0.323389	0	main		NM_175127	Fbxo28	F-box protei	NM_175127	RefSeq	Mus muscu	FALSE	67948	Mm.30737	Q8BIG4	chr1	GO:000815	biological_p	GO:000557	cellular_con	GO:000367	molecular_f	○
17230668	283.7418	311.7881	0.9100469	-0.135987	0	main		NM_17738	Mia3	melanoma i	NM_17738	RefSeq	Mus muscu	FALSE	338366	Mm.41152	Q8BI84	chr1	GO:000206	chondrocyte	GO:000578	endoplasmi	GO:000367	molecular_f	○
17230760	51.96034	85.06554	0.6108271	-0.711164	0	main		NM_14551	Mark1	MAP/microt	NM_14551	RefSeq	Mus muscu	FALSE	226778	Mm.7445	Q8VHJ5	chr1	GO:000022	microtubule	GO:000573	cytoplasm ,	GO:000016	nucleotide b	○
17231461	215.5273	203.6139	1.0585098	0.0820346	0	main		NM_00795	Esr1	estrogen rec	NM_00795	RefSeq	Mus muscu	FALSE	13982	Mm.9213 /,	P19785	chr10	GO:000154	antral ovaria	GO:000563	nucleus // r	GO:000104	core promot	○
17232483	15.28952	13.23052	1.155625	0.2086734	0	main		XR_380237	LOC102632	uncharacter	XR_380237	RefSeq	PREDICTE	FALSE	102632938	---	Q8BG92	chr10	---	---	---	---	---	---	○
17232734	169.2554	158.2847	1.0693099	0.0966801	0	main		NM_00116	Cdk19	cyclin-deper	NM_00116	RefSeq	Mus muscu	FALSE	78334	Mm.200924	Q8BWD8	chr10	GO:000646	protein phos	GO:000557	cellular_con	GO:000016	nucleotide b	○
17233437	198.1677	215.519	0.9194906	-0.121093	0	main		NM_00119	Lims1	LIM and ser	NM_00119	RefSeq	Mus muscu	FALSE	110829	Mm.57734	Q99JW4	chr10	GO:000716	cell-matrix a	GO:000588	plasma mer	GO:000551	protein bind	○
17233457	663.1248	1143.976	0.5796667	-0.786704	0	main		NM_01124	Ranbp2	RAN bindin	NM_01124	RefSeq	Mus muscu	FALSE	19386	Mm.43169	Q9ERU9	chr10	GO:000645	protein foldi	GO:000563	nucleus // r	GO:000372	RNA bindin	○
17235211	219.8713	400.6118	0.5488388	-0.865546	0	main		NM_02156	Midn	midnolin	NM_02156	RefSeq	Mus muscu	FALSE	59090	Mm.14381	Q3TPJ7	chr10	GO:003313	negative reg	GO:000563	nucleus // r	GO:001990	kinase bindi	○
17236182	1261.031	1672.027	0.754193	-0.406994	0	main		NM_01159	Timp3	tissue inhibi	NM_01159	RefSeq	Mus muscu	FALSE	21859	Mm.4871	P39876	chr10	GO:001046	negative reg	GO:000557	extracellular	GO:000485	enzyme inh	○
17236439	16.5119	15.49385	1.0657067	0.0918105	0	main		NM_00112	Anks1b	ankyrin repe	NM_00112	RefSeq	Mus muscu	FALSE	77531	Mm.44060	Q8BIZ1	chr10	GO:000815	biological_p	GO:000563	nucleus // c	GO:004687	ephrin recep	○
17238449	193.3304	198.2105	0.9753792	-0.035965	0	main		NM_17279	Ankrd52	ankyrin repe	NM_17279	RefSeq	Mus muscu	FALSE	237615	Mm.440177	Q8BTI7	chr10	GO:000815	biological_p	GO:000557	cellular_con	GO:000367	molecular_f	○
17238571	297.3772	268.5456	1.107362	0.147127	0	main		NM_02887	Dnajc14	DnaJ (Hsp4	NM_02887	RefSeq	Mus muscu	FALSE	74330	Mm.29691	Q921R4	chr10	GO:000681	transport //	GO:000578	endoplasmi	GO:000166	G-protein co	○
17239234	28.0104	24.57605	1.1397438	0.1887095	0	main		NM_00111	Grm1	glutamate re	NM_00111	RefSeq	Mus muscu	FALSE	14816	Mm.48298	P97772	chr10	GO:000018	activation of	GO:000563	nucleus // p	GO:000163	PLC activat	○
17240123	11.87797	11.32564	1.0487681	0.0686957	0	main		XM_00651	Clvs2	clavesin 2	XM_00651	RefSeq	PREDICTE	FALSE	215890	Mm.94461	Q8BG92	chr10	GO:000681	transport //	GO:000562	intracellular	GO:000521	transporter a	○
17240226	378.1627	234.4308	1.6131101	0.6898449	0	main		NM_00853	Marcks	myristoylate	NM_00853	RefSeq	Mus muscu	FALSE	17118	Mm.30059	P26645	chr10	---	---	GO:000573	cytoplasm ,	GO:000377	actin bindin	○
17241032	201.7627	187.1108	1.078306	0.1087667	0	main		NM_02908	Ddit4	DNA-damag	NM_02908	RefSeq	Mus muscu	FALSE	74747	Mm.21697	Q9D3F7	chr10	GO:000166	response to	GO:000562	intracellular	GO:007188	14-3-3 prote	○
17243509	82.39014	139.9786	0.588591	-0.764663	0	main		NM_01091	Nfyb	nuclear tran	NM_01091	RefSeq	Mus muscu	FALSE	18045	Mm.24599	P63139	chr10	GO:000635	transcriptior	GO:000562	intracellular	GO:000367	DNA bindin	○
17245095	322.5288	384.7924	0.8381891	-0.254652	0	main		NM_00103	Cnot2	CCR4-NOT	NM_00103	RefSeq	Mus muscu	FALSE	72068	Mm.35155	Q8C5L3	chr10	GO:000012	negative reg	GO:000563	nucleus // c	GO:000122	RNA polym	○
17245188	245.1456	293.1326	0.8362959	-0.257915	0	main		NM_17779	Frs2	fibroblast gr	NM_17779	RefSeq	Mus muscu	FALSE	327826	Mm.13596	Q8C180	chr10	GO:000018	activation of	GO:000573	cytoplasm ,	GO:000506	transmemb	○
17245587	439.5294	454.9009	0.9662091	-0.049593	0	main		NM_00116	Mon2	MON2 hom	NM_00116	RefSeq	Mus muscu	FALSE	67074	Mm.169924	Q80TL7	chr10	GO:000681	transport //	GO:000580	trans-Golgi	GO:000508	ARF guanyl	○
17246268	48.08744	51.18897	0.9394102	-0.090173	0	main		NM_01177	Ikzf4	IKAROS far	NM_01177	RefSeq	Mus muscu	FALSE	22781	Mm.35864	Q8C208	chr10	GO:000635	transcriptior	GO:000563	nucleus	GO:000367	nucleic acid	○
17247448	286.4043	315.9281	0.906549	-0.141543	0	main		ENSMUST	Ppp3r1	protein phos	ENSMUST	ENSEMBL	havana:kno	FALSE	19058	Mm.41840	Q63810	chr11	GO:000156	patterning o	GO:000562	intracellular	GO:000472	phosphopro	○
17247519	177.3747	168.062	1.0554123	0.0778067	0	main		NM_03352	Spred2	sprouty-rela	NM_03352	RefSeq	Mus muscu	FALSE	114716	Mm.266627	Q924S7	chr11	GO:000018	inactivation	GO:000563	nucleus // c	GO:000517	stem cell fa	○
17247533	1017.681	1084.556	0.9383388	-0.091819	0	main		ENSMUST	Rab1	RAB1, mem	ENSMUST	ENSEMBL	havana:kno	FALSE	19324	Mm.271944	P62821	chr11	GO:000004	autophagic	GO:000013	Golgi memb	GO:000016	nucleotide b	○
17247550	413.364	423.2663	0.976605	-0.034153	0	main		ENSMUST	Peli1	pellino 1	ENSMUST	ENSEMBL	havana:kno	FALSE	67245	Mm.28957	Q8C669	chr11	GO:000020	protein poly	GO:000563	nucleus	GO:000484	ubiquitin-pr	○
17248213	433.511	864.8309	0.5012668	-0.996349	0	main		NM_00129	Cpeb4	cytoplasmic	NM_00129	RefSeq	Mus muscu	FALSE	67579	Mm.339792	Q7TN98	chr11	GO:000293	response to	GO:000563	nucleus // r	GO:000016	nucleotide b	○
17248288	127.1214	143.4328	0.8862785	-0.174168	0	main		NM_17736	Sh3pxd2b	SH3 and PX	NM_17736	RefSeq	Mus muscu	FALSE	268396	Mm.22761	A2AAY5	chr11	GO:000150	skeletal syst	GO:000210	podosome	GO:001031	phosphatidy	○
17248476	1037.724	939.384	1.1046856	0.1436359	0	main		NM_14596	Pank3	pantothenat	NM_14596	RefSeq	Mus muscu	FALSE	211347	Mm.255044	Q8R2W9	chr11	GO:001593	coenzyme A	GO:000573	cytoplasm ,	GO:000016	nucleotide b	○
17253307	210.5211	296.9527	0.7089382	-0.496268	0	main		NM_00102	Nufip2	nuclear frag	NM_00102	RefSeq	Mus muscu	FALSE	68564	Mm.42899	Q5F2E7	chr11	---	---	GO:000563	nucleus // c	GO:000372	RNA bindin	○
17254933	283.0973	393.6081	0.7192365	-0.475462	0	main		NM_01668	Vezf1	vascular en	NM_01668	RefSeq	Mus muscu	FALSE	22344	Mm.46628	Q5SXC3	chr11	GO:000152	angiogenesi	GO:000563	nucleus // r	GO:000367	nucleic acid	○
17255443	257.5068	225.9709	1.1395574	0.1884735	0	main		NM_20160	Zfp652	zinc finger p	NM_20160	RefSeq	Mus muscu	FALSE	268469	Mm.38903	Q5DU09	chr11	GO:000635	transcriptior	GO:000563	nucleus	GO:000367	nucleic acid	○
17255727	75.58215	61.25826	1.2338279	0.3031412	0	main		NM_001081	Osbpl7	oxysterol bir	NM_001081	RefSeq	Mus muscu	FALSE	71240	Mm.19045	A2A716	chr11	GO:000681	transport //	GO:000577	autophagic	GO:001548	cholesterol	○
17255775	78.28211	106.8942	0.7323326	-0.449429	0	main		NM_13865	Socs7	suppressor	NM_13865	RefSeq	Mus muscu	FALSE	192157	Mm.34339	Q8VHQ2	chr11	GO:000828	insulin rece	GO:000563	nucleus // r	---	---	○
17255828	163.7507	181.5189	0.9021138	-0.148619	0	main		NM_139311	Mllt6	myeloid/lym	NM_139311	RefSeq	Mus muscu	FALSE	246198	Mm.23685	B1AR09	chr11	GO:000815	biological_p	GO:000557	cellular_con	GO:004687	metal ion bi	○
17256991	44.79544	38.2034	1.1725511	0.2296508	0	main		NM_00111	Adam11	a disintegrir	NM_00111	RefSeq	Mus muscu	FALSE	11488	Mm.89854	Q9R1V4	chr11	GO:000650	proteolysis	GO:001602	membrane	GO:000422	metalloendo	○
17257235	112.4936	120.3888	0.9344191	-0.097858	0	main		NM_01678	Itgb3	integrin beta	NM_01678	RefSeq	Mus muscu	FALSE	16416	Mm.87150	O54890	chr11	GO:000193	positive reg	GO:000563	nucleus // p	GO:000375	protein disu	○
17257801	72.32794	65.87026	1.0980364	0.1349258	0	main		NM_01573	Axin2	axin2	NM_01573	RefSeq	Mus muscu	FALSE	12006	Mm.71710	O88566	chr11	GO:000175	somitogene	GO:000562	intracellular	GO:000487	signal trans	○
17258789	174.3007	226.4071	0.7698553	-0.377341	0	main		NM_19802	Tnrc6c	trinucleotide	NM_19802	RefSeq	Mus muscu	FALSE	217351	Mm.40272	Q3UHC0	chr11	GO:000170	endoderm f	GO:000557	cellular_con	GO:000016	nucleotide b	○
17261289	53.34941	45.55436	1.1711153	0.2278832	0	main		NM_14601	Eml6	echinoderm	NM_14601	RefSeq	Mus muscu	FALSE	237711	Mm.445271	Q5SQM0	chr11	GO:000815	biological_p	GO:000573	cytoplasm ,	GO:000367	molecular_f	○
17261896	26.70852	24.7414	1.0795072	0.1103729	0	main		NM_01025	Gabra1	gamma-ami	NM_01025	RefSeq	Mus muscu	FALSE	14394	Mm.43966	P62812	chr11	GO:000681	transport //	GO:000588	plasma mer	GO:000489	GABA-A re	○
17262055	49.51683	56.09911	0.8826669	-0.180059	0	main		NM_17252	Nipal4	NIPA-like do	NM_17252	RefSeq	Mus muscu	FALSE	214112	Mm.22525	Q8BZF2	chr11	GO:000681	transport //	GO:001602	membrane	GO:001509	magnesium	○
17262964	31.10429	28.15368	1.1048037	0.1437901	0	main		NM_00102	Fat2	FAT tumor	NM_00102	RefSeq	Mus muscu	FALSE	245827	Mm.33936	Q5F226	chr11	GO:000715	cell adhesio	GO:000563	nucleus // p	GO:000550	calcium ion	○
17266264	647.6657	808.1497	0.801418	-0.319373	0	main		NM_14482	Taok1	TAO kinase	NM_14482	RefSeq	Mus muscu	FALSE	216965	Mm.34043	Q5F2E8	chr11	GO:000016	MAPK casc	GO:000573	cytoplasm ,	GO:000016	nucleotide b	○
17266498	243.4246	313.5163	0.7764336	-0.365065	0	main		NM_008702	Nlk	nemo like ki	NM_008702	RefSeq	Mus muscu	FALSE	18099	Mm.9001	O54949	chr11	GO:000016	MAPK casc	GO:000563	nucleus // c	GO:000016	nucleotide b	○
17266534	109.636	102.0037	1.0748238	0.1041001	0	main		NM_013571	Ksr1	kinase supp	NM_013571	RefSeq	Mus muscu	FALSE	16706	Mm.4745	Q61097	chr11	GO:000646	protein phos	GO:000573	cytoplasm ,	GO:000467	protein kina	○
17267632	101.3317	105.6088	0.9595005	-0.059644	0	main		NM_01950	Dgke	diacylglycer	NM_01950	RefSeq	Mus muscu	FALSE	56077	Mm.15369	Q9R1C6	chr11	GO:000720	protein kina	GO:000573	cytoplasm ,	GO:000016	nucleotide b	○
17270621	236.9771	276.8301	0.8560381	-0.224253	0	main		NM_001081	Kansl1	KAT8 regula	NM_001081	RefSeq	Mus muscu	FALSE	76719	Mm.13641	Q80TG1	chr11	GO:001656	chromatin m	GO:000012	histone acet	GO:004399	histone acet	○
17272095	64.37485	96.8969	0.6643644	-0.589953	0	main		NM_008211	H3f3b	H3 histone,	NM_008211	RefSeq	Mus muscu	FALSE	15081	Mm.37156	P84244	chr11	GO:000164	osteoblast d	GO:000022	nuclear chrc	GO:000097	RNA polym	○
17272530	986.7911	1443.771	0.6834817	-0.549025	0	main		NM_01135	Srsf2	serine/argin	NM_01135	RefSeq	Mus muscu	FALSE	20382	Mm.21841	Q62093	chr11	GO:000639	mRNA proc	GO:000563	nucleus // r	GO:000016	nucleotide b	○
17273819	248.0828	307.9908	0.8054877	-0.312066	0	main		NM_00109	Atad2b	ATPase fam	NM_00109	RefSeq	Mus muscu	FALSE	320817	Mm.21096	E9Q166	chr12	GO:000815	biological_p	GO:000563	nucleus	GO:000016	nucleotide b	○
17277017	39.7174	37.5067	1.0589415	0.0826228	0	main		XM_00651	Rgs6	regulator of	XM_00651	RefSeq	PREDICTE	FALSE	50779	Mm.15301	Q9Z2H2	chr12	GO:000716	signal trans	GO:000573	cytoplasm ,	GO:000487	signal trans	○
17277177	52.09187	48.52398	1.0735284	0.1023603	0	main		NM_028821	Dnal1	dynein, axo	NM_028821	RefSeq	Mus muscu	FALSE	105000	Mm.10152	Q05A62	chr12	GO:000815	biological_p	GO:000557	cellular_con	GO:000367	molecular_f	○
17277387	115.658	250.5789	0.4615632	-1.1154	0	main	2Down	ENSMUST	Fos	FBJ osteosa	ENSMUST	ENSEMBL	havana:puta	FALSE	14281	Mm.24651	P01101	chr12	GO:000635	regulation o	GO:000563	nucleus // r	GO:000097	RNA polym	○
17277521	74.09139	58.45456	1.267504	0.3419903	0	main		NM_17735	Vash1	vasohibin 1	NM_17735	RefSeq	Mus muscu	FALSE	238328	Mm.216101	Q8C1W1	chr12	GO:000152	angiogenesi	GO:000557	extracellular	GO:000367	molecular_f	○
17279210	355.8349	385.0033	0.9242386	-0.113663	0	main		NM_00102	Klc1	kinesin light	NM_00102	RefSeq	Mus muscu	FALSE	16593	Mm.278357	O88447	chr12	GO:000688	intracellular	GO:000562	intracellular	GO:000377	microtubule	○
17280913	210.4908	167.5096	1.2565895	0.3295134	0	main		NM_021361	Nova1	neuro-oncol	NM_021361	RefSeq	Mus muscu	FALSE	664883	Mm.24719	Q9JKN6	chr12	GO:000039	mRNA splic	GO:000563	nucleus // r	GO:000372	RNA bindin	○
17281228	388.6653	432.9735	0.8976653	-0.15575	0	main		NM_00100	Ralgapa1	Ral GTPase	NM_00100	RefSeq	Mus muscu	FALSE	56784	Mm.29218	Q6GYP7	chr12	GO:000635	regulation o	GO:000563	nucleus // c	GO:000509	GTPase act	○
17284839	51.56115	54.55101	0.9451915	-0.081321	0	main		NM_17729	Itgb8	integrin beta	NM_17729	RefSeq	Mus muscu	FALSE	320910	Mm.21700	Q0VBD0	chr12	GO:000157	ganglioside	GO:001602	membrane	GO:000510	receptor bin	○
17286595	342.7743	444.4544	0.7712249	-0.374776	0	main		NM_00103	Rreb1	ras responsi	NM_00103	RefSeq	Mus muscu	FALSE	68750	Mm.49110	Q3UH06	chr13	GO:000635	transcriptior	GO:000563	nucleus // c	GO:000367	nucleic acid	○
17286962	470.676	611.6155	0.7695619	-0.377891	0	main		NM_15378	Mylip	myosin regu	NM_15378	RefSeq	Mus muscu	FALSE	218203	Mm.21285	Q8BM54	chr13	GO:000692	cellular com	GO:000562	intracellular	GO:000484	ubiquitin-pr	○
17286998	38.23375	32.43024	1.1789537	0.237507	0	main		NM_001081	Rbm24	RNA bindin	NM_001081	RefSeq	Mus muscu	FALSE	666794	Mm.38269	D3Z4I3	chr13	GO:001083	regulation o	GO:000563	nucleus // c	GO:000016	nucleotide b	○
17287144	44.78688	46.63666	0.9603364	-0.058388	0	main		AK029314	Tes3-ps	testis derive	AK029314	GenBank H	Mus muscu	FALSE	54339	Mm.44147	Q9QZ73	chr13	---	---	GO:000015	ubiquitin lig	---	---	○
17289196	82.20768	62.01216	1.3256703	0.406722	0	main		NM_17258	Lhfpl2	lipoma HMC	NM_17258	RefSeq	Mus muscu	FALSE	218454	Mm.31655	Q8BGA2	chr13	GO:000815	biological_p	GO:001602	membrane	GO:000367	molecular_f	○
17289824	189.1224	404.4613	0.4675908	-1.096681	0	main	2Down	NM_17259	Mier3	mesoderm i	NM_17259	RefSeq	Mus muscu	FALSE	218613	Mm.31012	Q3UHF3	chr13	GO:000635	transcriptior	GO:000563	nucleus // c	GO:000367	DNA bindin	○
17290121	383.4963	534.5063	0.7174776	-0.478994	0	main		XM_00651	Paip1	polyadenyla	XM_00651	RefSeq	PREDICTE	FALSE	218693	Mm.49024	Q8VE62	chr13	GO:000641	regulation o	GO:000573	cytoplasm ,	GO:000372	RNA bindin	○
17290363	155.3877	158.4648	0.9805818	-0.02829	0	main		NM_00103	Wdr37	WD repeat	NM_00103	RefSeq	Mus muscu	FALSE	207615	Mm.284654	Q8CBE3	chr13	GO:000815	biological_p	GO:000557	cellular_con	GO:000367	molecular_f	○
17290815	262.2838	241.5116	1.0860091	0.1190362	0	main		NM_019491	Rala	v-ral simian	NM_019491	RefSeq	Mus muscu	FALSE	56044	Mm.27348	P63321	chr13	GO:000091	cytokinesis	GO:000588	plasma mer	GO:000016	nucleotide b	○
17292174	355.5998	314.4709	1.1307876	0.177328	0	main		NM_00119	Atxn1	ataxin 1	NM_00119	RefSeq	Mus muscu	FALSE	20238	Mm.34268	P54254	chr13	GO:000635	transcriptior	GO:000563	nucleus // r	GO:000367	DNA bindin	○
17292346	339.4914	423.4393	0.8017475	-0.31878	0	main		NM_01107	Phf2	PHD finger	NM_01107	RefSeq	Mus muscu	FALSE	18676	Mm.48621	Q9WTU0	chr13	GO:000635	transcriptior	GO:000563	nucleus // r	GO:000090	sulfonate di	○
17292732	156.933	170.0451	0.9228905	-0.115769	0	main		NM_00114	Rnf44	ring finger p	NM_00114	RefSeq	Mus muscu	FALSE	105239	Mm.25366	Q3UHJ8	chr13	GO:000815	biological_p	GO:000557	cellular_con	GO:000827	zinc ion bin	○
17292759	61.13007	42.76512	1.4294376	0.5154476	0	main		NM_03361	Sncb	synuclein, b	NM_03361	RefSeq	Mus muscu	FALSE	104069	Mm.20084	Q91ZZ3	chr13	GO:000726	synaptic tra	GO:000563	nucleus // c	GO:000550	calcium ion	○
17293085	204.4518	273.2763	0.7481505	-0.4186	0	main		NM_02987	Hnrnpa0	heterogenec	NM_02987	RefSeq	Mus muscu	FALSE	77134	Mm.490274	Q9CX86	chr13	GO:000695	inflammator	GO:000563	nucleus // r	GO:000016	nucleotide b	○
17296142	370.2949	591.9007	0.6256031	-0.67668	0	main		NM_00112	Gpbp1	GC-rich pro	NM_00112	RefSeq	Mus muscu	FALSE	73274	Mm.57286	Q6NXH3	chr13	GO:000635	transcriptior	GO:000563	nucleus // r	GO:000367	DNA bindin	○
17297359	237.9575	225.8601	1.0535615	0.0752745	0	main		NM_00111	Thrb	thyroid horn	NM_00111	RefSeq	Mus muscu	FALSE	21834	Mm.32563	P37242	chr14	GO:000012	negative reg	GO:000079	nuclear chrc	GO:000367	DNA bindin	○
17297913	898.0315	821.9045	1.0926227	0.1277953	0	main		NM_00747	Arf4	ADP-ribosyl	NM_00747	RefSeq	Mus muscu	FALSE	11843	Mm.29776	P61750	chr14	GO:000647	protein ADP	GO:000562	intracellular	GO:000016	nucleotide b	○
17299217	44.12502	50.95481	0.8659638	-0.207621	0	main		NM_01963	Styx	serine/threo	NM_01963	RefSeq	Mus muscu	FALSE	56291	Mm.202561	Q60969	chr14	GO:000647	protein deph	GO:000573	cytoplasm ,	GO:000472	phosphopro	○
17299316	127.8254	157.564	0.8112602	-0.301763	0	main		NM_08084	Socs4	suppressor	NM_08084	RefSeq	Mus muscu	FALSE	67296	Mm.42588	Q91ZA6	chr14	GO:000717	negative reg	GO:000557	cellular_con	GO:000367	molecular_f	○
17300292	297.1501	235.6604	1.260925	0.3344825	0	main		NM_02299	Lrp10	low-density	NM_02299	RefSeq	Mus muscu	FALSE	65107	Mm.47271	Q7TQH7	chr14	GO:000662	lipid metabo	GO:001602	integral com	GO:000504	low-density	○
17300860	355.2199	446.2243	0.7960568	-0.329057	0	main		NM_02949	Zmym2	zinc finger,	NM_02949	RefSeq	Mus muscu	FALSE	76007	Mm.31417	Q9CU65	chr14	GO:000635	transcriptior	GO:000563	nucleus // F	GO:000551	protein bind	○
17301225	33.48871	27.66383	1.2105594	0.2756739	0	main		NM_17762	Fam167a	family with	NM_17762	RefSeq	Mus muscu	FALSE	219148	Mm.37882	Q6P1G6	chr14	GO:000815	biological_p	GO:000557	cellular_con	GO:000367	molecular_f	○
17301849	30.26217	40.01425	0.7562848	-0.402998	0	main		ENSMUST	Gm16549	predicted ge	ENSMUST	ENSEMBL	havana:kno	FALSE	---	---	Q8BX90	chr14	---	---	---	---	---	---	○
17302600	45.80589	50.52592	0.906582	-0.141491	0	main		NM_19886	Slitrk5	SLIT and N	NM_19886	RefSeq	Mus muscu	FALSE	75409	Mm.235097	Q810B7	chr14	GO:000726	synaptic tra	GO:001602	membrane	GO:000367	molecular_f	○
17303941	218.0668	193.7652	1.1254178	0.1704607	0	main		NM_01882	Ap3m1	adaptor-rela	NM_01882	RefSeq	Mus muscu	FALSE	55946	Mm.37626	Q9JKC8	chr14	GO:000681	transport //	GO:000562	intracellular	---	---	○
17305662	520.9209	595.9213	0.8741438	-0.194057	0	main		NM_14605	Fermt2	fermitin fam	NM_14605	RefSeq	Mus muscu	FALSE	218952	Mm.21001	Q8CIB5	chr14	GO:000715	cell adhesio	GO:000172	stress fiber	GO:000554	phosphatidy	○
17306230	188.8597	207.4168	0.9105323	-0.135218	0	main		NM_20163	Chd8	chromodom	NM_20163	RefSeq	Mus muscu	FALSE	67772	Mm.289934	Q09XV5	chr14	GO:000170	in utero eml	GO:000563	nucleus // r	GO:000016	nucleotide b	○
17307709	212.3038	205.0916	1.0351658	0.0498618	0	main		XM_00651	Hmbox1	homeobox c	XM_00651	RefSeq	PREDICTE	FALSE	219150	Mm.344074	Q8BJA3	chr14	GO:000635	transcriptior	GO:000563	nucleus // c	GO:000367	DNA bindin	○
17307935	103.3587	173.6408	0.5952443	-0.748446	0	main		NM_02803	Ppp2r2a	protein phos	NM_02803	RefSeq	Mus muscu	FALSE	71978	Mm.273997	Q6P1F6	chr14	GO:000647	protein deph	GO:000015	protein phos	GO:000472	protein serir	○
17308132	217.3462	245.1689	0.8865162	-0.173781	0	main		NM_026331	Slc25a37	solute carrie	NM_026331	RefSeq	Mus muscu	FALSE	67712	Mm.29363	Q920G8	chr14	GO:000681	transport //	GO:000573	mitochondri	GO:000538	iron ion tran	○
17308165	85.0218	82.31371	1.0328996	0.0467001	0	main		ENSMUST	Gm21464	predicted ge	ENSMUST	ENSEMBL	havana:kno	FALSE	100862085	Mm.29144	Q920G8	chr14	GO:000681	transport //	GO:000573	mitochondri	GO:000538	iron ion tran	○
17308525	657.1865	788.4019	0.8335679	-0.262628	0	main		NM_20763	Fndc3a	fibronectin t	NM_20763	RefSeq	Mus muscu	FALSE	319448	Mm.205421	Q8BX90	chr14	GO:000728	spermatid d	GO:000166	acrosomal v	GO:004482	poly(A) RN	○
17309774	26.01733	29.32752	0.8871302	-0.172782	0	main		NM_010201	Fgf14	fibroblast gr	NM_010201	RefSeq	Mus muscu	FALSE	14169	Mm.206362	P70379	chr14	GO:000725	JNK cascac	GO:000557	extracellular	GO:000510	receptor bin	○
17310872	381.6093	311.0828	1.226713	0.2947977	0	main		NM_00830	Sdc2	syndecan 2	NM_00830	RefSeq	Mus muscu	FALSE	15529	Mm.23426	P43407	chr15	GO:000739	nervous sys	GO:001602	membrane	GO:000551	protein bind	○
17311272	117.3688	118.9235	0.9869269	-0.018985	0	main		NM_01176	Zfpm2	zinc finger p	NM_01176	RefSeq	Mus muscu	FALSE	22762	Mm.39496	Q8CCH7	chr15	GO:000012	negative reg	GO:000563	nucleus // r	GO:000107	nucleic acid	○
17314421	18.83454	20.39221	0.9236145	-0.114637	0	main		NM_00116	Pdzrn4	PDZ domai	NM_00116	RefSeq	Mus muscu	FALSE	239618	Mm.30982	B9EKP7	chr15	GO:000815	biological_p	GO:000557	cellular_con	GO:004687	metal ion bi	○
17315500	31.42917	25.73942	1.221052	0.2881246	0	main		NM_01046	Hoxc10	homeobox C	NM_01046	RefSeq	Mus muscu	FALSE	209448	Mm.31665	P31257	chr15	GO:000150	skeletal syst	GO:000563	nucleus // c	GO:000367	DNA bindin	○
17315810	532.1091	705.8835	0.75382	-0.407708	0	main		NM_027707	Nipbl	Nipped-B h	NM_027707	RefSeq	Mus muscu	FALSE	71175	Mm.24032	Q6KCD5	chr15	GO:000012	negative reg	GO:000563	nucleus // S	GO:000368	chromatin b	○
17316845	65.56257	58.41259	1.1224048	0.1665931	0	main		NM_00128	Sybu	syntabulin (	NM_00128	RefSeq	Mus muscu	FALSE	319613	Mm.20771	Q8BHS8	chr15	GO:006117	regulation o	GO:000579	Golgi appar	GO:000801	microtubule	○
17316956	168.1638	193.3805	0.8696006	-0.201575	0	main		ENSMUST	Trps1	trichorhinop	ENSMUST	ENSEMBL	havana:puta	FALSE	83925	Mm.30466	Q8BZ62	chr15	GO:000012	negative reg	GO:000563	nucleus // r	GO:000367	DNA bindin	○
17316977	26.61115	27.01605	0.9850126	-0.021786	0	main		NR_035444	Mir1907	microRNA 1	NR_035444	RefSeq	Mus muscu	FALSE	100316685	---	Q925H1	chr15	---	---	---	---	---	---	○
17319299	252.4587	309.8194	0.8148576	-0.29538	0	main		NM_00120	Sun2	Sad1 and U	NM_00120	RefSeq	Mus muscu	FALSE	223697	Mm.20271	Q8BJS4	chr15	GO:000699	nuclear env	GO:000078	nuclear chrc	GO:000551	protein bind	○
17320583	187.5397	216.8393	0.8648787	-0.20943	0	main		NM_00103	Cpne8	copine VIII	NM_00103	RefSeq	Mus muscu	FALSE	66871	Mm.290991	Q9DC53	chr15	GO:000815	biological_p	GO:007006	extracellular	GO:000367	molecular_f	○
17322261	459.7737	431.9658	1.0643752	0.0900068	0	main		ENSMUST	Atf7	activating tr	ENSMUST	ENSEMBL	ensembl:kn	FALSE	---	---	Q7TNN1	chr15	---	---	---	---	---	---	○
17322263	542.6584	591.0241	0.9181663	-0.123173	0	main		NM_14606	Atf7	activating tr	NM_14606	RefSeq	Mus muscu	FALSE	223922	Mm.208714	Q8R0S1	chr15	GO:000635	regulation o	GO:003439	nuclear peri	GO:000813	transcriptior	○
17322359	141.1824	104.1711	1.3552934	0.4386052	0	main		NM_01386	Zfp385a	zinc finger p	NM_01386	RefSeq	Mus muscu	FALSE	29813	Mm.14099	Q8VD12	chr15	GO:000635	transcriptior	GO:000079	nuclear chrc	GO:000203	p53 binding	○
17322950	92.95651	85.33616	1.089298	0.1233987	0	main		NM_02896	Snx29	sorting nexi	NM_02896	RefSeq	Mus muscu	FALSE	74478	Mm.325831	Q9D3S3	chr16	GO:000815	biological_p	GO:000587	kinesin com	GO:003509	phosphatidy	○
17323465	159.4473	180.2454	0.8846123	-0.176883	0	main		NM_02334	Snap29	synaptosom	NM_02334	RefSeq	Mus muscu	FALSE	67474	Mm.271992	Q9ERB0	chr16	GO:000004	autophagic	GO:000573	cytoplasm ,	GO:001990	syntaxin bin	○
17327445	15.47195	13.26748	1.1661559	0.2217607	0	main		ENSMUST	Dennd1b	DENN/MAD	ENSMUST	ENSEMBL	ensembl_lir	FALSE	329260	Mm.337604	Q3U1T9	chr16	GO:000681	transport //	GO:000573	cytoplasm ,	GO:000508	guanyl-nucl	○
17327465	309.0158	528.1785	0.5850594	-0.773345	0	main		NM_01180	Ets2	E26 avian le	NM_01180	RefSeq	Mus muscu	FALSE	23872	Mm.290207	P15037	chr16	GO:000635	transcriptior	GO:000563	nucleus // r	GO:000097	RNA polym	○
17327482	50.936	51.22802	0.9942996	-0.008247	0	main		ENSMUST	Gm15342	predicted ge	ENSMUST	ENSEMBL	havana:kno	FALSE	---	Mm.399491	Q921C3	chr16	---	---	---	---	---	---	○
17328104	55.21127	60.51356	0.9123785	-0.132296	0	main		NM_001271	Socs1	suppressor	NM_001271	RefSeq	Mus muscu	FALSE	12703	Mm.130	O35716	chr16	GO:000193	regulation o	GO:000562	intracellular	GO:000515	insulin-like	○
17329258	92.12485	118.6727	0.7762935	-0.365326	0	main		ENSMUST	Igf2bp2	insulin-like	ENSMUST	ENSEMBL	havana:kno	FALSE	319765	Mm.489442	Q5SF07	chr16	GO:000641	regulation o	GO:000563	nucleus // c	GO:000016	nucleotide b	○
17331418	76.68375	145.4918	0.5270658	-0.923945	0	main		NM_02805	Zfp654	zinc finger p	NM_02805	RefSeq	Mus muscu	FALSE	72020	Mm.25960	Q9DAU9	chr16	GO:000635	transcriptior	GO:000563	nucleus	GO:000367	DNA bindin	○
17332395	170.6023	251.0268	0.6796179	-0.557204	0	main		NM_00110	Brwd1	bromodoma	NM_00110	RefSeq	Mus muscu	FALSE	93871	Mm.240871	Q921C3	chr16	GO:000635	transcriptior	GO:000563	nucleus // r	GO:000551	protein bind	○
17332628	194.4698	191.0261	1.0180274	0.0257764	0	main		NM_174847	C2cd2	C2 calcium-	NM_174847	RefSeq	Mus muscu	FALSE	207781	Mm.1465	E9Q3C1	chr16	GO:000815	biological_p	GO:000563	nucleus // c	GO:000367	molecular_f	○
17334241	188.232	237.5832	0.7922782	-0.335921	0	main		NM_00108	Rnps1	ribonucleic	NM_00108	RefSeq	Mus muscu	FALSE	19826	Mm.1951	Q99M28	chr17	GO:000018	nuclear-tran	GO:000563	nucleus // c	GO:000016	nucleotide b	○
17335550	114.5701	101.6232	1.127401	0.1730008	0	main		NM_198647	Tbc1d22b	TBC1 doma	NM_198647	RefSeq	Mus muscu	FALSE	381085	Mm.328934	Q6PAT2	chr17	GO:000815	biological_p	GO:000557	cellular_con	GO:000367	molecular_f	○
17338460	43.92234	36.53804	1.202099	0.2655557	0	main		NM_027452	Lrfn2	leucine rich	NM_027452	RefSeq	Mus muscu	FALSE	70530	Mm.133607	Q80TG9	chr17	---	---	GO:000588	plasma mer	GO:000551	protein bind	○
17338521	83.08208	96.95976	0.8568718	-0.222849	0	main		NM_01388	Plcl2	phospholipa	NM_01388	RefSeq	Mus muscu	FALSE	224860	Mm.217362	Q8K394	chr17	GO:000232	B cell prolife	GO:000573	cytoplasm	GO:000443	phosphatidy	○
17339973	174.6721	217.6629	0.8024891	-0.317446	0	main		NM_134117	Pkdcc	protein kina	NM_134117	RefSeq	Mus muscu	FALSE	106522	Mm.311974	Q5RJI4	chr17	GO:000150	skeletal syst	GO:000579	Golgi appar	GO:000016	nucleotide b	○
17340323	217.4165	303.9398	0.7153275	-0.483324	0	main		NM_18097	Foxn2	forkhead bo	NM_18097	RefSeq	Mus muscu	FALSE	14236	Mm.112824	D3Z6Z3	chr17	GO:000635	transcriptior	GO:000563	nucleus // i	GO:000367	DNA bindin	○
17340756	1248.215	1358.052	0.9191217	-0.121672	0	main		NM_00115	Qk	quaking	NM_00115	RefSeq	Mus muscu	FALSE	19317	Mm.38413	Q9QYS9	chr17	GO:000157	vasculogene	GO:000563	nucleus // c	GO:000372	RNA bindin	○
17345038	647.5317	811.4113	0.7980314	-0.325483	0	main		NM_009847	Cd2ap	CD2-associ	NM_009847	RefSeq	Mus muscu	TRUE	12488	Mm.218637	Q9JLQ0	chr17	GO:000704	cell cycle //	GO:000172	ruffle // cyt	GO:000517	vascular en	○
17345134	41.16046	31.27957	1.3158896	0.3960384	0	main		NM_00114	Runx2	runt related	NM_00114	RefSeq	Mus muscu	TRUE	12393	Mm.391013	Q08775	chr17	GO:000150	skeletal syst	GO:000079	nuclear chrc	GO:000097	RNA polym	○
17347680	490.6622	931.9779	0.5264741	-0.925566	0	main		NM_001001	Zfp36l2	zinc finger p	NM_001001	RefSeq	Mus muscu	TRUE	12193	Mm.259321	P23949	chr17	GO:000028	nuclear-tran	GO:000563	nucleus // c	GO:000367	DNA bindin	○
17348238	200.9488	276.0688	0.7278939	-0.4582	0	main		NM_00127	Rab18	RAB18, me	NM_00127	RefSeq	Mus muscu	TRUE	19330	Mm.132802	P35293	chr18	GO:000681	transport //	GO:000562	intracellular	GO:000016	nucleotide b	○
17348591	17.7663	19.43399	0.9141869	-0.129439	0	main		NM_00104	Cabyr	calcium-bin	NM_00104	RefSeq	Mus muscu	TRUE	71132	Mm.17974	Q9D424	chr18	GO:001972	calcium-me	GO:000562	intracellular	GO:000550	calcium ion	○
17349243	289.953	371.9801	0.7794852	-0.359406	0	main		NM_01194	Map3k2	mitogen-act	NM_01194	RefSeq	Mus muscu	TRUE	26405	Mm.211762	Q61083	chr18	GO:000016	MAPK casc	GO:000563	nucleus // c	GO:000016	nucleotide b	○
17349572	242.5387	254.2783	0.9538317	-0.068193	0	main		NM_02642	Paip2	polyadenyla	NM_02642	RefSeq	Mus muscu	TRUE	67869	Mm.126534	Q9D6V8	chr18	GO:000641	regulation o	GO:000573	cytoplasm ,	GO:000090	translation r	○
17349671	299.7853	469.3047	0.6387861	-0.646595	0	main		NM_17537	Ankhd1	ankyrin repe	NM_17537	RefSeq	Mus muscu	TRUE	108857	Mm.482287	E9PUR0	chr18	GO:000815	biological_p	---	---	GO:004482	poly(A) RN	○
17349713	288.4999	385.6921	0.7480057	-0.418879	0	main		ENSMUST	Ankhd1	ankyrin repe	ENSMUST	ENSEMBL	havana:puta	TRUE	108857	Mm.482287	F6RUI8	chr18	GO:000815	biological_p	---	---	GO:004482	poly(A) RN	○
17349807	73.48066	74.36163	0.9881529	-0.017194	0	main		NM_00100	Pcdhac1	protocadher	NM_00100	RefSeq	Mus muscu	TRUE	353236	Mm.30850	O88689	chr18	GO:000715	cell adhesio	GO:000588	plasma mer	GO:000550	calcium ion	○
17350011	698.5485	691.2709	1.0105279	0.0151091	0	main		NM_02299	Ndfip1	Nedd4 fami	NM_02299	RefSeq	Mus muscu	TRUE	65113	Mm.10249	Q8R0W6	chr18	GO:000276	regulation o	GO:000557	extracellular	GO:000487	signal trans	○
17351594	440.16	416.0981	1.0578275	0.0811043	0	main		NM_00108	Tcf4	transcriptior	NM_00108	RefSeq	Mus muscu	TRUE	21413	Mm.4269	Q60722	chr18	GO:000012	negative reg	GO:000563	nucleus // r	GO:000097	RNA polym	○
17352212	100.4986	94.76816	1.060468	0.0847011	0	main		NM_14609	Zadh2	zinc binding	NM_14609	RefSeq	Mus muscu	TRUE	225791	Mm.147052	Q8BGC4	chr18	GO:005511	oxidation-re	GO:000573	mitochondri	GO:000827	zinc ion bin	○

17519967	77.80013	63.36783	1.2277544	0.296022	0	main		NM_011162	Tpbg	trophoblast	NM_011627	RefSeq	Mus muscu	TRUE	21983	Mm.20864	Q9Z0L0	chr9	---	---	GO:000573	cytoplasm	---	---	○
17520815	381.8084	686.8726	0.5558649	-0.847194	0	main		NM_001110	Msl2	male-specifi	NM_001110	RefSeq	Mus muscu	TRUE	77853	Mm.326206	Q69ZF8	chr9	GO:004398	histone H4-	GO:007248	MSL compl	GO:000827	zinc ion bin	○
17522848	205.7395	257.2575	0.7997415	-0.322394	0	main		NM_001048	Azi2	5-azacytidin	NM_001048	RefSeq	Mus muscu	TRUE	27215	Mm.92705	Q9QYP6	chr9	GO:000027	mitotic cell	GO:000573	cytoplasm	GO:000551	protein bind	○
17523081	70.94463	40.75385	1.740808	0.7997571	0	main		NM_007399	Acvr2b	activin rece	NM_007399	RefSeq	Mus muscu	TRUE	11481	Mm.390239	P27040	chr9	GO:000150	skeletal sys	GO:000562	cell // cytop	GO:000016	nucleotide b	○
17526130	339.0828	396.8731	0.8543859	-0.22704	0	main		NM_007616	Cbl	Casitas B-lin	NM_007616	RefSeq	Mus muscu	TRUE	12402	Mm.266871	P22682	chr9	GO:000716	cell surface	GO:000563	nucleus // c	GO:000178	phosphotyro	○
17528714	235.3805	249.4519	0.9435907	-0.083767	0	main		NM_001255	Tcf12	transcriptior	NM_001255	RefSeq	Mus muscu	TRUE	21406	Mm.171615	Q61286	chr9	GO:000635	transcriptior	GO:000563	nucleus // t	GO:000367	DNA bindin	○
17529713	331.4807	529.5917	0.6259175	-0.675956	0	main		NM_001114	U2surp	U2 snRNP-l	NM_001114	RefSeq	Mus muscu	TRUE	67958	Mm.292742	Q6NV83	chr9	GO:000639	RNA proces	GO:000563	nucleus // r	GO:000016	nucleotide b	○
17530930	64.3563	59.80752	1.076057	0.1057545	0	main		NM_001042	Sema3b	sema domai	NM_001042	RefSeq	Mus muscu	TRUE	20347	Mm.4083	Q62177	chr9	GO:000727	multicellular	GO:000557	extracellular	GO:000487	receptor act	○
17530955	986.2798	842.2397	1.1710203	0.2277661	0	main		NM_008138	Gnai2	guanine nuc	NM_008138	RefSeq	Mus muscu	TRUE	14678	Mm.196464	P08752	chr9	GO:000018	activation of	GO:000563	nucleus // c	GO:000016	nucleotide b	○
17531734	28.70505	28.00312	1.0250661	0.035717	0	main		NM_016852	Stac	src homolog	NM_016852	RefSeq	Mus muscu	TRUE	20840	Mm.1414	P97306	chr9	GO:003460	cellular resp	GO:000573	cytoplasm	GO:004687	metal ion bi	○
17533416	512.7594	858.501	0.5972729	-0.743538	0	main		NM_010028	Ddx3x	DEAD/H (A	NM_010028	RefSeq	Mus muscu	TRUE	13205	Mm.289662	Q62167	chrX	GO:000237	immune sys	GO:000563	nucleus // c	GO:000016	nucleotide b	○
17535208	1145.401	546.4041	2.0962526	1.0678126	0	main	2Up	NM_001290	Fmr1	fragile X mr	NM_001290	RefSeq	Mus muscu	TRUE	14265	Mm.3451	P35922	chrX	GO:000681	transport	GO:000563	nucleus // c	GO:000372	RNA bindin	○
17535241	124.9131	151.5649	0.8241559	-0.279011	0	main		ENSMUST(	Styx	serine/threo	ENSMUST(	ENSEMBL	havana:kno	TRUE	56291	Mm.202561	Q60969	chrX	GO:000647	protein dept	GO:000573	cytoplasm	GO:000472	phosphopro	○
17538018	16.33215	16.62154	0.9825895	-0.025339	0	main		NM_013724	Nrk	Nik related l	NM_013724	RefSeq	Mus muscu	TRUE	27206	Mm.482319	Q9R0G8	chrX	GO:000646	protein phos	GO:000573	cytoplasm	GO:000016	nucleotide b	○
17538395	9.817351	10.32762	0.9505918	-0.073102	0	main		NM_001033	Zcchc16	zinc finger,	NM_001033	RefSeq	Mus muscu	TRUE	619287	Mm.387961	Q3URY0	chrX	GO:000815	biological_p	GO:000557	cellular_con	GO:000367	nucleic acid	○
17538658	24.19338	22.67239	1.0670856	0.0936759	0	main		NM_001271	Wnk3	WNK lysine	NM_001271	RefSeq	Mus muscu	TRUE	279561	Mm.441474	Q80XP9	chrX	GO:000646	protein phos	GO:000573	cytoplasm	GO:000016	nucleotide b	○
17539828	24.83115	25.36139	0.9790926	-0.030483	0	main		NM_019461	Usp27x	ubiquitin sp	NM_019461	RefSeq	Mus muscu	TRUE	54651	Mm.483107	Q8CEG8	chrX	GO:000650	proteolysis	GO:000557	cellular_con	GO:000823	peptidase ac	○
17541343	21.40386	20.20307	1.059436	0.0832965	0	main		NM_001290	Smarca1	SWI/SNF re	NM_001290	RefSeq	Mus muscu	TRUE	93761	Mm.229151	Q6PGB8	chrX	GO:000073	DNA strand	GO:000079	nuclear chr	GO:000016	nucleotide b	○
17543840	12.03887	12.28752	0.979764	-0.029494	0	main		NM_001007	C77370	expressed s	NM_001007	RefSeq	Mus muscu	TRUE	245555	Mm.381907	Q5DTT1	chrX	GO:000008	mitotic S ph	GO:000563	nucleus // c	GO:000388	DNA-directe	○
17544102	56.45731	66.44284	0.8497125	-0.234953	0	main		ENSMUST(	Brwd3	bromodoma	ENSMUST(	ENSEMBL	ensembl_ha	TRUE	382236	Mm.426127	A2AHJ4	chrX	GO:000701	cytoskeletor	GO:000557	cellular_con	GO:000551	protein bind	○
17544939	360.4171	267.6529	1.346584	0.4293042	0	main		NM_001007	Tsc22d3	TSC22 dom	NM_001007	RefSeq	Mus muscu	TRUE	14605	Mm.22216	Q9Z2S7	chrX	GO:000012	negative reg	GO:000563	nucleus // c	GO:000370	sequence-sp	○
17545078	95.12606	93.64679	1.0157963	0.0226111	0	main		NM_019490	Ammecr1	Alport syndr	NM_019490	RefSeq	Mus muscu	TRUE	56068	Mm.143724	Q9JHT5	chrX	GO:000815	biological_p	GO:000557	cellular_con	GO:000367	molecular_f	○
17545618	57.85563	41.40395	1.3973457	0.4826889	0	main		XM_006528	Ptchd1	patched dor	XM_006528	RefSeq	PREDICTE	TRUE	211612	Mm.218811	Q14B62	chrX	GO:000722	smoothened	GO:000588	plasma mer	GO:000815	hedgehog re	○
17545629	13.29709	15.85833	0.8384925	-0.25413	0	main		NM_011077	Phex	phosphate r	NM_011077	RefSeq	Mus muscu	TRUE	18675	Mm.2529	P70669	chrX	GO:000650	proteolysis	GO:000578	endoplasmi	GO:000422	metalloendo	○
17546834	541.8898	1081.035	0.5012694	-0.996342	0	main		NM_012008	Ddx3y	DEAD (Asp	NM_012008	RefSeq	Mus muscu	TRUE	26900	Mm.302938	Q62095	chrY	GO:000620	ATP catabo	GO:000563	nucleus // c	GO:000016	nucleotide b	○
17547616	769.094	810.2198	0.9492412	-0.075153	0	main		---	---	---	X91866	GenBank	M.musculus	TRUE	---	---	P84244	chr11	GO:000633	nucleosome	GO:000078	nucleosome	GO:000367	DNA bindin	○
17547837	85.62926	88.08841	0.9720832	-0.040848	0	main		ENSMUST(	Gm21464	predicted ge	ENSMUST(	ENSEMBL	havana:kno	TRUE	100862085	Mm.291443	Q920G8	chr14	GO:000681	transport	GO:000573	mitochondri	GO:000538	iron ion tran	○
17547846	92.70303	94.7348	0.9785531	-0.031278	0	main		ENSMUST(	Gm21464	predicted ge	ENSMUST(	ENSEMBL	havana:kno	TRUE	100862085	Mm.291443	Q920G8	chr14	GO:000681	transport	GO:000573	mitochondri	GO:000538	iron ion tran	○
17548283	948.6991	1613.575	0.5879486	-0.766238	0	main		NM_008211	H3f3b	H3 histone,	NM_008211	RefSeq	Mus muscu	TRUE	15081	Mm.371563	P84244	chr3	GO:000164	osteoblast d	GO:000022	nuclear chr	GO:000097	RNA polym	○
17548518	1182.456	1200.466	0.9849975	-0.021808	0	main		NM_001081	Gm12657	predicted ge	NM_001081	RefSeq	Mus muscu	TRUE	667250	Mm.449778	P84244	chr6	---	---	---	---	---	---	○
17548946	826.8755	1431.395	0.5776711	-0.79168	0	main		NM_008211	H3f3b	H3 histone,	NM_008211	RefSeq	Mus muscu	TRUE	15081	Mm.371563	P84244	chr1	GO:000164	osteoblast d	GO:000022	nuclear chr	GO:000097	RNA polym	○

Supplementary Table 6. Validated and predicted target genes for Mir221 and Mir222

RGS6	SUN2	ARID1A	KHDRBS2	KLF3	GRM1	GBX2	PHEX
CDKN1B	ARHGEF7	DDIT4	CPNE8	ANKIB1	RREB1	HNRNPA0	MAGI1
CXCL12	ARF4	NIPAL4	MLLT6	FGF14	PTCHD1	DDX3Y	ANKS1B
TCF12	BRWD1	TPBG	RPH3A	S100PBP	VASH1	INSIG1	CAPRIN2
RFX7	RALGAPA1	MEGF9	ATP1B1	ERBB4	CMTM4	FERMT2	LRP10
SEC62	ZFPM2	CNR1	POGZ	EMX2	SPPL3	SPRED2	ZFP90
GABRA1	KIAA1370	NFYB	REV1	CD2AP	MEX3A	HDGF	
HECTD2	ANGPTL2	TSC22D3	USP27X	PHF2	ZNF654	PELI1	
KIT	MIDN	CDK19	CDKN1C	PDGFA	MAPK10	VKORC1L1	
VGLL4	DPP8	FOS	KIAA1267	PLEKHA6	ZEB2	TEAD1	
PAIP1	CHSY1	TOX	MESDC1	CNOT2	ACVR2B	FBXO28	
TP53BP2	MIER3	NAA25	RNPS1	AJAP1	MARCKS	MARK1	
NAP1L5	C3orf70	MSL2	VAPB	CDH2	AAK1	SMARCA1	
ZFAND5	CASZ1	ASPH	CBFB	ADAM11	NFAT5	EFCAB14	
NRK	NSMCE4A	GPM6A	KIAA0368	ITGB8	NDFIP1	PPP6C	
IRX5	YWHAG	AGFG1	LPPR1	HOXA7	STX1B	RC3H2	
DCUN1D1	EIF3J	HIPK1	PAK1	BAZ2B	ANKRD52	CAMK1D	
CLVS2	FOXN2	NFATC3	SPATS2L	TAOK1	TCF4	RFX3	
LRRTM2	CD4	ZCCHC16	CBL	FAM167A	EIF4E3	UBE2E3	
ETV3	DCUN1D4	IGDCC4	CTCF	PBX3	TRPS1	PDCD10	
AP3B2	GPBP1	CREBZF	C11orf87	C14orf147	THRB	U2SURP	
PPP3R1	UBN2	TLE3	HIPK2	SLITRK5	DGKE	DDX3X	
RIMS3	ZNF385A	DNAJC14	TP53INP1	LHFPL2	SLC1A2	THSD7B	
DCAF12	PRUNE	ZFP36L2	FRS2	PTBP2	RNF165	MAGI2	
ZNF652	ARNT	PPP2R2A	ESR1	AMMECR1	C16orf52	PGAP1	
DMRT3	UBE2J1	ZMYM2	SMARCA5	CAPRIN1	AGPS	BBC3	
CCDC64	PCDHA9	BRWD3	GNAI2	FOXP1	OSBPL7	STMN1	
EML6	PCDHAC2	NLK	VEZF1	ZNF618	PVRL1	CABYR	
CACNB4	PCDHAC1	SEMA3B	TCF7L2	SRSF2	DNAL1	MED12L	
PLEKHA2	PCDHA13	HNRNPA3	H3F3A	IKZF4	E2F2	HELQ	
NRG1	PCDHA12	IPO7	DKK2	GALNTL4	TNRC6C	SLC25A37	
NTF3	PCDHA11	ANKHD1	IGF2BP2	MAP3K2	SOCS7	MYBL1	
FAM38B	PCDHA10	STYX	DENND1B	C16orf45	SNX29	SYBU	
SCD5	PCDHA8	FMR1	RNF44	AP3M1	WASF2	FAM214A	
MIA3	PCDHA7	SNCB	PKDCC	CEP350	KCNA1	KLC1	
RBM24	PCDHA6	RUNX2	ETS2	TIMP3	KIAA2022	PANK3	
FNDC3A	PCDHA5	METTL10	C17orf63	ATAD2B	RIMBP2	ADAM22	
NOVA1	PCDHA4	WDR37	FAT2	RANBP2	RALA	SNAP29	
TMCC1	PCDHA3	LOC388630	SEC23IP	MON2	FKTN	MCMDC2	
BCL2L11	PCDHA2	BEND4	SLC4A4	PHC2	MAP3K10	PHACTR4	
WDR47	PCDHA1	ST8SIA1	TIPARP	CUX1	SNAP25	CAMTA1	
EIF5A2	GNAI3	ROD1	NUFIP2	SOCS1	ITIH5	ASB4	
HMBOX1	SHANK2	KIAA0494	ARL6IP1	FOXP2	PI15	URI1	
WNK3	SBK1	AZI2	ZADH2	NANOS1	PCDH10	ZBTB41	
C18orf25	ATF7	RAB1A	IGSF3	RAB3GAP2	FNIP2	RAB18	
MYLIP	PAIP2	ITGB3	SH3PXD2B	DLG2	CPEB4	LIMS1	
KIF16B	RSBN1L	HOXC10	PDIK1L	YTHDC1	STAC	GUCY1A2	
BMF	ETS1	ZNF629	KSR1	GAB1	PDZRN4	ATF2	
IRF2	AXIN2	QKI	ATXN1	C2CD2	SDC2	CHD8	
PLCL2	NIPBL	LRFN2	SH3BP4	TBC1D22B	HIPK3	ASB7	

Supplementary Table 7. Expression of candidate target genes of miR-221-3p and miR-222-3p in Mir221/222flox/y and Mir221/222AdipoKO mice fed with stardard (STD) and high fat-high sucrose (HFHS) chow.

Annotation	Expression value				Ratio				Keyword
Gene Symbol	STD flox/y	HFHS flox/y	STD AdipoKO	HFHS AdipoKO	STD AdipoKO / STD flox_y	HFHS AdipoKO / HFHS flox_y	HFHS flox_y / STD flox_y	HFHS AdipoKO / STD AdipoKO	miR221/222 target gene
Igf2bp2	118.6727	92.12485	111.7554	233.6214	0.94171111	2.535921632	0.776293537	2.090470796	○
Foxp2	53.29913	25.92172	46.43985	56.3454	0.871305967	2.173675204	0.486344149	1.213298493	○
Ddit4	187.1108	201.7627	482.7296	383.8727	2.579913078	1.902594979	1.078306009	0.795212682	○
Tiparp	370.4981	370.9203	243.0674	629.3118	0.656055726	1.696622698	1.001139547	2.589042381	○
Gm13034	89.3279	42.14671	66.82102	71.24998	0.748041989	1.690522938	0.471820226	1.06628094	○
Cdkn1c	139.7296	64.02979	86.02513	99.0863	0.615654307	1.547503123	0.458240702	1.151829704	○
Gm17275	38.15434	25.35535	28.33733	38.61103	0.742702665	1.522796175	0.664546943	1.362550036	○
Ppp2r2a	173.6408	103.3587	136.4849	156.1966	0.786018609	1.511209023	0.59524432	1.144424035	○
Caprin2	105.009	84.21983	107.7583	127.1511	1.026181565	1.509752513	0.802024874	1.17996572	○
Fos	250.5789	115.658	96.99457	173.6935	0.387081953	1.501785436	0.461563204	1.790754885	○
Uri1	666.848	366.2552	624.7025	515.4158	0.936798941	1.407258655	0.549233409	0.825058008	○
Mark1	85.06554	51.96034	72.25445	73.05361	0.849397418	1.405949422	0.610827134	1.011060357	○
Casz1	67.4341	63.58655	83.56946	87.91584	1.239275975	1.382616921	0.942943555	1.052009191	○
Itgb8	54.55101	51.56115	53.44313	71.05316	0.979690935	1.378036758	0.945191482	1.329509705	○
Agfg1	594.9557	470.1974	450.3722	646.7574	0.756984428	1.375501864	0.790306572	1.436050893	○
Etv3	409.6244	143.7052	342.2083	197.4402	0.835419716	1.37392523	0.350821875	0.576959121	○
Tle3	812.1421	684.8116	767.2126	920.5015	0.944677785	1.344167505	0.843216477	1.199799769	○
Ddx3x	858.501	512.7594	664.2457	688.9457	0.773727346	1.343604232	0.597272921	1.037185036	○
Cpne8	216.8393	187.5397	240.7783	249.4114	1.110399729	1.329912547	0.864878737	1.035854975	○
Pvrl1	127.8629	150.1472	130.7448	199.2742	1.022538985	1.327192249	1.174282767	1.524146276	○
Pdzrn4	20.39221	18.83454	22.20171	24.96736	1.088734865	1.325615598	0.923614459	1.124569234	○
Ets2	528.1785	309.0158	364.8452	406.857	0.690761173	1.316621998	0.585059407	1.115149658	○
Smarca1	20.20307	21.40386	22.6035	28.04365	1.118815111	1.310214606	1.059436016	1.240677329	○